AD-A087 335 DAVID W TAYLOR NAVAL SHIP RESEARCH AND DEVELOPMENT CE—ETC F/G 13/10
HEAD AND FOLLOWING WAVE EXCITING FORCE EXPERIMENTS ON TWO SWATH—ETC(U)
JUN 80 J A FEIN, R STAHL

UNCLASSIFIED DTNSRDC/SPD-0928-01 NL

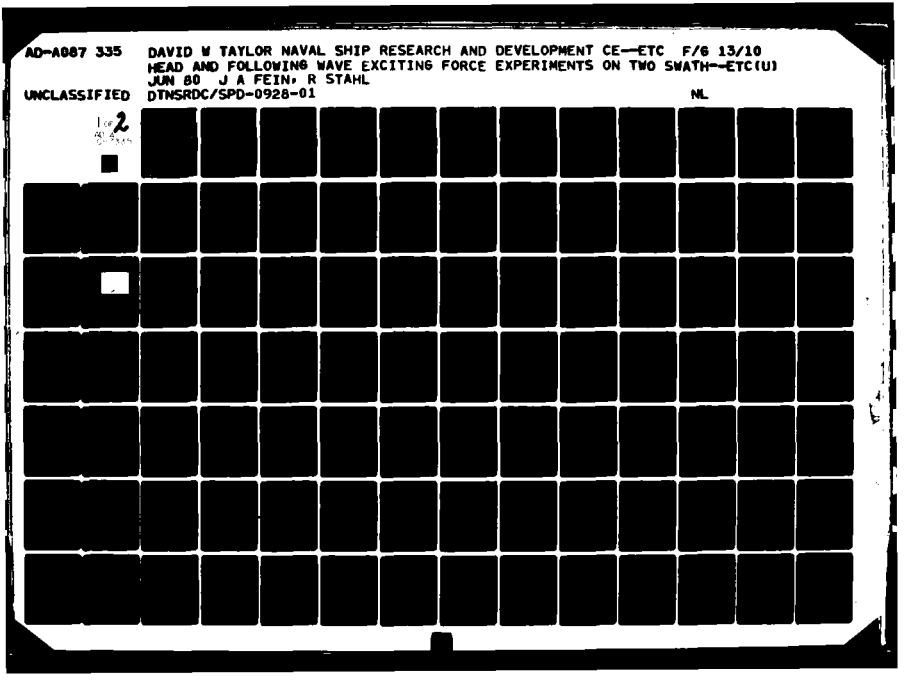


A
73

DAVID W. TAYLOR NAVAL SHIP RESEARCH AND DEVELOPMENT CENTER

Bethesda, Md. 20084

HEAD AND FOLLOWING WAVE EXCITING FORCE EXPERIMENTS ON TWO SWATH CONFIGURATIONS

J.A. FEIN
AND
R. STAHL

SHIP PERFORMANCE DEPARTMENT

JUNE 1980

DTNSRDC/SPD-0928-01

DTNSRDC/SPD-0928-01
HEAD AND FOLLOWING WAVE EXCITING FORCE EXPERIMENTS ON TWO SWATH CONFIGURATIONS

MAJOR DTNSRDC ORGANIZATIONAL COMPONENTS

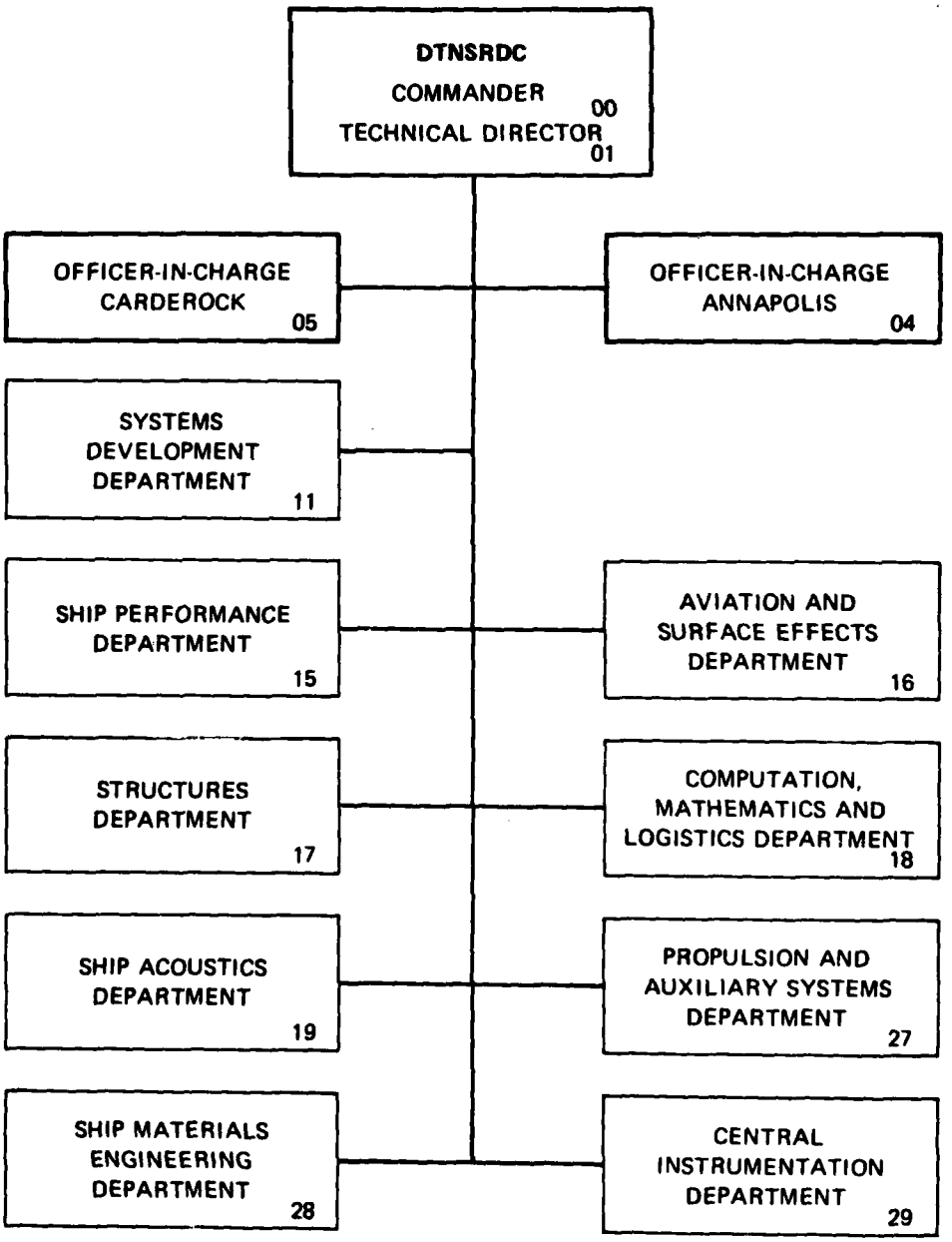

UNCLASSIFIED

SECURITY CLASSIFICATION OF THIS PAGE (When Data Entered)

REPORT DOCUMENTATION PAGE

READ INSTRUCTIONS BEFORE COMPLETING FORM

(14) 1. REPORT NUMBER: DTNSRDC/SPD-0928-01

2. GOVT ACCESSION NO.: AD-A087 335

3. RECIPIENT'S CATALOG NUMBER:

(6) 4. TITLE (and Subtitle): HEAD AND FOLLOWING WAVE EXCITING FORCE EXPERIMENTS ON TWO SWATH CONFIGURATIONS

5. TYPE OF REPORT & PERIOD COVERED:

6. PERFORMING ORG. REPORT NUMBER:

(10) 7. AUTHOR(s): J.A. FEIN, R. STAHL

8. CONTRACT OR GRANT NUMBER(s): (11) Jun 80

9. PERFORMING ORGANIZATION NAME AND ADDRESS: David W. Taylor Naval Ship R&D Center, Ship Performance Department, Bethesda, MD 20084 (16) F43412

10. PROGRAM ELEMENT, PROJECT, TASK AREA & WORK UNIT NUMBERS: Program Task Area SF 4341211, Task 19424

11. CONTROLLING OFFICE NAME AND ADDRESS: Naval Sea Systems Command, Code 031R, Washington, DC 20362 (17) SF4341121

12. REPORT DATE: June 1980 (12) 222

13. NUMBER OF PAGES:

14. MONITORING AGENCY NAME & ADDRESS (if different from Controlling Office): PE 62543N

15. SECURITY CLASS. (of this report): 387614 UNCLASSIFIED

15a. DECLASSIFICATION/DOWNGRADING SCHEDULE:

16. DISTRIBUTION STATEMENT (of this Report)

APPROVED FOR PUBLIC RELEASE: DISTRIBUTION UNLIMITED

17. DISTRIBUTION STATEMENT (of the abstract entered in Block 20, if different from Report)

18. SUPPLEMENTARY NOTES

19. KEY WORDS (Continue on reverse side if necessary and identify by block number)

SWATH Ships

Wave Excitations

Model Experiments

20. ABSTRACT (Continue on reverse side if necessary and identify by block number)

The heave force, surge force and pitch moment on a captive model due to regular waves have been obtained for two SWATH configurations. Exciting forces in head seas have been obtained for the SWATH 6D model and the SSP KAIMALINO model, and following-sea excitations have been obtained for the SWATH 6D model. The forces, moments and phase angles are presented for a range of regular wave frequencies. The experiments were conducted with and without propulsion which was found to have no effect on the coefficients.

DD FORM 1 JAN 73 1473 EDITION OF 1 NOV 65 IS OBSOLETE S/N 0102-LF-014-6601

UNCLASSIFIED 387694

SECURITY CLASSIFICATION OF THIS PAGE (When Data Entered)

TABLE OF CONTENTS

LIST OF TABLES

LIST OF FIGURES

ABSTRACT

The heave force, surge force and pitch moment on a captive model due to regular waves have been obtained for two SWATH configurations. Exciting forces in head seas have been obtained for the SWATH 6D model and the SSP KAIMALINO model, and following-sea excitations have been obtained for the SWATH 6D model. The forces, moments and phase angles are presented for a range of regular wave frequencies. The experiments were conducted with and without propulsion which was found to have no effect on the coefficients.

ADMINISTRATIVE INFORMATION

The work described herein was performed for the Small Waterplane Area Twin Hull (SWATH) Ship Development Office (Code 1110) in the Systems Development Office of DTNSRDC. Funding was provided by Work Unit 1110-200. The funding source was the SWATH Ship Exploratory Development Program under the Ships, Subs and Boats Program Task Area SF 43411211, Task 19424. The Program Manager was Mr. Schuler, Code 031R, of the Naval Sea Systems Command, Washington, D.C.

INTRODUCTION

In general SWATH motions are smaller than the motions of similar sized monohulls since the low waterplane reduces the wave exciting forces. On the other hand, SWATH motions are quite dependent on small changes in design parameters such as GM, waterplane area and fin size. Thus SWATH seakeeping design optimization is more complex and potentially more rewarding than seakeeping design for monohulls. The ability to predict seakeeping motions is essential to this design process.

Interest in the excitation forces and moments on a SWATH has centered around the need for data to compare with the computed excitations generated by the SWATH motion prediction program and to use in empirically based math models. The experimental work of Lee and Murray[1*] obtained exciting forces for SWATH 6A but did not produce good agreement with theory for pitching moment. The current effort was intended to broaden the scope of the previous effort, validate the experimental technique through calibrations, and provide data for a configuration that exists in full scale. Following sea as well as head sea excitations were conducted in order to expand the data base. The SWATH 6D configuration was chosen for this investigation because it represented a current state of the art design and was readily available for testing.

This report contains a description of the models, a discussion of the test technique, presentation of the data, discussion of the results and pertinent conclusions. The report demonstrates a reasonable technique for obtaining exciting forces and moments in head and following seas, shows that powering of the model does not affect the results and provides data for comparison with computed values.

DESCRIPTION OF MODELS

Two SWATH models were used in this experiment. The first was a 1/22.5 scale model (DTNSRDC Model 5337) of a 2900 metric ton developmental SWATH type craft designated as SWATH 6D. A new set of tandem struts was constructed for this model though the lower hulls are the same ones used for previous SWATH 6 experiments. This set of struts was constructed of fiberglass such that 40% of the waterplane area of each strut could be free flooding or be tested intact. However, only the intact configuration was examined in these experiments. Craft particulars for the intact configuration of the 6D are presented in Table 1. A sketch of the model is given in Figure 1.

---

* References are listed on page 11.

Fin shape and size were the same as for the previous SWATH 6A model. The forward fins of the SWATH 6D were fixed at zero angle of attack while the angle of attack on the aft set was variable and could be changed by means of a remotely controlled actuator.

The second model (DTNSRDC Model 5267) was of the Stable Semi-Submerged Platform (SSP). It is a 7.8 scale geosym of the original configuration of the SSP workboat built by the Naval Ocean Systems Center, Kailua, Hawaii. Model particulars are given in Table 1 and a photograph is given in Figure 2. The SSP design represents the state of tandem strut design in 1970, while the SWATH 6D was intended to investigate design approach rather than an actual prototype. The two configurations represent a range of design alternatives as far as strut length is concerned. A complete discussion of the design philosophy is contained in Lamb and Fein.[2]

DESCRIPTION OF EXPERIMENTAL TECHNIQUE

The wave exciting forces and moments were obtained by towing the fully captive model through regular or transient waves. Forces were measured by means of four-inch block gages oriented to measure drag force and lift force at two places on the model equidistant from the LCG on the model centerline. Pitch pivots were mounted in line with the gage systems. The moment in pitch was obtained by multiplying the difference between the lift gages by the moment arm which was half the distance between the gages (0.93 m for both models). Positions of the gages are given in Table 2. Wave height was measured by two sonic transducers, one located 5.9 meters ahead of the model LCG and the other attached to the model bow.

Calibrations were conducted to assure that the block gage system measured the proper forces without cross talk between directions. Moments generated about the reference point by either longitudinal or

vertical forces were properly reflected in the moment calculated by taking the lift force difference. No coupling between net lift force and net longitudinal force was found. The accuracy of the force transducers was better than $\pm$0.2 kg.

The model was at level trim and the fin positions were zero for the experiment except for some SWATH 6D conditions where the effect of fin angle was investigated. Propulsion was not used during most of the experiment for either model, but for some SWATH 6D conditions it was applied at the self-propulsion point to demonstrate that the use of power had little effect on the oscillatory exciting forces.

Regular wave exciting forces in head seas were obtained by running the model into the waves for at least 10 cycles of data. A range of wave periods from 1.25 to 3.75 seconds was explored. Amplitude of the waves was kept between 7.6 cm and 13 cm to insure linearity. In following regular waves the tests were carried out by either letting the longer waves overtake the model or letting the model catch up with the shorter, slower waves. When wave speed was near model speed it was not possible to obtain sufficient cycles of good data. Following sea excitations were conducted only for the SWATH 6D.

The data was analyzed on the carriage for the regular wave results. Forces and moments were computed and combined with the encountered wave translated to the CG to obtain amplitude and phase of the vertical force, longitudinal force and pitch moment.

The transient wave results were obtained in head seas by running the model into a packet of waves of continuously varying frequency, generated by a taped signal. The transient wave must be met when the frequencies are spread apart yet not spread so far that the wave lengths exceed the run length. The transient wave produces the results of a series of regular waves in a single run. The data must be analyzed by Fourier transform to produce the amplitude and phase of the forces for each single frequency contained in the transient wave.

ANALYSIS AND PRESENTATION OF DATA

The data presented in this report treats only the regular wave exciting force experiments in head and following seas, not the transient wave work. The transient wave effort essentially duplicated the regular wave data and the results will be included in a separate report on that technique. The experimental data over the encounter frequency range is presented for longitudinal force, $F_{10}(e)$, vertical force, $F_{30}(e)$, pitch moment, $F_{50}(e)$, and the three associated phase angles: a_1, a_3, a_5 in three appendices. Head sea SWATH 6D exciting force experimental results are given in Appendix A. The following sea SWATH 6D experimental results are presented in Appendix B. The head sea SSP exciting force data are contained in Appendix C.

The data analysis follows Fein and Murray[3]. The nomenclature is based on standard seakeeping terminology as given in Lee and Murray[1]. Nondimensionalization equations are given as follows:

Encounter frequency $\mu_e = \omega_e \sqrt{L/g}$,

where ω_e is encounter frequency in rad/sec
L is nominal ship length in meters and
g is gravitational constant in m/sec^2.

Longitudinal force $F_{10}(e) = \frac{\overline{F}_{10}\, L}{mgh}$, (positive forward)

where $\overline{F}_{10}$ is the measured force amplitude in newtons
m is mass of the ship in kg and
h is wave height in meters.

Similarly, vertical force is defined as:

$$F_{30}(e) = \frac{\overline{F}_{30}\, L}{mgh} \text{ , (positive down)}$$

and pitch moment is given by:

$$F_{50}(e) = \frac{F_{50}}{mgh} \text{ , (positive bow down)}$$

where F_{50} is the measured moment amplitude in newton-meters.

DISCUSSION OF RESULTS

HEAD WAVES, SWATH 6D

The excitation forces and moments in terms of amplitude and phase are given in Figures 3 to 32 (Appendix A) for the SWATH 6D in head seas. Five speeds were evaluated corresponding to 0, 4, 10, 20 and 28 knots full scale.

Longitudinal exciting force amplitude is presented in Figures 3 through 7. The data shows no effects due to powering, fin angles or wave height. The linearity was checked by repeating a frequency at various wave steepnesses. Two examples of this linearity are seen at μ_e = 1.1 and 1.8 in Figure 3. The data trends are consistent for the five speeds, showing only a shift due to speed. The very high frequency points show some scatter but most of the data is very reasonable.

The phase associated with longitudinal force, α_1, is given in Figures 8 through 12. The phase angle is roughly 90 degrees over most frequencies at all speeds. The higher frequencies do show a shift; however they may be related to the scatter in the force. A phase lead of 90 degrees is reasonable as it coincides with the wave trough approaching the bow resulting in maximum longitudinal force (positive forward).

The vertical force in Figures 13 to 17 also shows a similarity of trends with speed and no effect due to nonlinearity, propulsion or fin angles. The trough in the data varies from μ_e = 1.8 at zero speed to μ_e = 4 at 20 and 28 knots.

The phase associated with vertical force, a_3, is given in Figures 18 to 22. The results show very consistent trends at the various speeds, tending to zero at low frequencies. This is reasonable since the vertical force (positive down) should be in phase with long waves.

Nondimensional pitch exciting moment is shown in Figures 23 to 27. The magnitude of the pitch moment increases with speed though the trends remain the same. Very importantly, the data is unaffected by the use of powering and fin angles. The constant force due to powering is not an influence on the oscillatory exciting force. Oscillatory lift on the fin is probably small.

Moment phase a_5 is given in Figures 28 to 32 for the SWATH 6D in head regular waves. The moment tends to -90 or 270 degrees at low speed, and near zero at the middle speeds. Since pitch moment is positive bow down, the 90 degree lag is reasonable for long waves, as moment lags behind the wave.

FOLLOWING WAVES, SWATH 6D

Appendix B contains the results from the following sea exciting force experiments on the SWATH 6D, which is the first SWATH configuration to have undergone this type of experiment. The results are presented in Figures 33 to 62. Since in the figures the data is plotted against encounter frequencies, interesting anomalies are apparent. At higher speeds and higher encounter frequencies in this experiment a limiting frequency is evident. For long waves, the waves travel much faster than the ship and ω_e increases as ω increases. For shorter waves, when the wave velocity is only slightly greater than the ship, ω_e decreases with ω. Hence for any given speed there is a maximum ω_e in following waves where the waves are overtaking the ship. When the ship travels faster and overtakes the shortest waves the encounter frequency becomes negative as the ship speed is greater than the wave speed. At a full scale speed of 10 knots the maximum μ_e is 1.3, at 20 knots it is about

0.62, and at 28 knots the μ_e maximum is 0.44. This tendency in the data illustrates an important factor in the analysis of following sea excitation. Another facet of the following sea data is the difficulty in obtaining excitation data near zero frequency of encounter. By definition no results can be obtained unless a cycle of encounter is recorded. Thus results near zero encounter are subject to inaccuracies and scatter.

The longitudinal forces and phases versus encounter frequency are presented in Figures 33 to 42. Five full scale speeds (0, 4, 10, 20 and 28 knots) are explored. Data trends are similar at all speeds with a peak in the force data that shifts to lower encounter frequency as speed increases. The zero speed results agree substantially with the head sea results for magnitude while phase is shifted 180 degrees as expected since the wave direction has been reversed.

Following seas heave force and phase are given in Figures 43 to 52. The lower speed data shows a definite 180 degree phase shift from near zero to a 180 degree lead. Zero speed results show the same trends and values as the head sea cases. Figure 47 gives a good indication of the heave force at zero encounter frequency and the trends at negative encounters. Figure 52 is interesting as it shows what seems to be a linear relationship between phase and negative encounter frequency.

The pitch exciting moment magnitude and phase are given in Figures 53 to 62. The moment magnitude shows the same trends as the heave force at all speeds. The phase is 180 degrees out of phase from the head sea results as might be expected. There is very little scatter even near $\mu_e = 0$. The linear relationship for phase for negative encounters recurs in Figure 62. Also it is interesting to note that the magnitude of the exciting moment in following seas is about 20% less than the value in head seas over the frequency range. This is related to the much lower encounter frequencies in following seas and the more favorable phases between ship and wave.

HEAD WAVES, SSP

The SSP exciting force curves are contained in Appendix C (Figures 63 to 92). Speeds correspond to 0, 3, 7, 10 and 15.5 knots full scale. The longitudinal exciting force and phase are given in Figure 63 to 72. The data trends are similar to those seen for the SWATH 6D. SSP forces are of lower magnitude at lower speeds but the same at higher speeds. Phases are also similar in trends tending to a 90 degree lead at low frequency. The high frequency scatter present for the SWATH 6D is also apparent for the SSP.

Head wave heave exciting forces and phases are given in Figures 73 to 82. The data is consistent and shows no scatter. Nondimensional heave forces are a little larger than those for the SWATH 6D but trends such as peak and trough frequencies repeat closely. This indicates that theory may be able to predict SSP heave characteristics. Phase approaches zero at low frequency. Phase increases with increasing frequency at 7 knots (Figure 80) but decreases with frequency at the above hump speed of 15.5 knots.

Figures 83 to 92 give the pitch exciting moment and phase for the SSP. Pitch moment is greater for the SSP than for the SWATH 6D at all speeds. The trends also are somewhat different. This is due to the full span aft foil on the SSP which contributes a large oscillatory force, particularly at the higher speeds. Moment phase also shows some differences in trends. This tends to imply that present theory may have some trouble predicting SSP pitch motions.

CONCLUSIONS

This experimental program covers a wide range of test variables (in this case speed, frequency and wave height). The results describe the head and following wave excitation forces and moments for SWATH 6D and the head wave values for the SSP. Sufficient data is now available

to verify a force prediction program or to establish a data based program. The results are reasonable for both models. The SSP excitation moment data indicates that the full span foil has a major effect and may require new theoretical descriptions.

REFERENCES

1. Lee, C.M. and L. Murray, "Experimental Investigation of Hydrodynamic Coefficients of a SWATH Model," NSRDC Report SPD 747-01 (Jan 1977).

2. Lamb, G.R. and J.A. Fein, "The Developing Technology for SWATH Ships," presented at the AIAA/SNAME Advanced Marine Vehicles Conference, Baltimore (Oct 1979).

3. Fein, J.A. and L. Murray, "Wave Excitation and Vertical Plane Oscillation Experiments on a High Length-to-Beam Ratio Surface Effect Ship," NSRDC Report SPD 697-01 (July 1976).

TABLE 1

FULL SCALE GEOMETRIC AND OTHER PHYSICAL CHARACTERISTICS OF
SWATH 6D AND THE STABLE SEMI-SUBMERGED PLATFORM (SSP), BOTH TANDEM STRUT DESIGNS

	Units	SWATH 6D	SSP
Prototype to Model Scale Ratio		22.5	7.8
Overall Length (LOA)	Meters	73.15	26.40
Hull to Hull Centerline Separation	Meters	26.82	12.19
Displacement in Salt Water	Metric Tons	2946	193.0
Vertical Distance from Baseplane to Design Waterplane (Draft)	Meters	8.14	4.66
Longitudinal Distance from LCB to Aft Perpendicular	Meters	38.7	12.94
Submerged Hull, Each:			
Overall Length without Propellers	Meters	74.17	21.43
Length of Parallel Middle Body	Meters	40.48	17.68
Diameter of Parallel Middle Body	Meters	4.57	1.98
Forward Strut, Each:			
Chord at DWL	Meters	25.82	7.01
Maximum Thickness to Chord Ratio		.12	.15
Section		Lenticular	Lenticular
Aft Strut, Each:			
Chord at DWL	Meters	25.82	6.10
Maximum Thickness to Chord Ratio		.12	.15
Section		Lenticular	Lenticular
Forward Fin, Each:			
Span	Meters	2.56	1.83
Longitudinal Distance from Aft Perpendicular to ¼ Chord	Meters	57.1	21.47
Vertical Distance from Baseplane to Hinge Axis	Meters	2.29	0.99
Stern Fin			
Type		Two, All Movable	Full-Span Flapped
Chord	Meters	3.81	2.38
Span at Leading Edge	Meters	4.24	10.55
Vertical Distance from Baseplane to Chord Line	Meters	2.29	0.99
Longitudinal Distance from Aft Perpendicular to ¼ Chord	Meters	24.1	3.81

TABLE 2

EXPERIMENTAL WAVE EXCITATION X AND Z FORCE
MEASURING LOCATIONS IN FULL SCALE TERMS

	Units	SWATH 6D	SSP
Forward X,Z Forces			
Longitudinal Distance Forward of CB	Meters	20.57	7.13
Vertical Distance from Baseplane	Meters	18.71	8.60
Aft X,Z forces			
Longitudinal Distance Aft of CB	Meters	20.57	7.13
Vertical Distance from Baseplane	Meters	18.71	8.60

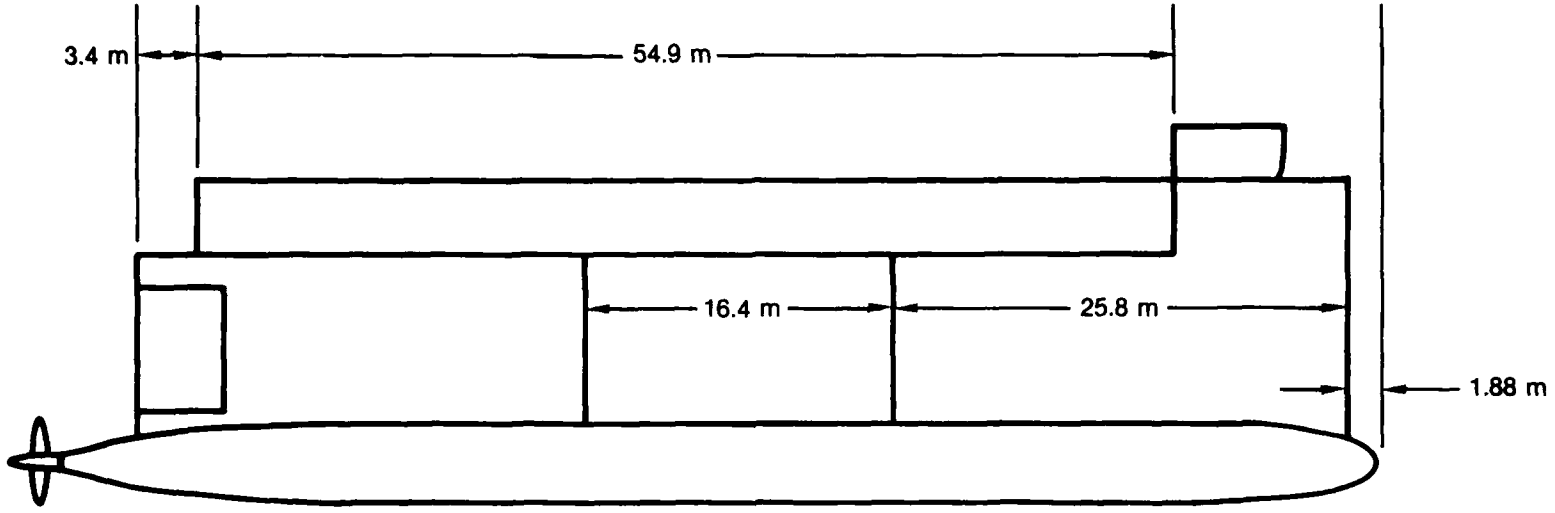

STRUT CONFIGURATION 6D

GM_L (Full) = 26.4 m
Strut Lengths = 25.8 m
Strut Thickness (max) = 3.1 m
Strut Gap = 16.4 m
Deck Width (max) = 29.6 m
Rudder = 7.2 m High
5.7 m Long

Figure 1 - Sketch of SWATH 6D Strut Configuration

Figure 2 - Photograph of a Bow View of the SSP Experimental Model

APPENDIX A

SWATH 6D HEAD SEA
EXCITING FORCE EXPERIMENTAL DATA

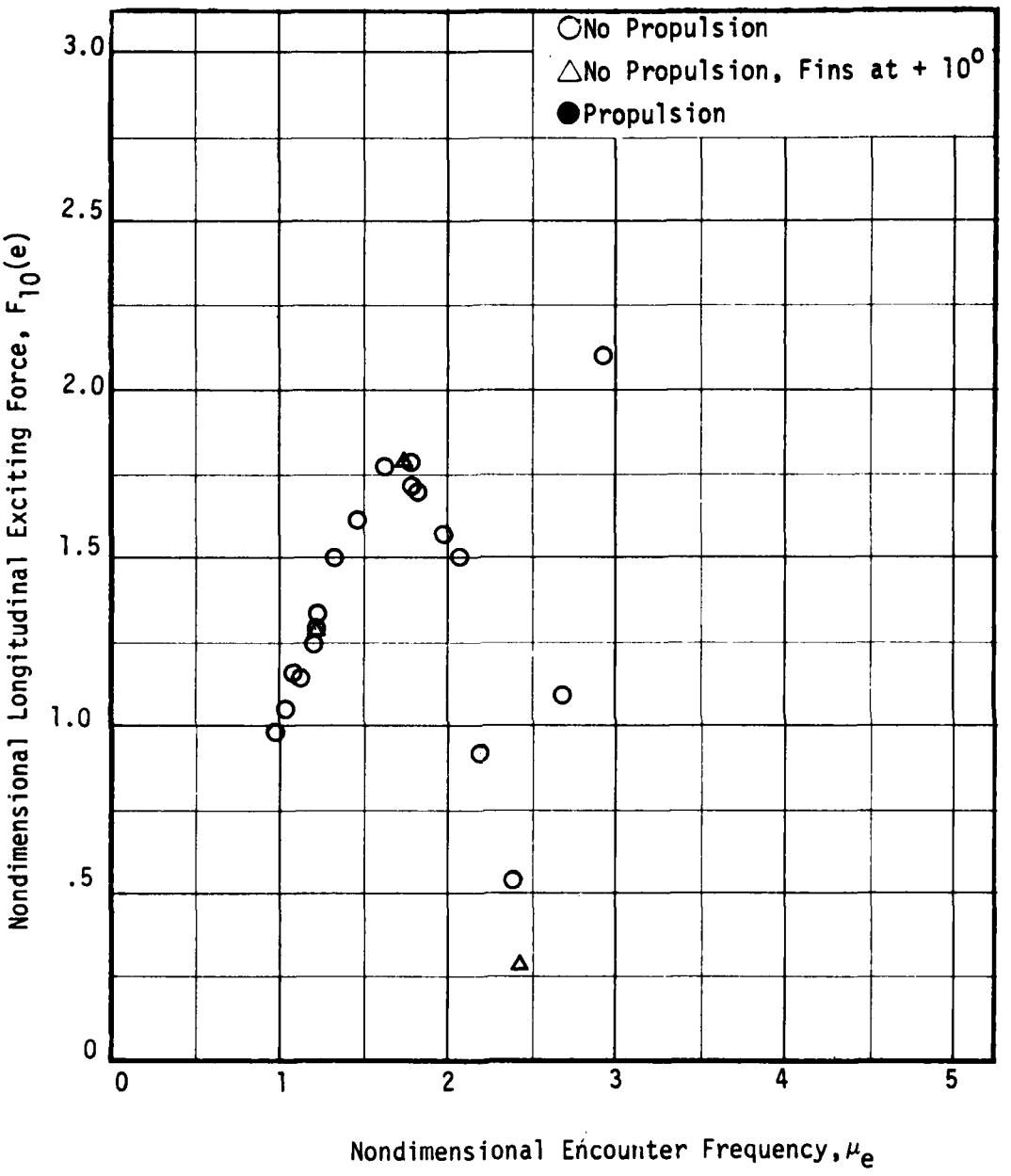

Figure 3 - Variation of Nondimensional Longitudinal Exciting Force, $F_{10}(e)$, with Nondimensional Encounter Frequency, μ_e, at Zero Speed for the SWATH 6D in Head Waves

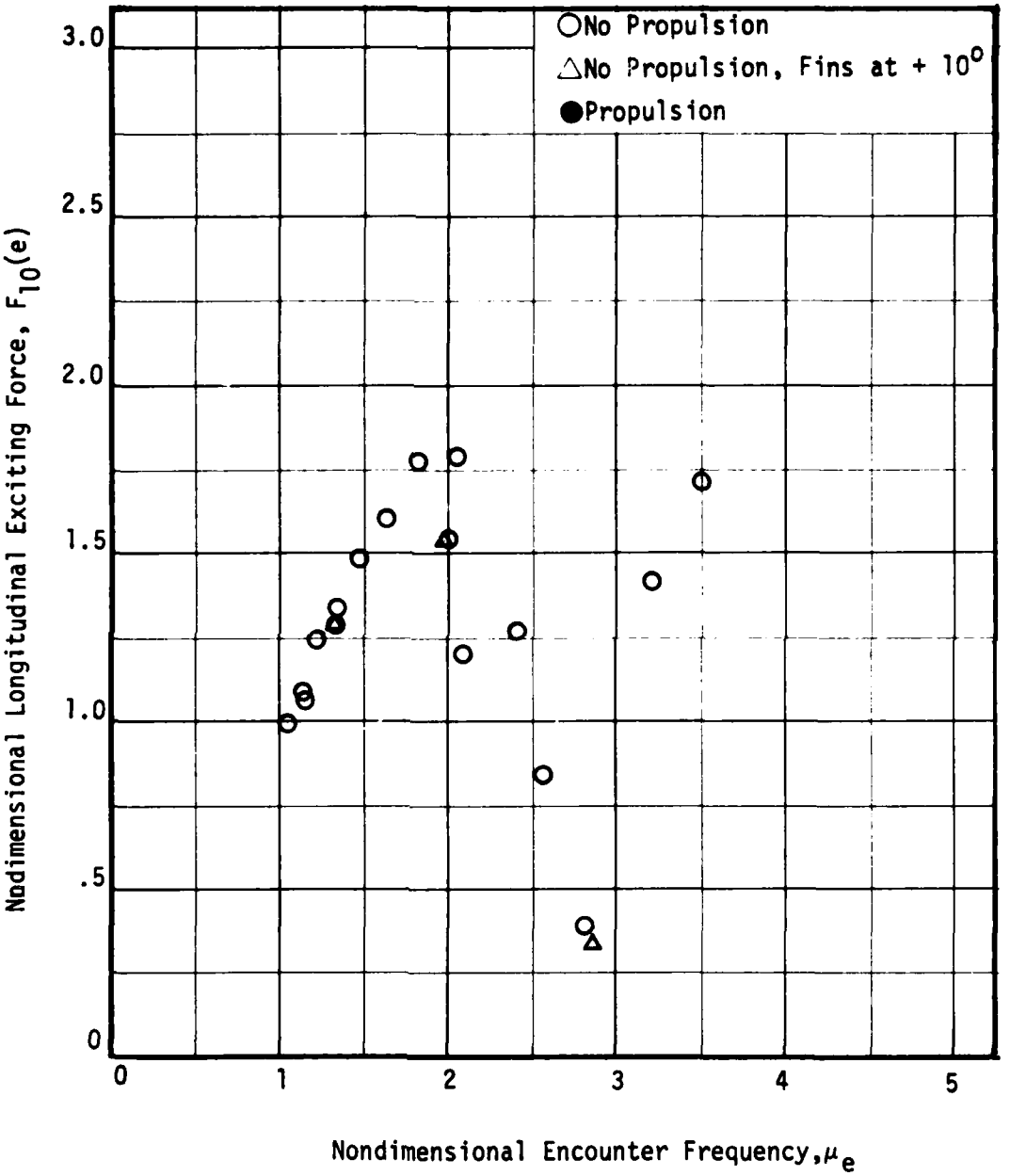

Figure 4 - Variation of Nondimensional Longitudinal Exciting Force, $F_{10}(e)$, with Nondimensional Encounter Frequency, μ_e, at a Full Scale Speed of 4 Knots for the SWATH 6D in Head Waves

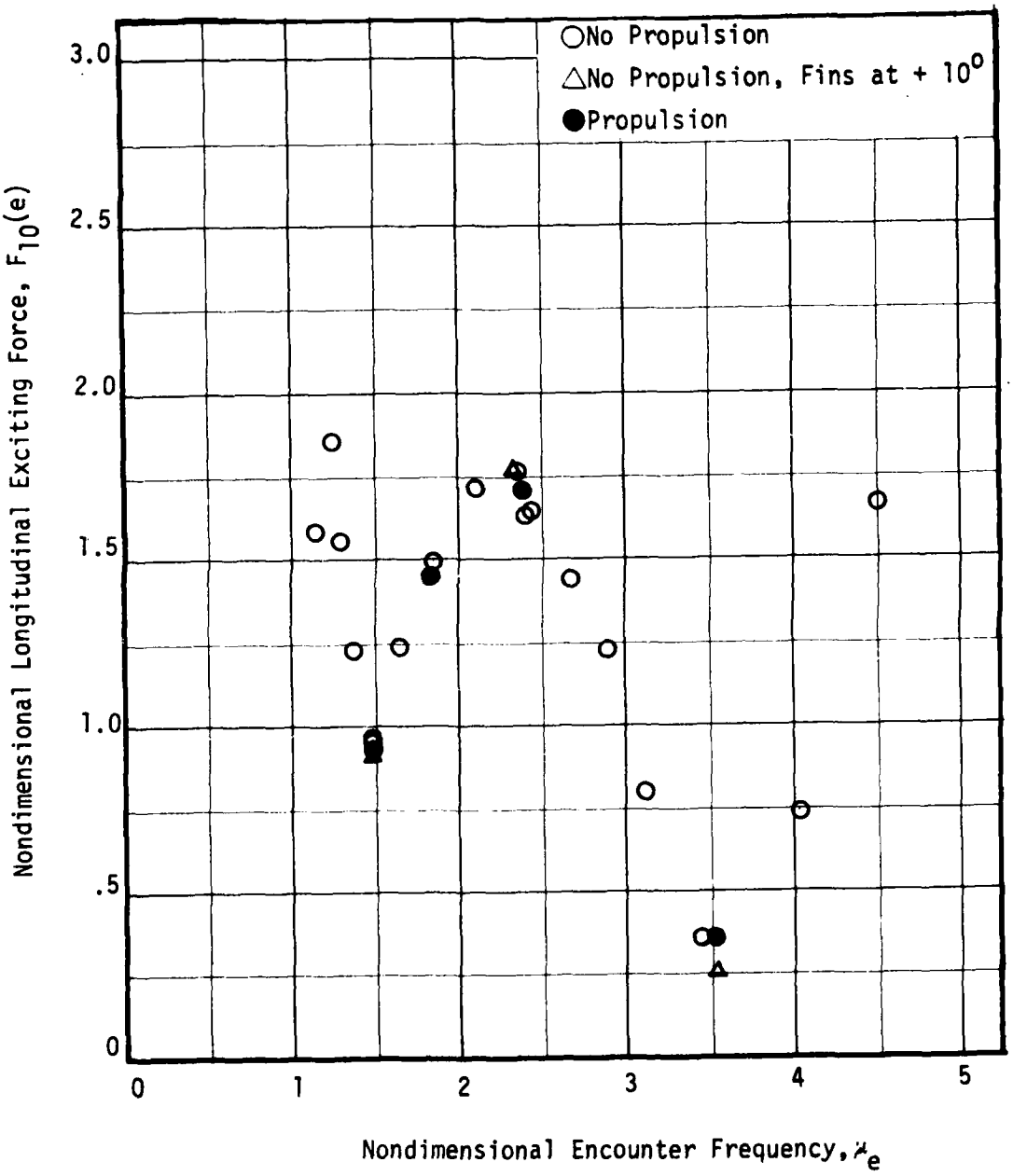

Figure 5 - Variation of Nondimensional Longitudinal Exciting Force, $F_{10}(e)$, with Nondimensional Encounter Frequency, μe, at a Full Scale Speed of 10 Knots for the SWATH 6D in Head Waves

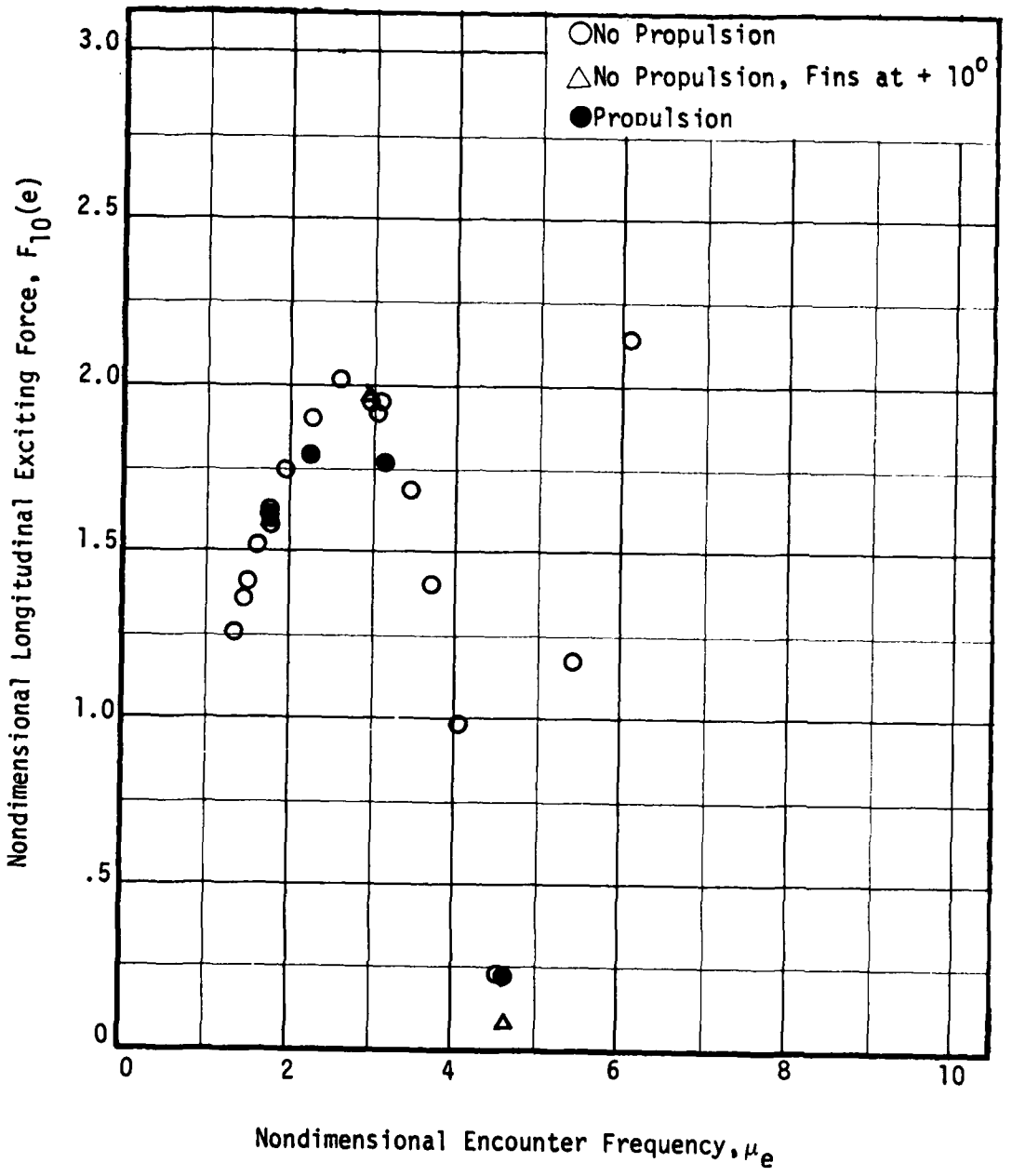

Figure 6 - Variation of Nondimensional Longitudinal Exciting Force, $F_{10}(e)$, with Nondimensional Encounter Frequency, μ_e, at a Full Scale Speed of 20 Knots for the SWATH 6D in Head Waves

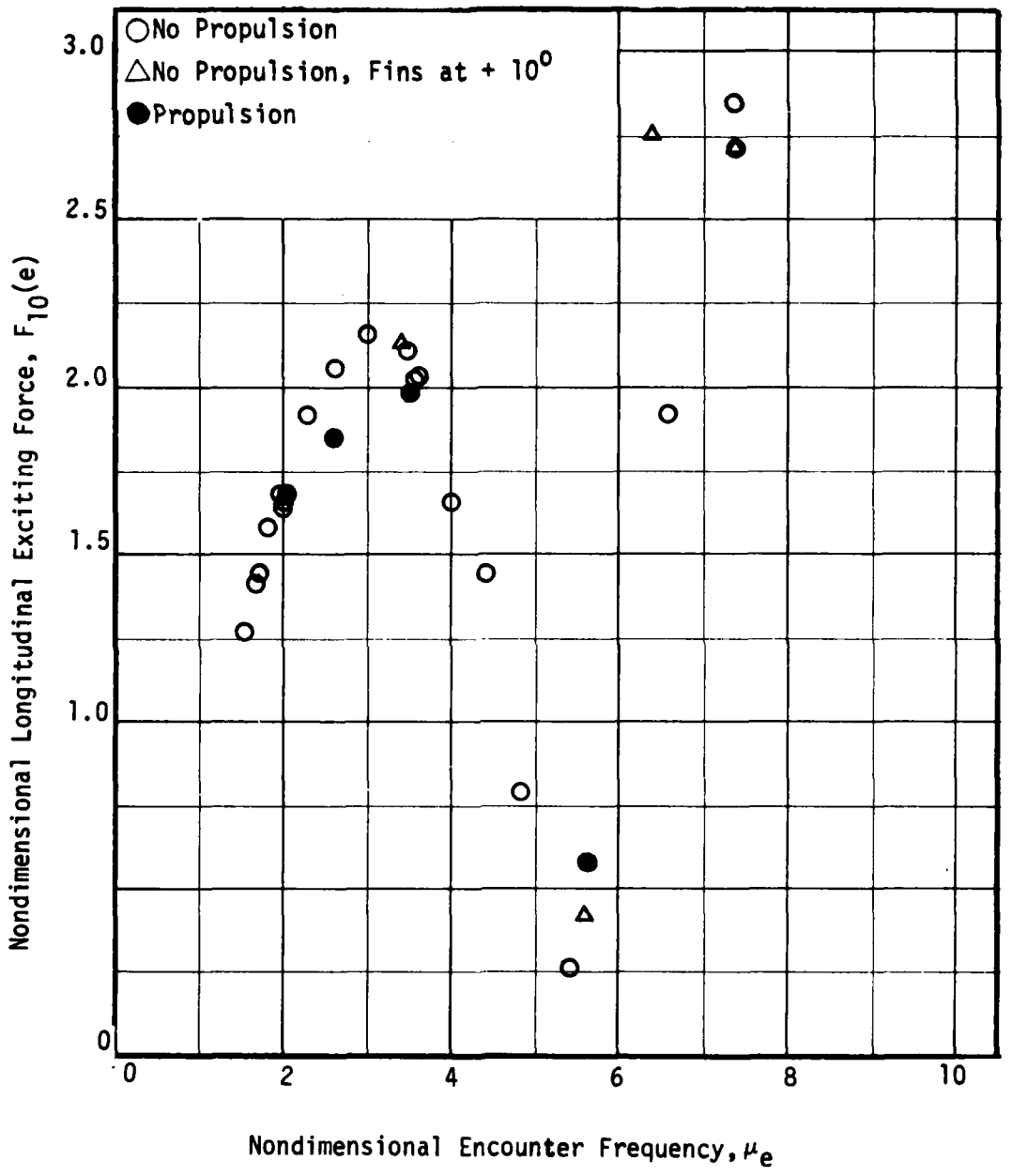

Figure 7 - Variation of Nondimensional Longitudinal Exciting Force, $F_{10}(e)$, with Nondimensional Encounter Frequency, μ_e, at a Full Scale Speed of 28 Knots for the SWATH 6D in Head Waves

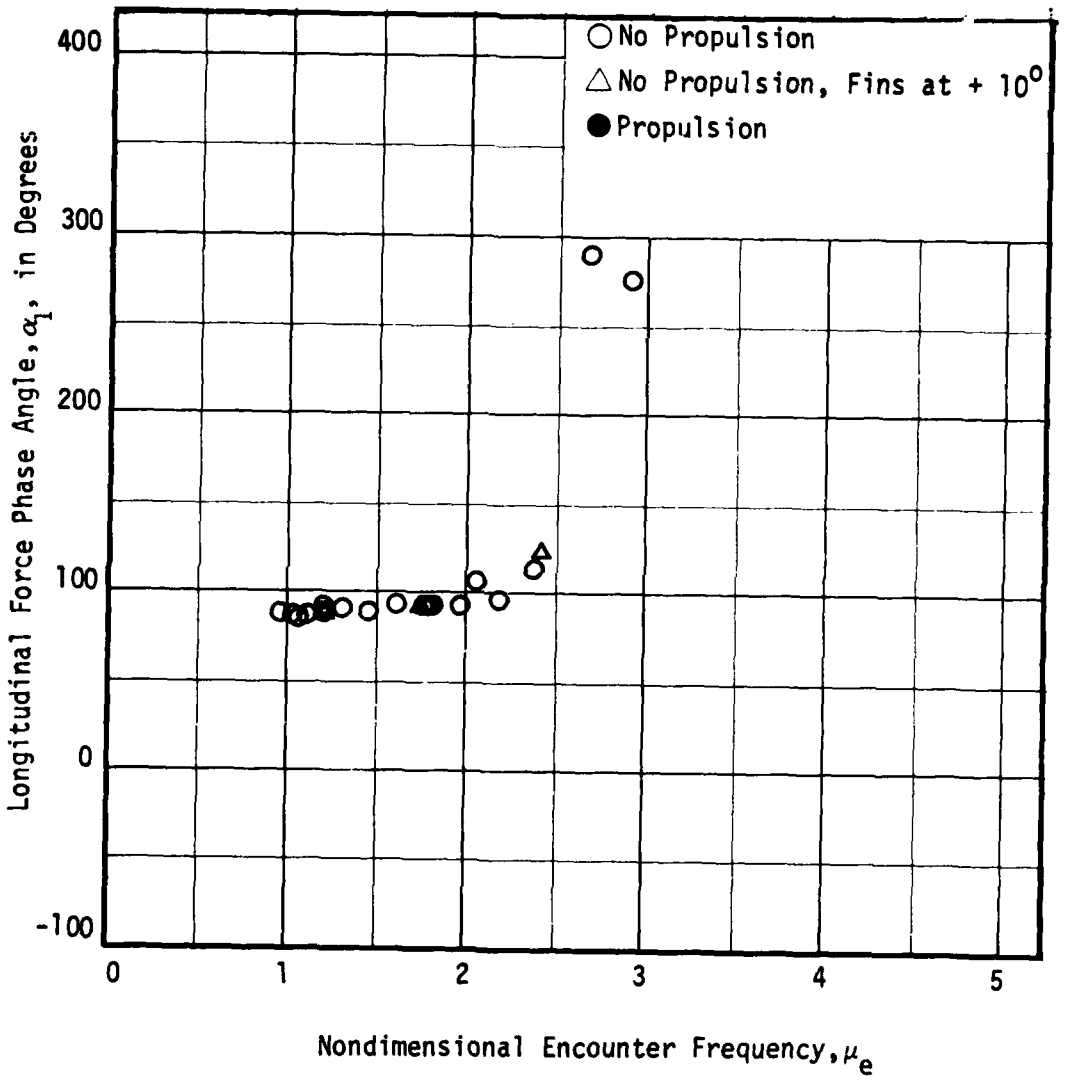

Figure 8 - Variation of Longitudinal Force Phase Angle, α_1, with Nondimensional Encounter Frequency, μ_e, at Zero Speed for the SWATH 6D in Head Waves

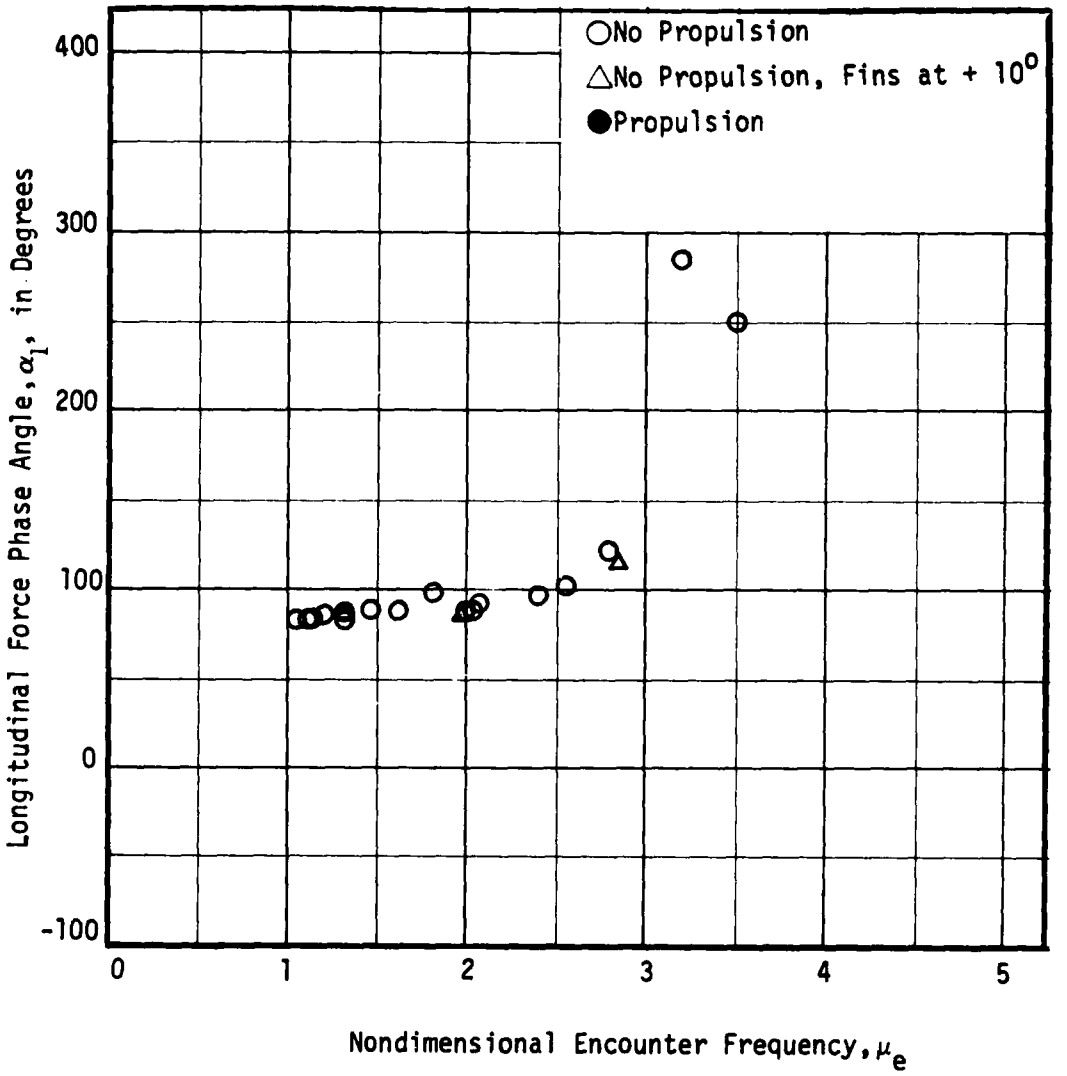

Figure 9 - Variation of Longitudinal Force Phase Angle, α_1, with Nondimensional Encounter Frequency, μ_e, at a Full Scale Speed of 4 Knots for the SWATH 6D in Head Waves

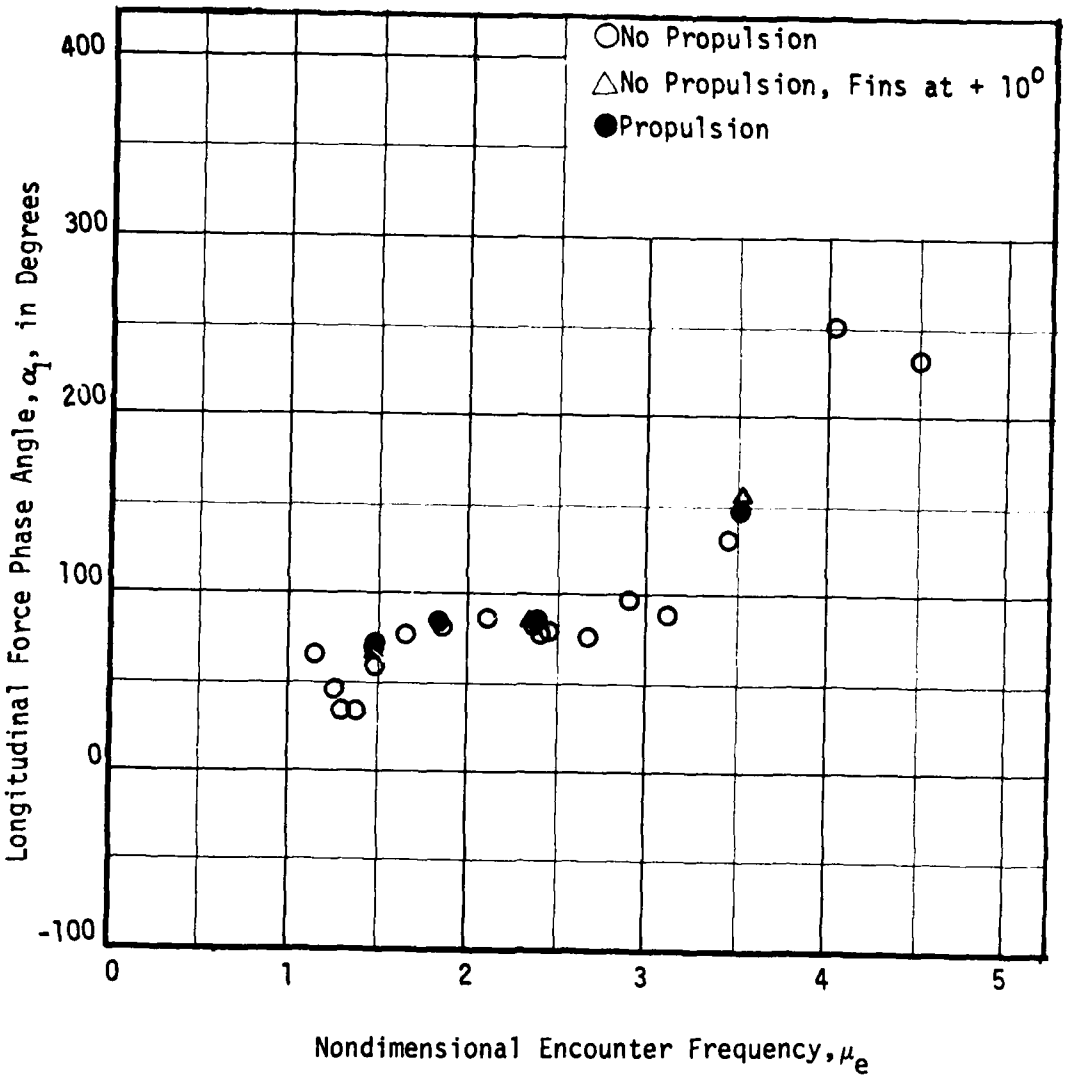

Figure 10 - Variation of Longitudinal Force Phase Angle, α_1, with Nondimensional Encounter Frequency, μ_e, at a Full Scale Speed of 10 Knots for the SWATH 6D in Head Waves

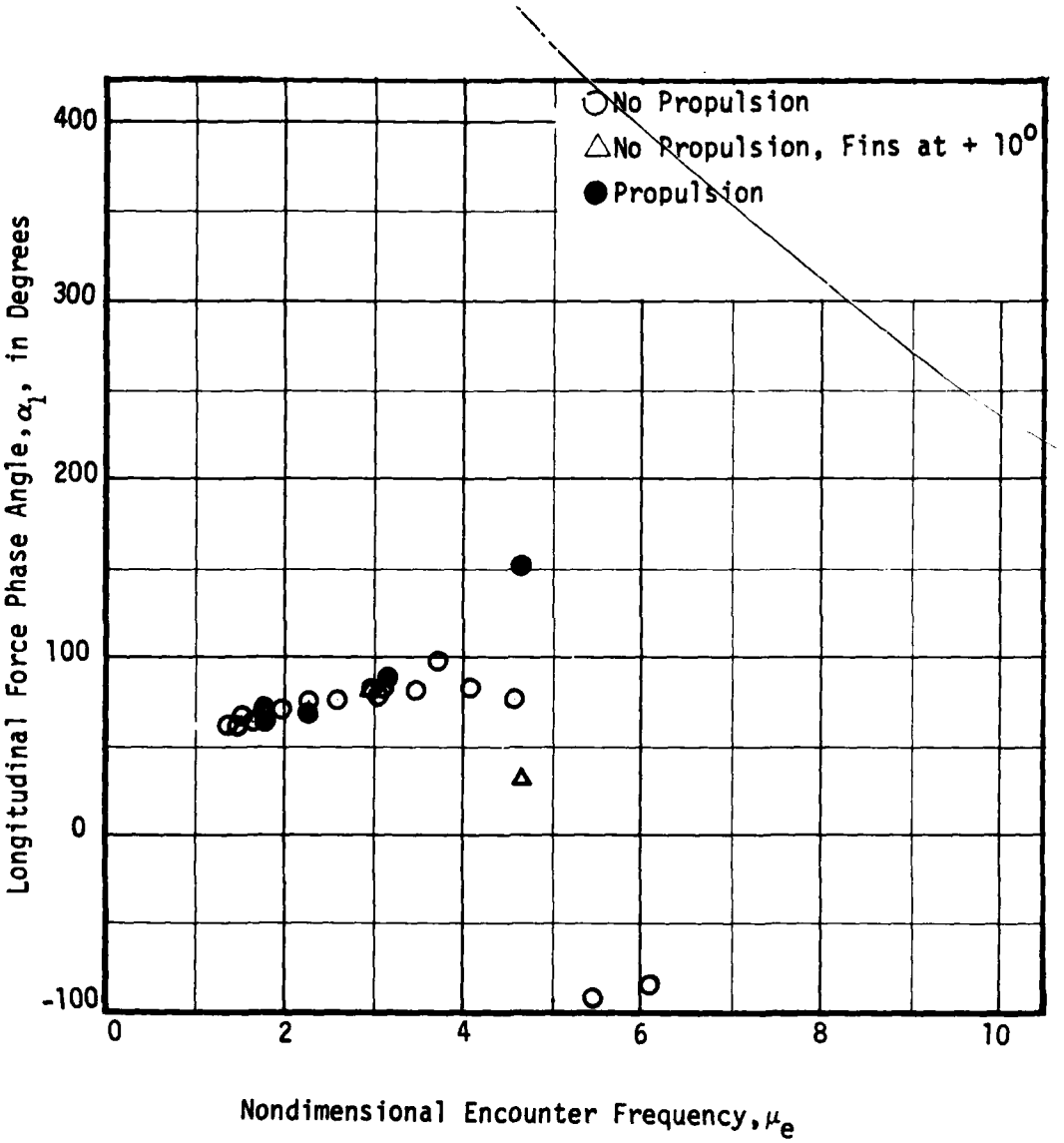

Figure 11 - Variation of Longitudinal Force Phase Angle, α_1, with Nondimensional Encounter Frequency, μ_e, at a Full Scale Speed of 20 Knots for the SWATH 6D in Head Waves

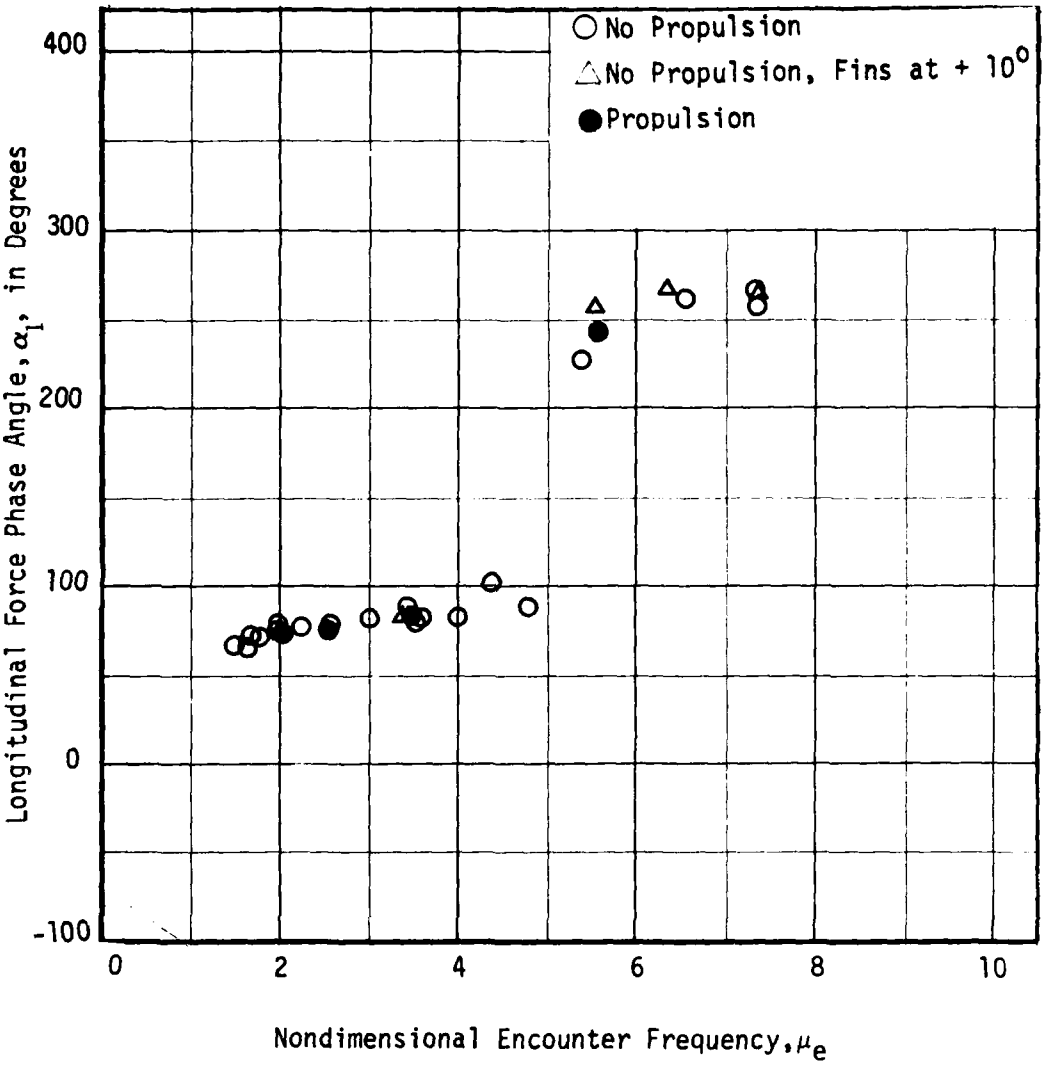

Figure 12 - Variation of Longitudinal Force Phase Angle, α_1, with Nondimensional Encounter Frequency, μ_e, at a Full Scale Speed of 28 Knots for the SWATH 6D in Head Waves

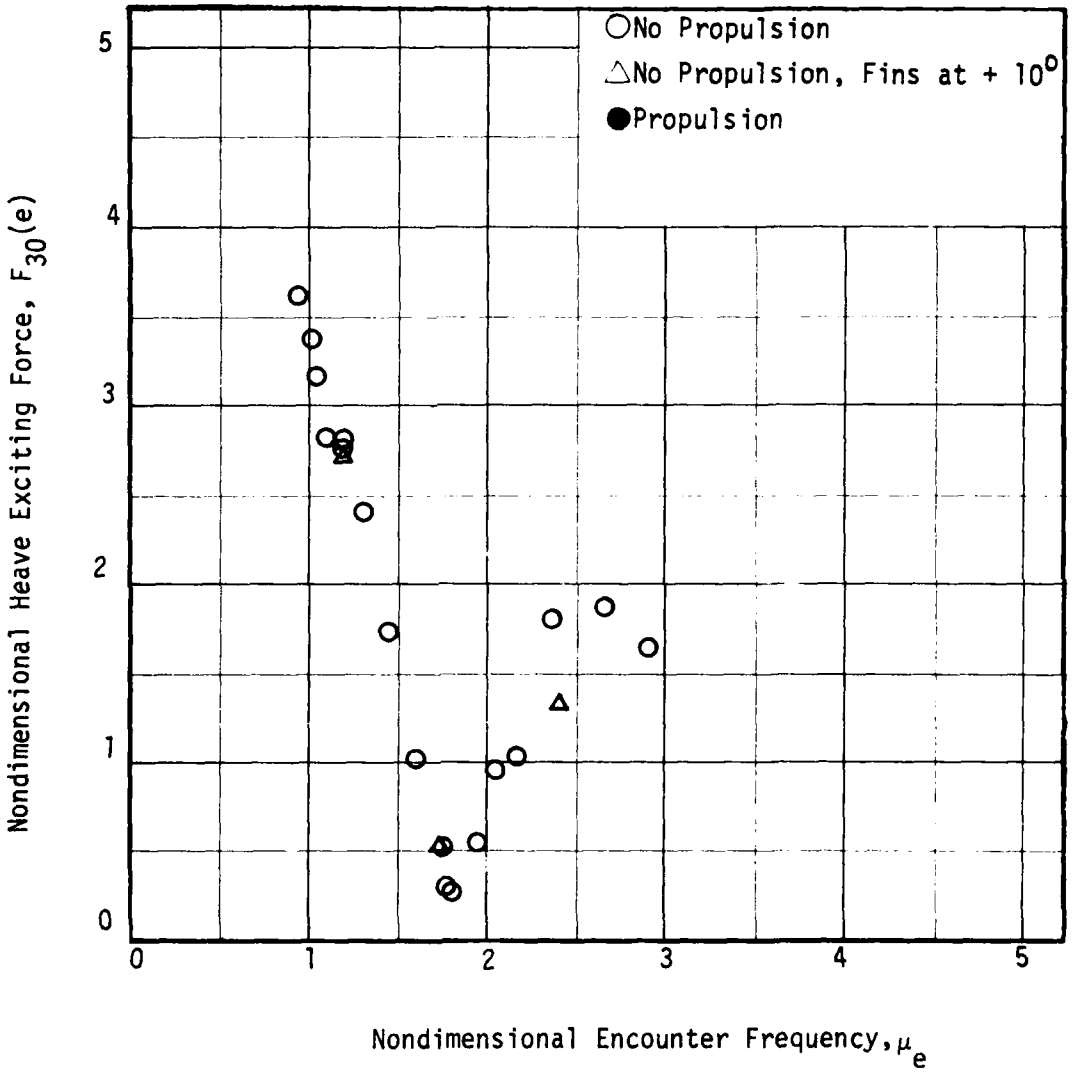

Figure 13 - Variation of Nondimensional Heave Exciting Force, $F_{30}(e)$, with Nondimensional Encounter Frequency, μ_e, at Zero Speed for the SWATH 6D in Head Waves

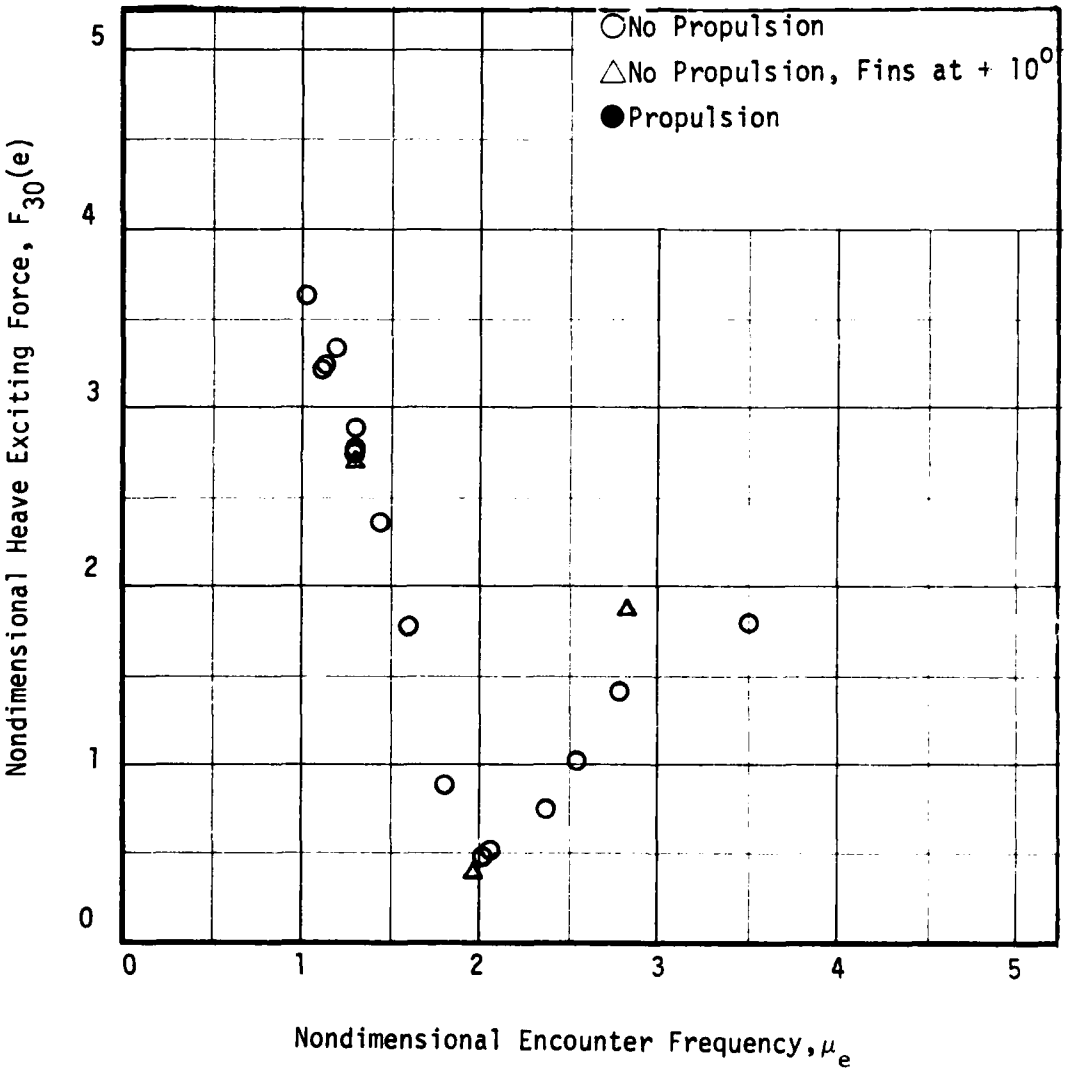

Figure 14 - Variation of Nondimensional Heave Exciting Force, $F_{30}(e)$, with Nondimensional Encounter Frequency, μ_e, at a Full Scale Speed of 4 Knots for the SWATH 6D in Head Waves

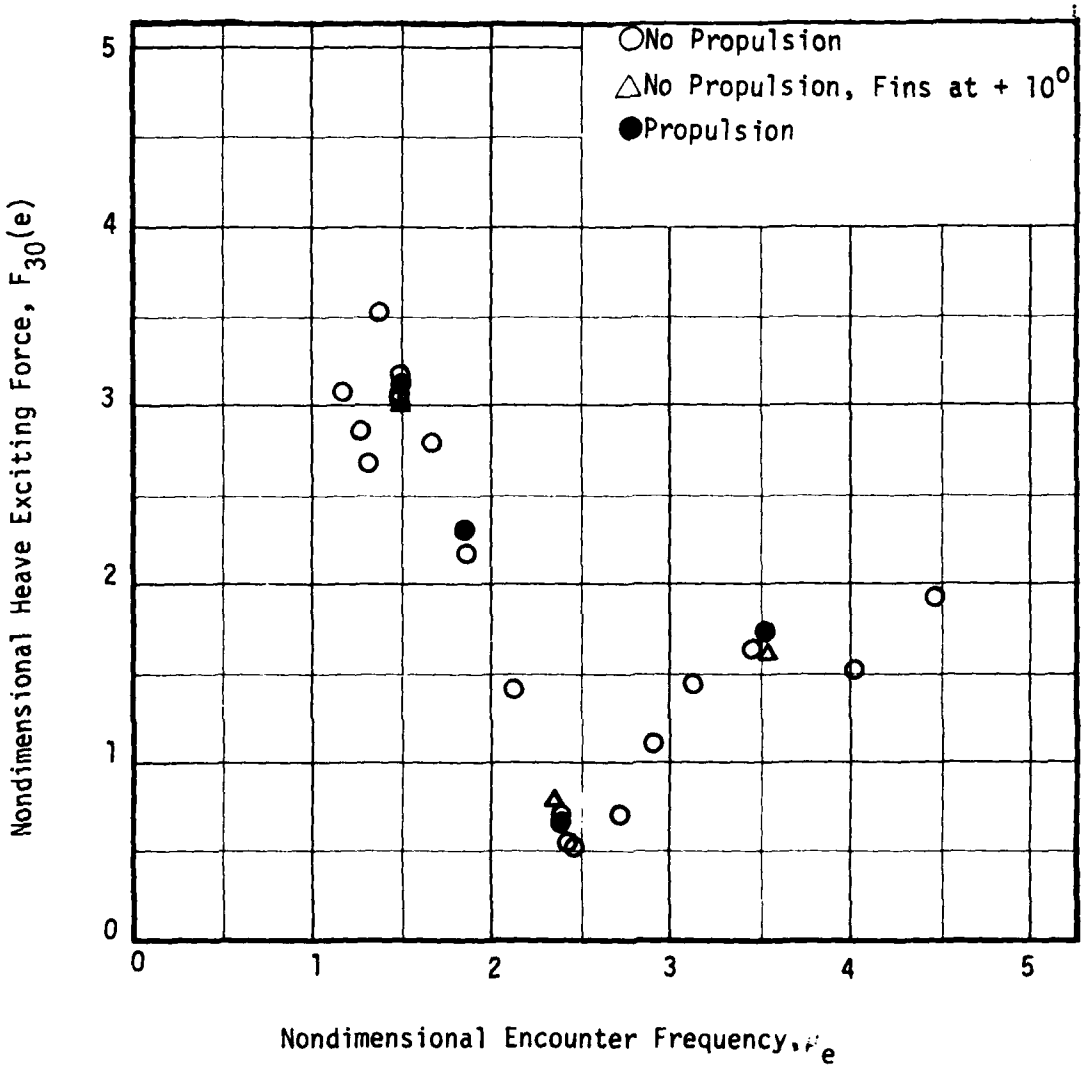

Figure 15 - Variation of Nondimensional Heave Exciting Force, $F_{30}(e)$, with Nondimensional Encounter Frequency, μ_e, at a Full Scale Speed of 10 Knots for the SWATH 6D in Head Waves

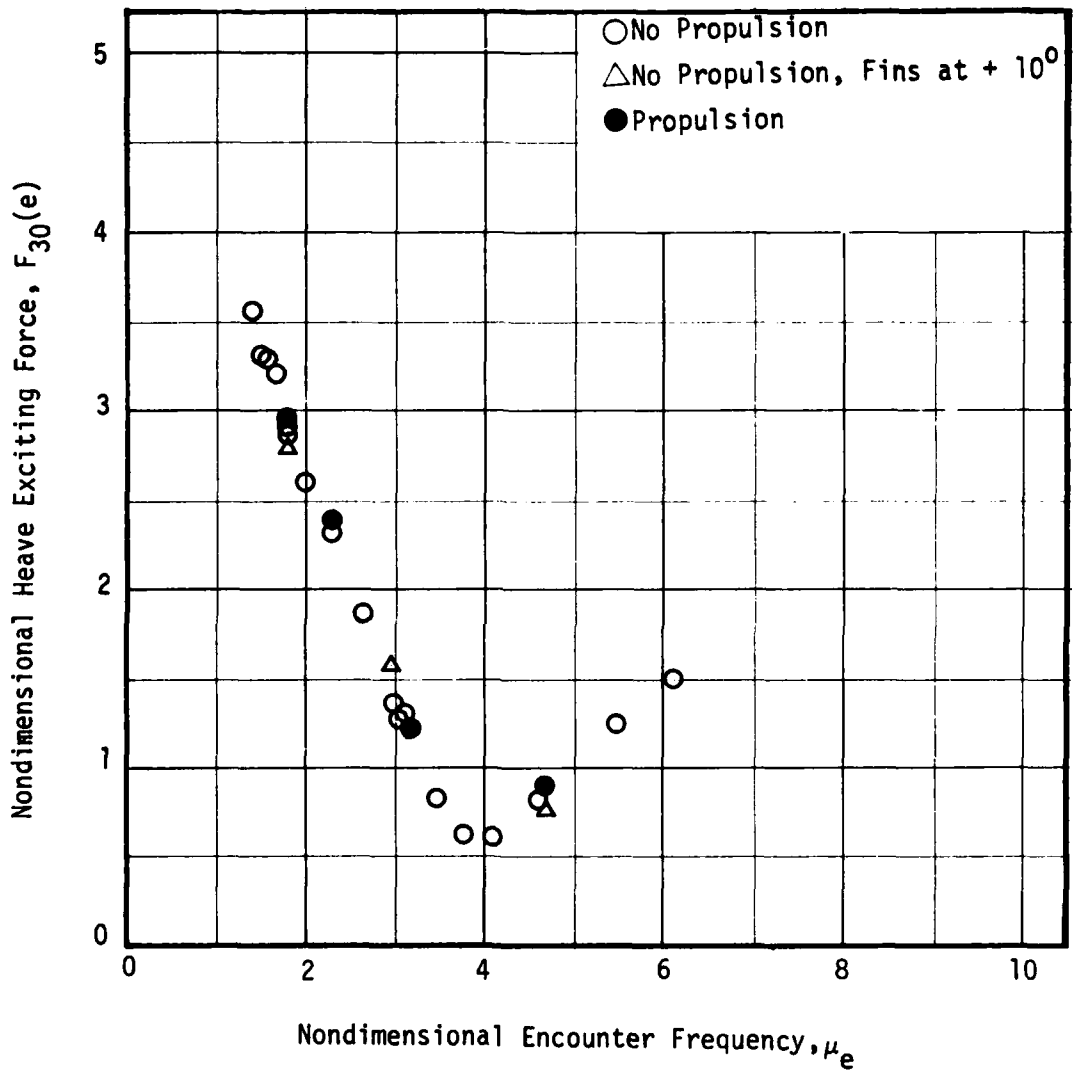

Figure 16 - Variation of Nondimensional Heave Exciting Force, $F_{30}(e)$, with Nondimensional Encounter Frequency, μ_e, at a Full Scale Speed of 20 Knots for the SWATH 6D in Head Waves

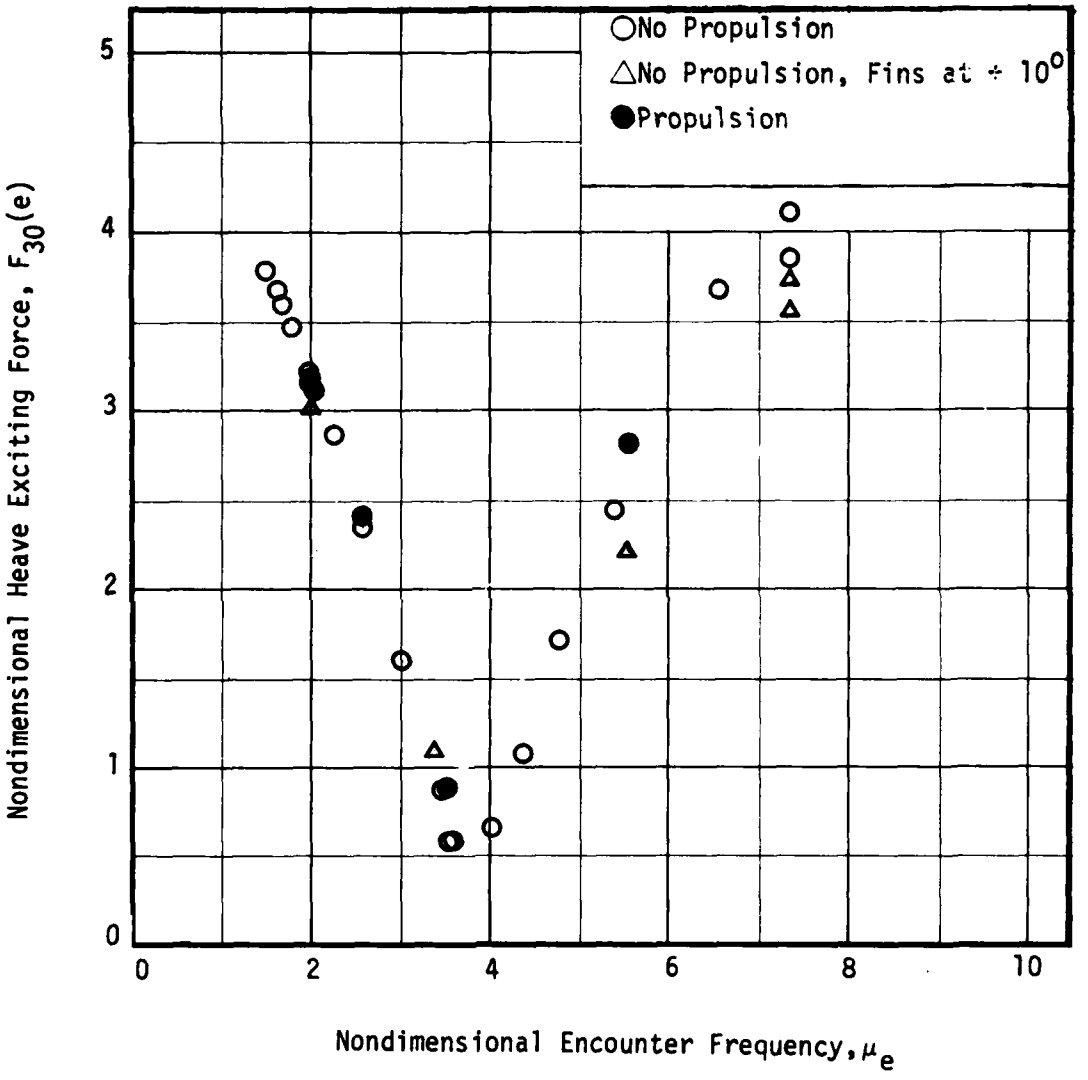

Figure 17 - Variation of Nondimensional Heave Exciting Force, $F_{30}(e)$, with Nondimensional Encounter Frequency, μ_e, at a Full Scale Speed of 28 Knots for the SWATH 6D in Head Waves

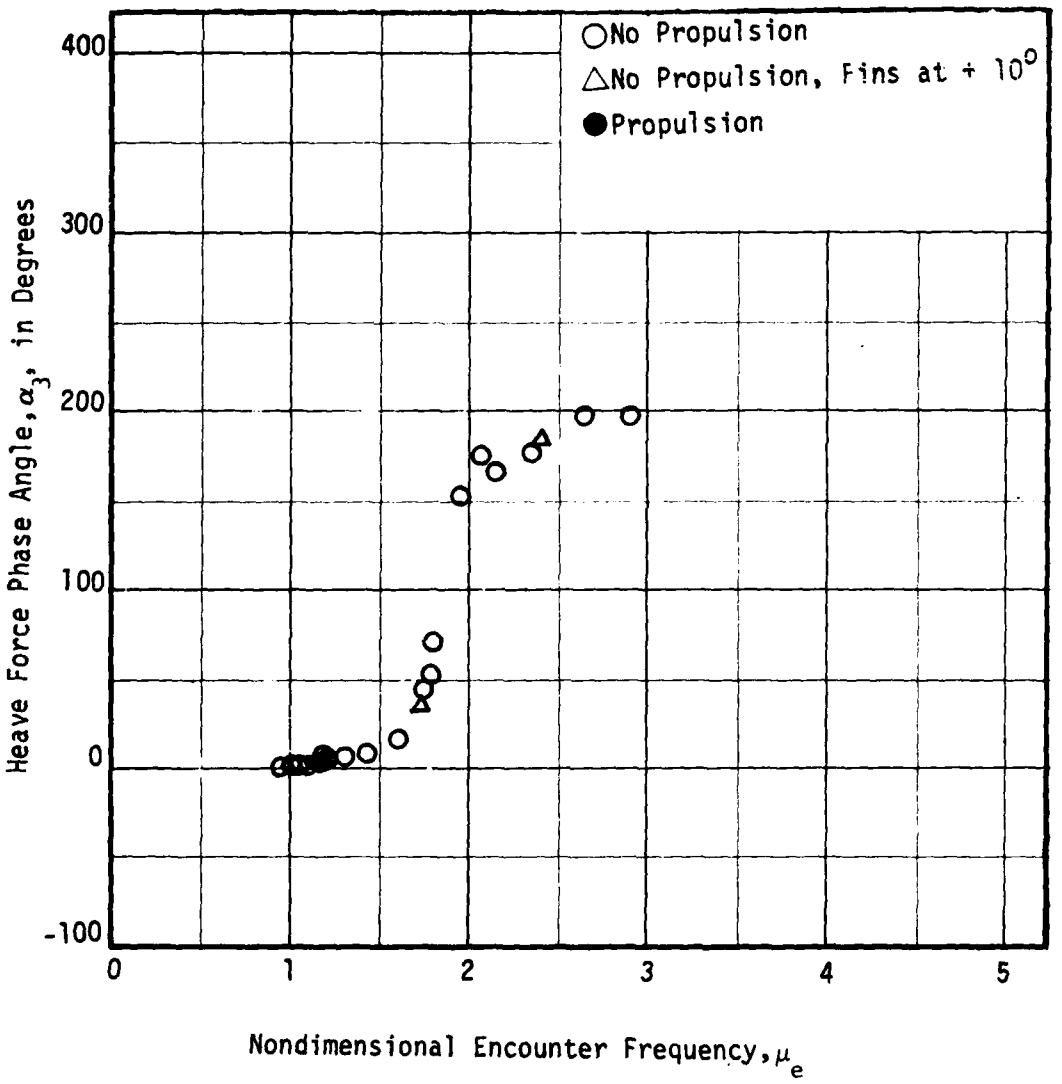

Figure 18 - Variation of Heave Force Phase Angle, α_3, with Nondimensional Encounter Frequency, μ_e, at Zero Speed for the SWATH 6D in Head Waves

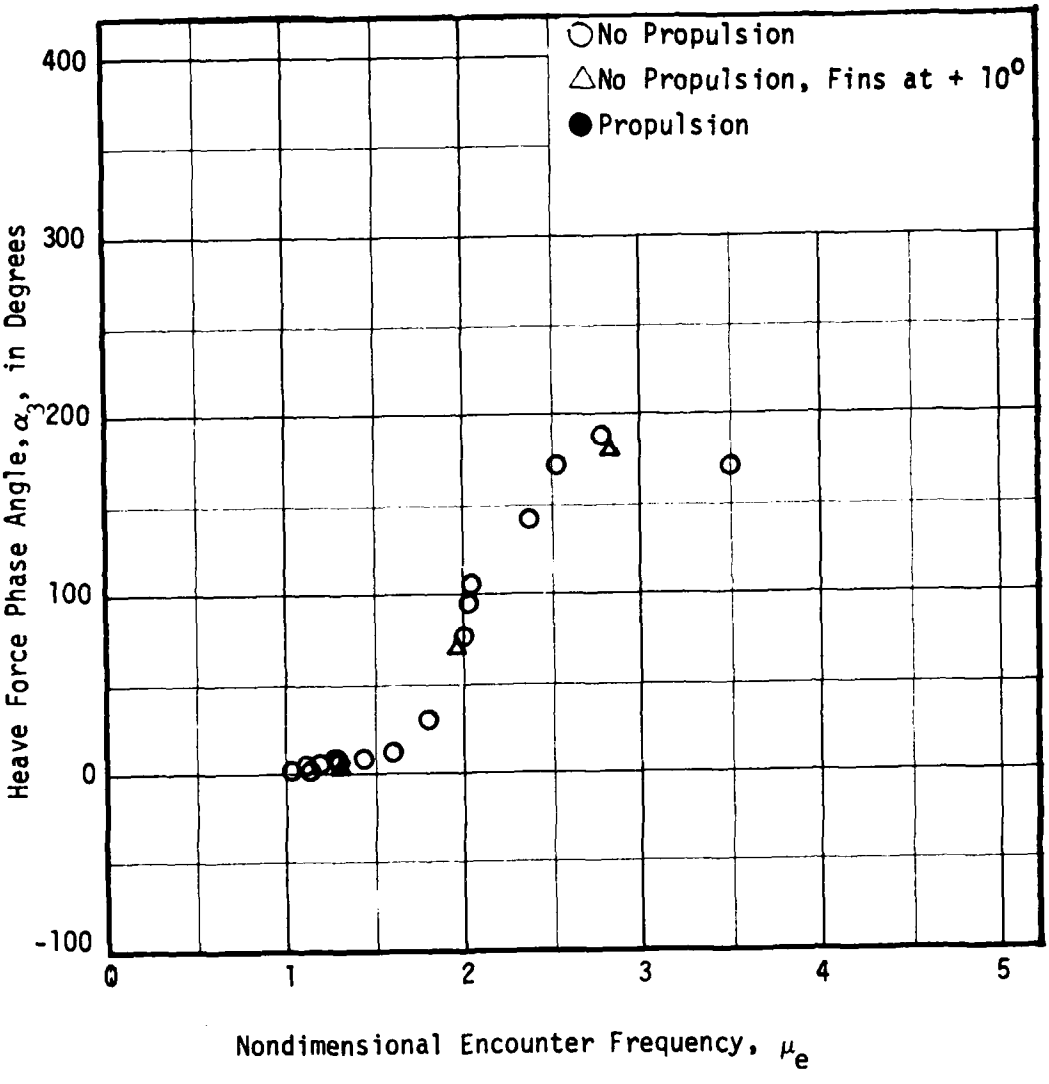

Figure 19 - Variation of Heave Force Phase Angle, α_3, with Nondimensional Encounter Frequency, μ_e, at a Full Scale Speed of 4 Knots for the SWATH 6D in Head Waves

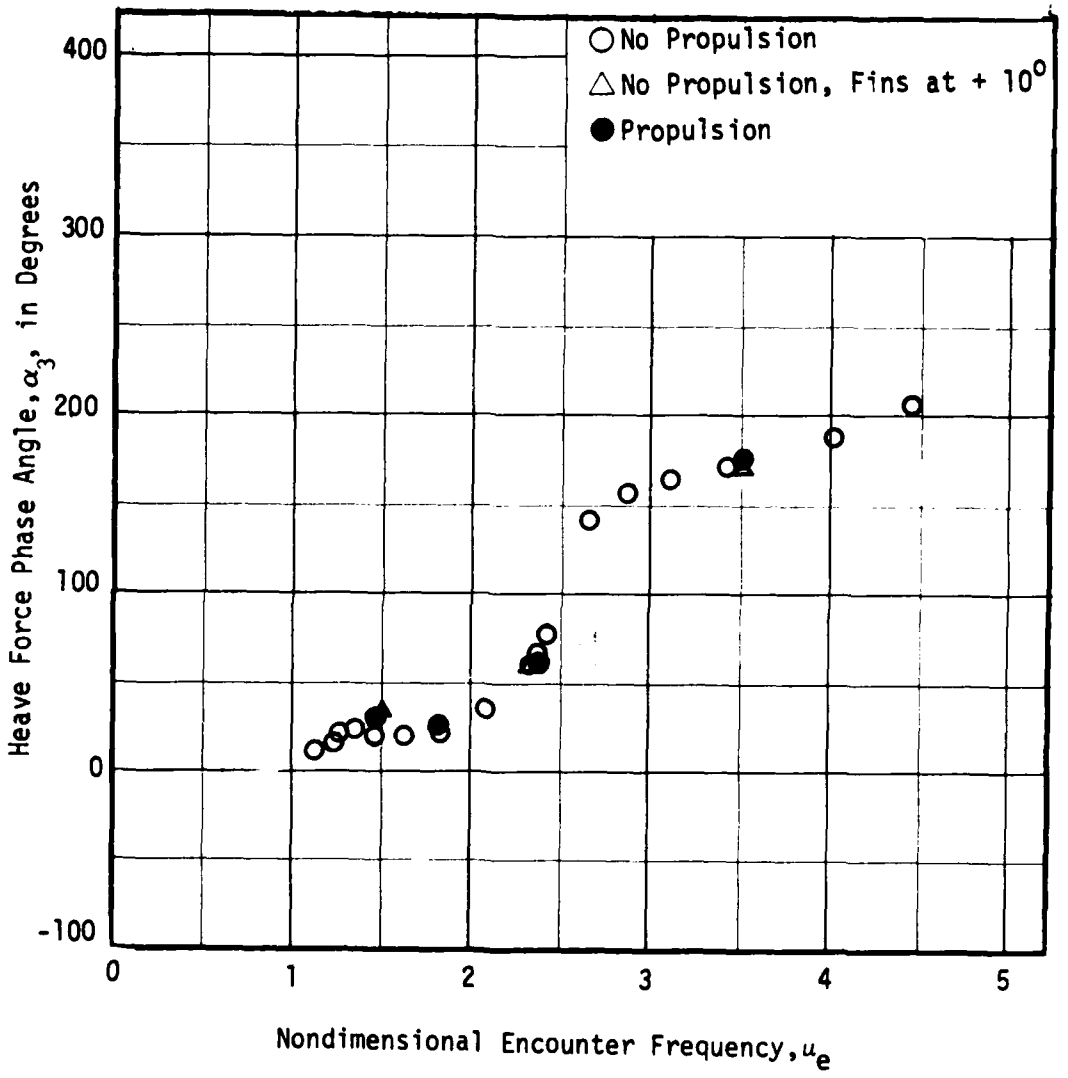

Figure 20 - Variation of Heave Force Phase Angle, α_3, with Nondimensional Encounter Frequency, μ_e, at a Full Scale Speed of 10 Knots for the SWATH 5D in Head Waves

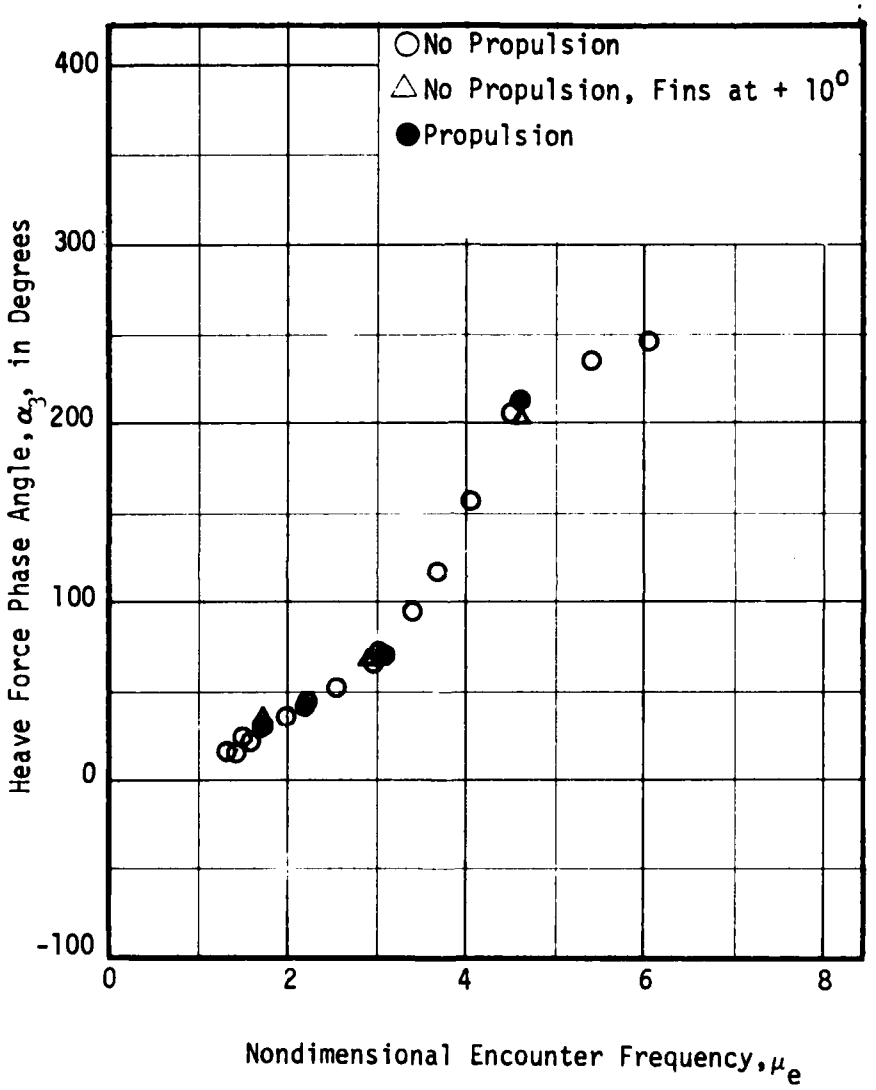

Figure 21 - Variation of Heave Force Phase Angle, α_3, with Nondimensional Encounter Frequency, μ_e, at a Full Scale Speed of 20 Knots for the SWATH 6D in Head Waves

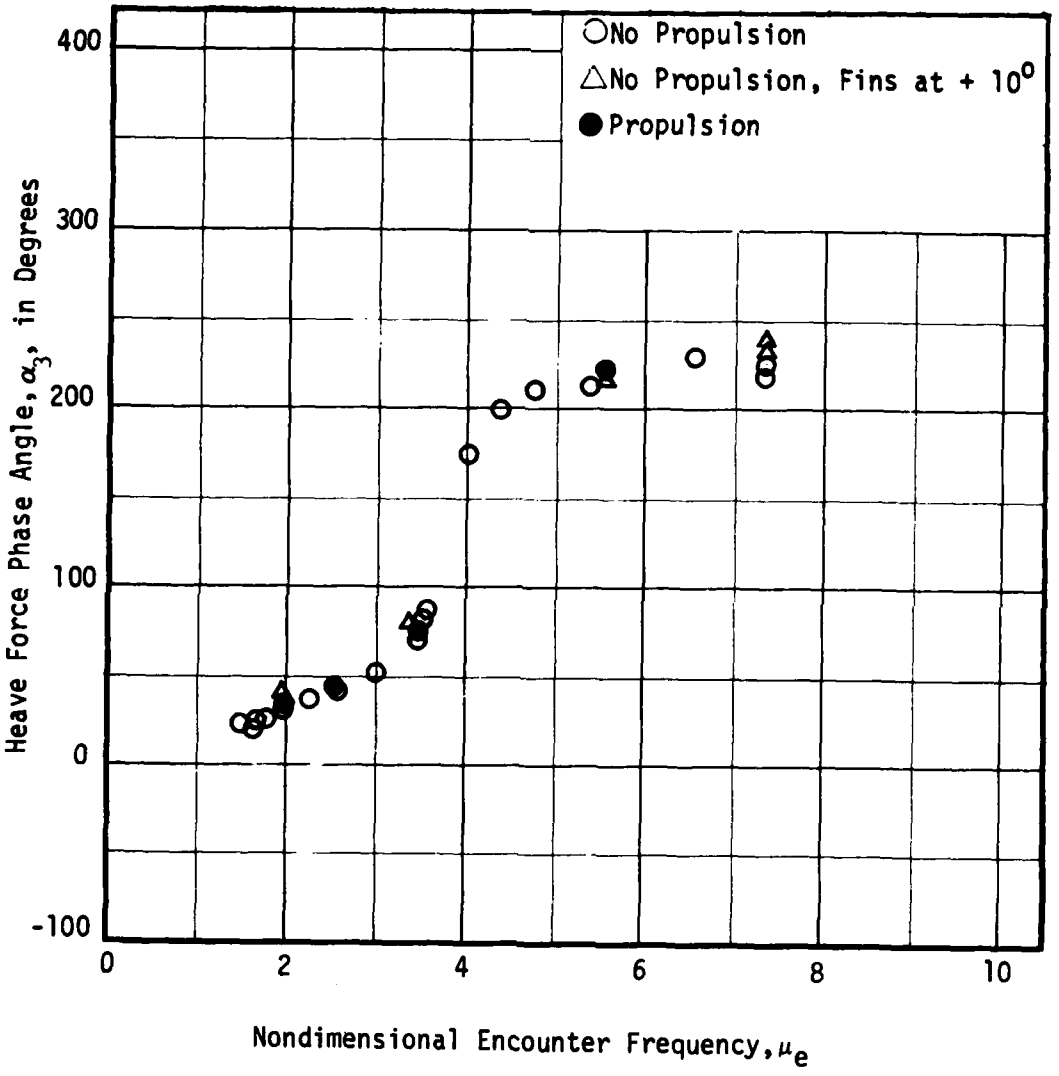

Figure 22 - Variation of Heave Force Phase Angle, α_3, with Nondimensional Encounter Frequency, μ_e, at a Full Scale Speed of 28 Knots for the SWATH 6D in Head Waves

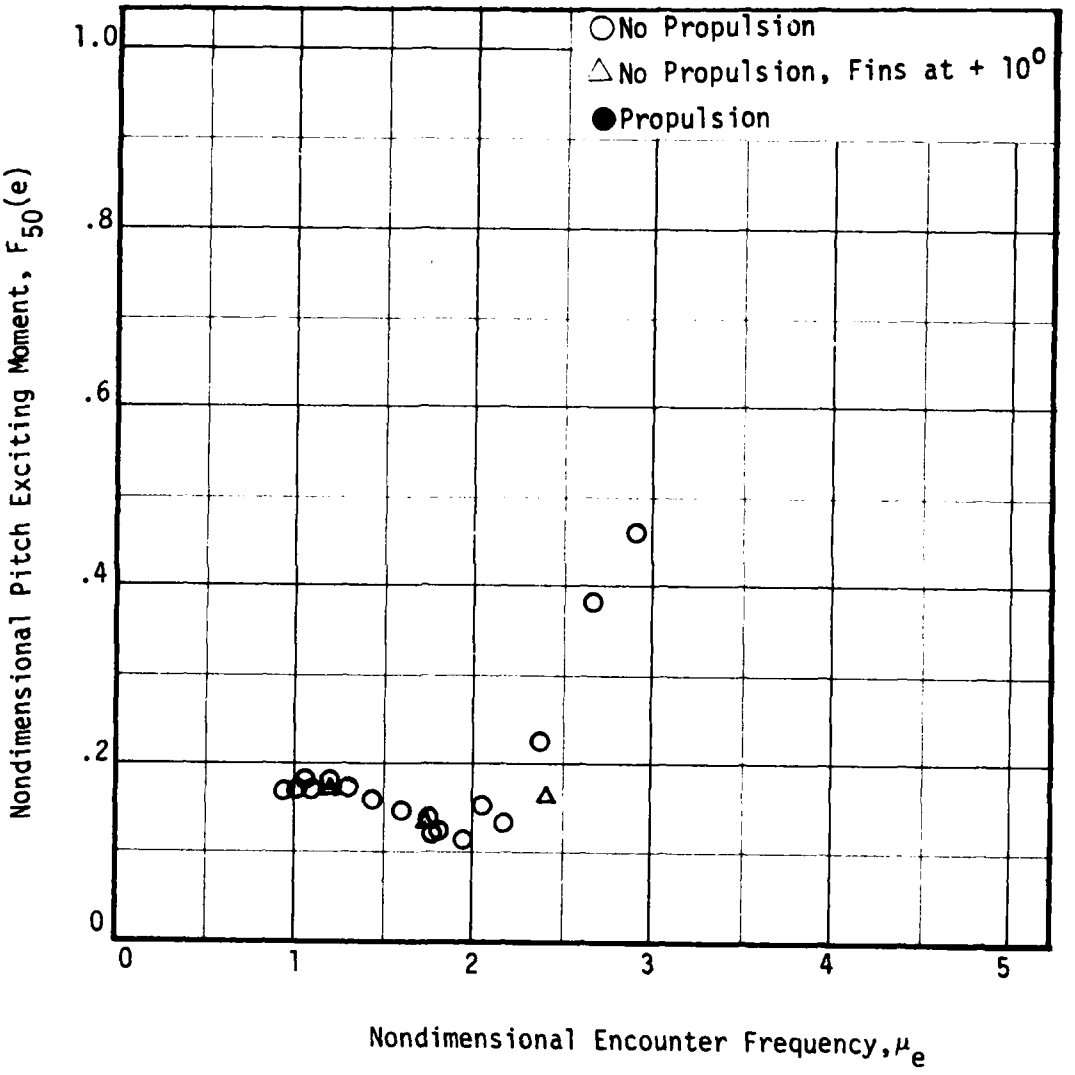

Figure 23 - Variations of Nondimensional Pitch Exciting Moment, $F_{50}(e)$, with Nondimensional Encounter Frequency, μ_e, at Zero Speed for the SWATH 6D in Head Waves

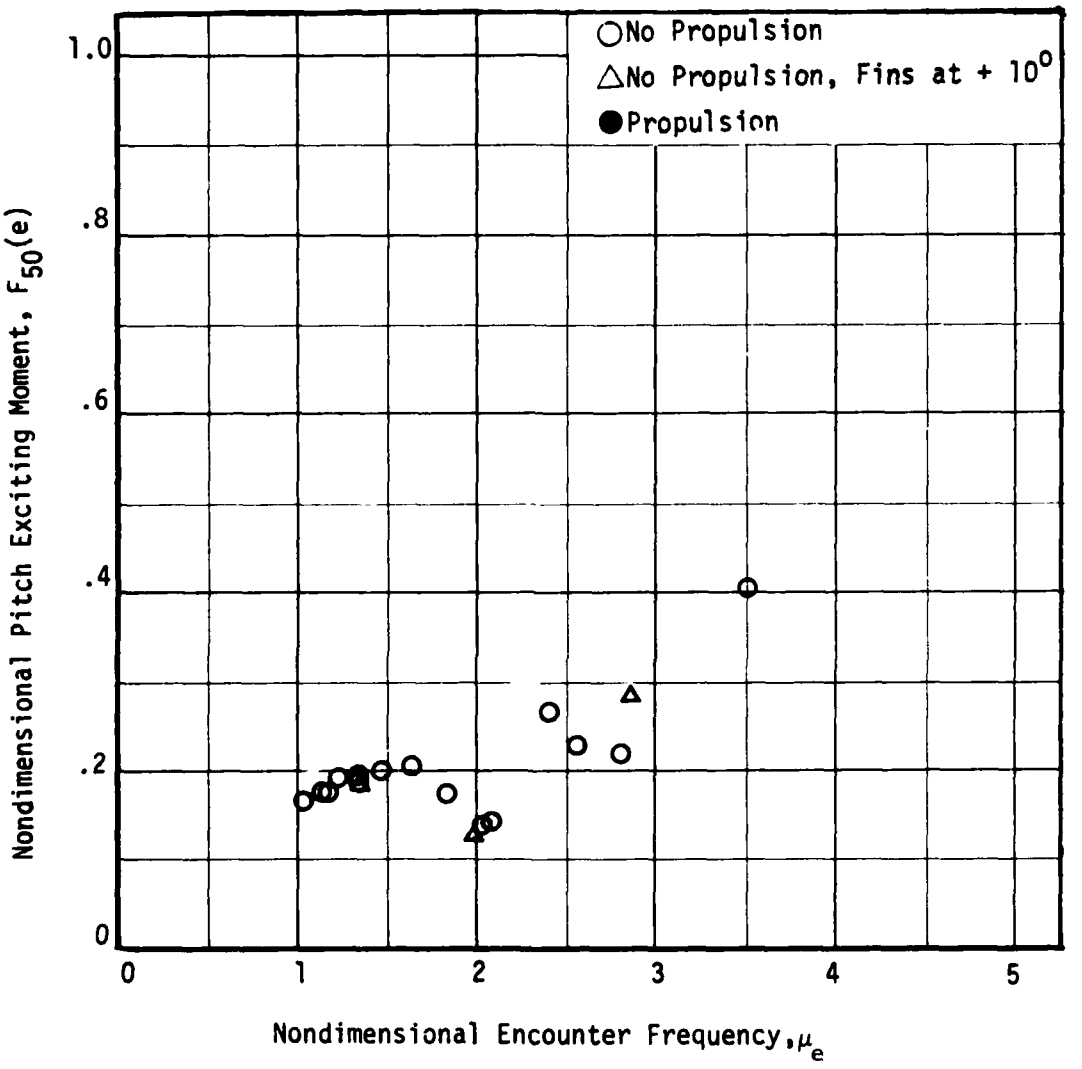

Figure 24 - Variation of Nondimensional Pitch Exciting Moment, $F_{50}(e)$, with Nondimensional Encounter Frequency, μ_e, at a Full Scale Speed of 4 Knots for the SWATH 6D in Head Waves

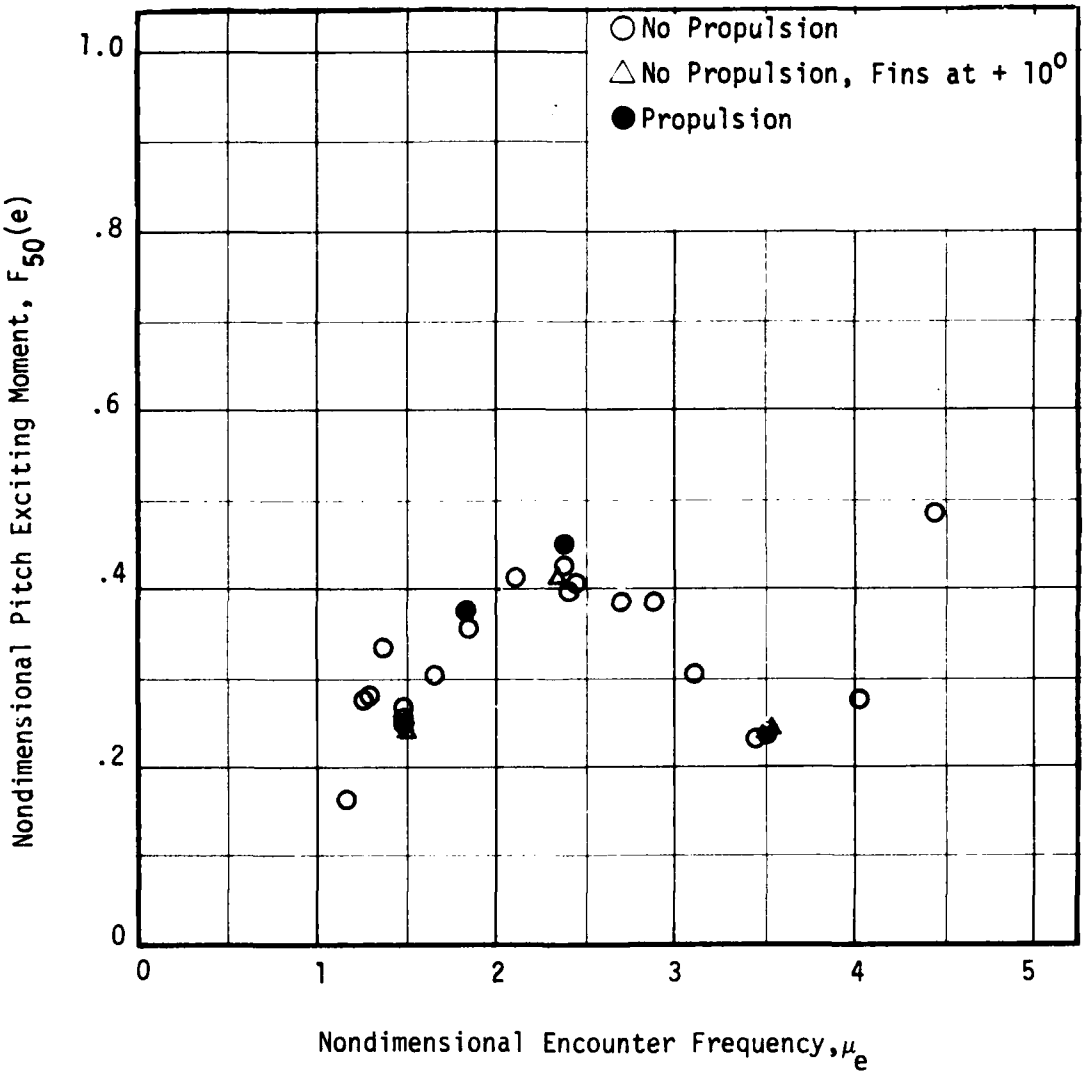

Figure 25 - Variation of Nondimensional Pitch Exciting Moment, $F_{50}(e)$, with Nondimensional Encounter Frequency, μ_e, at a Full Scale Speed of 10 Knots for the SWATH 6D in Head Waves

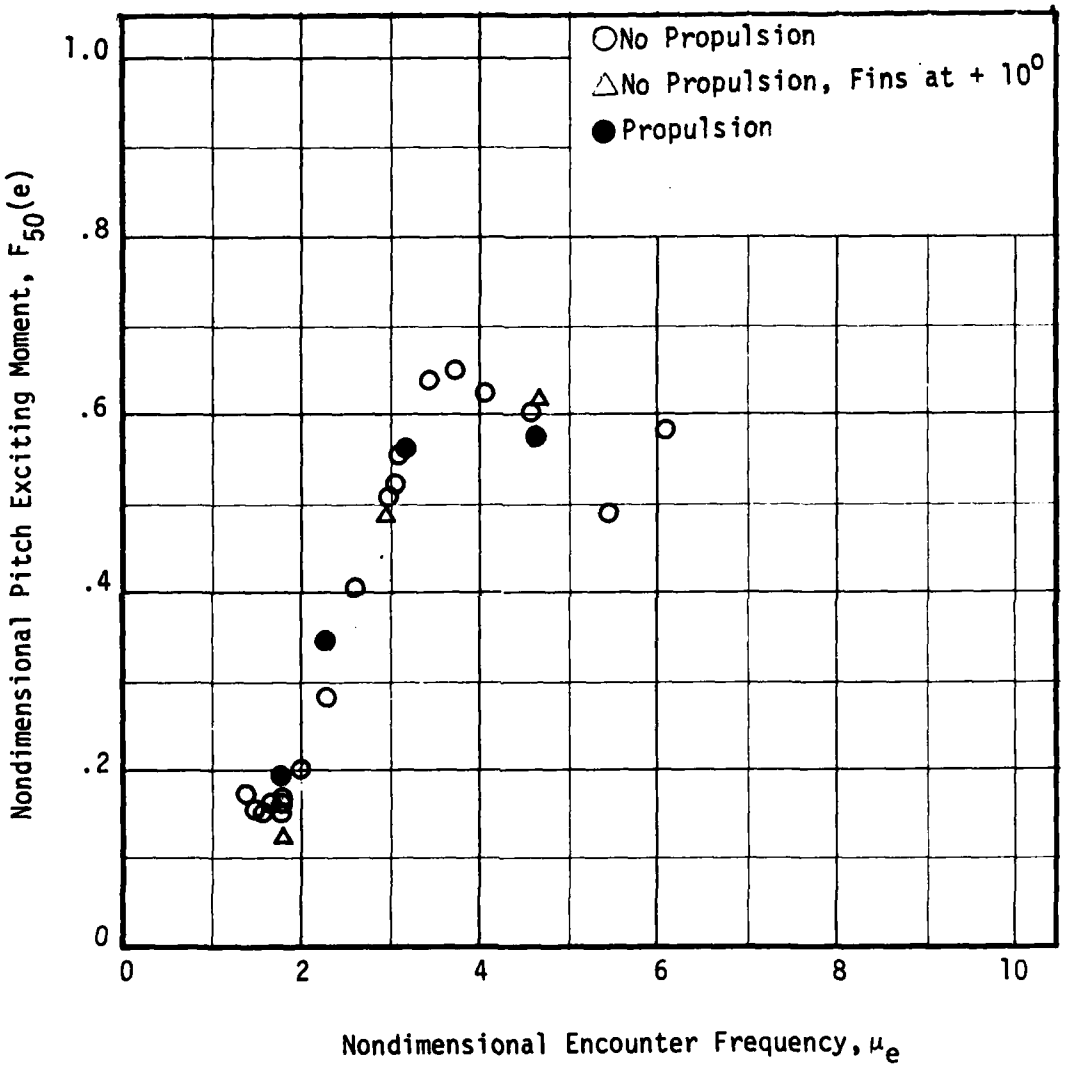

Figure 26 - Variation of Nondimensional Pitch Exciting Moment, $F_{50}(e)$, with Nondimensional Encounter Frequency, μ_e, at a Full Scale Speed of 20 Knots for the SWATH 6D in Head Waves

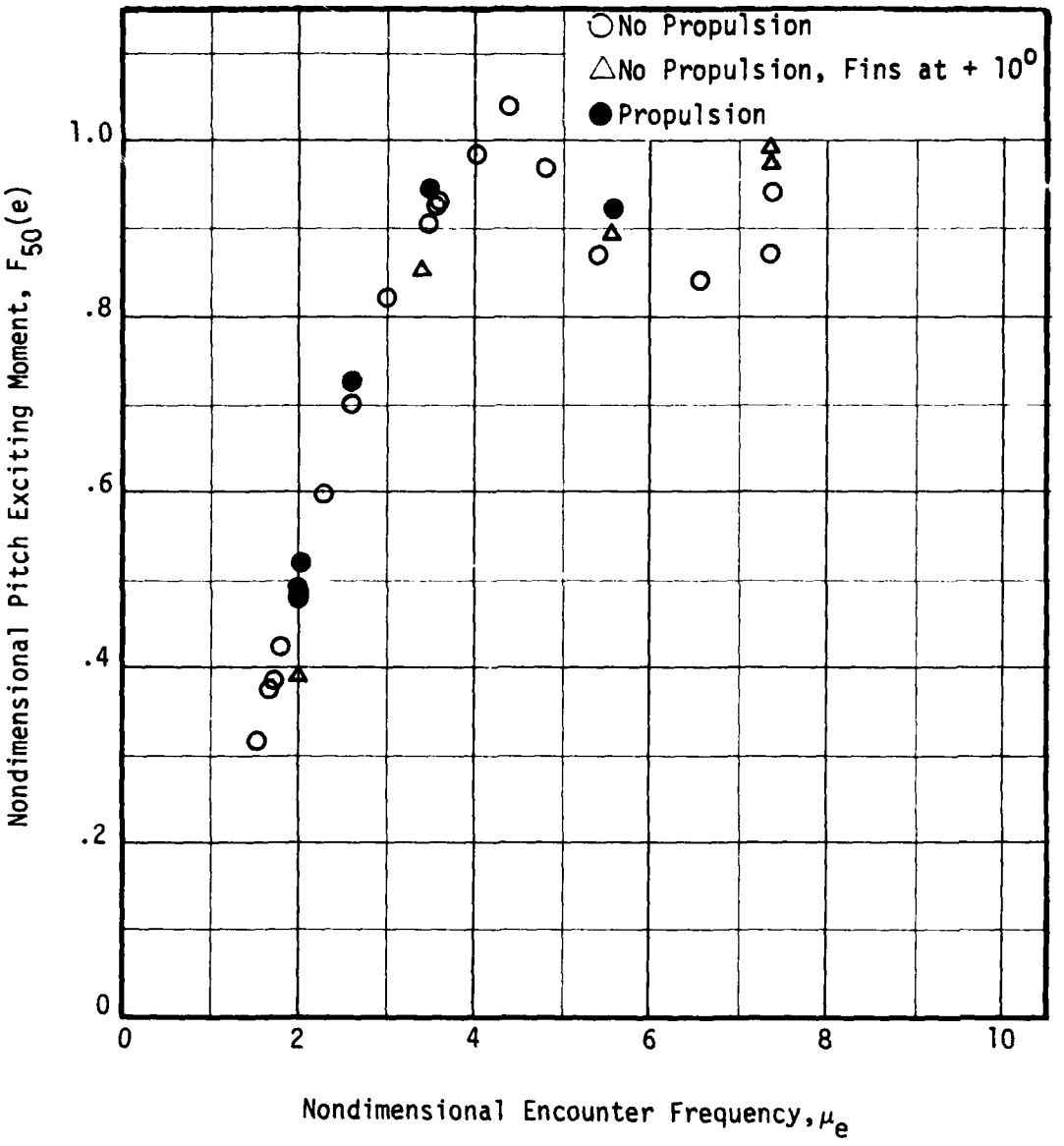

Figure 27 - Variation of Nondimensional Pitch Exciting Moment, $F_{50}(e)$, with Nondimensional Encounter Frequency, μ_e, at a Full Scale Speed of 28 Knots for the SWATH 6D in Head Waves

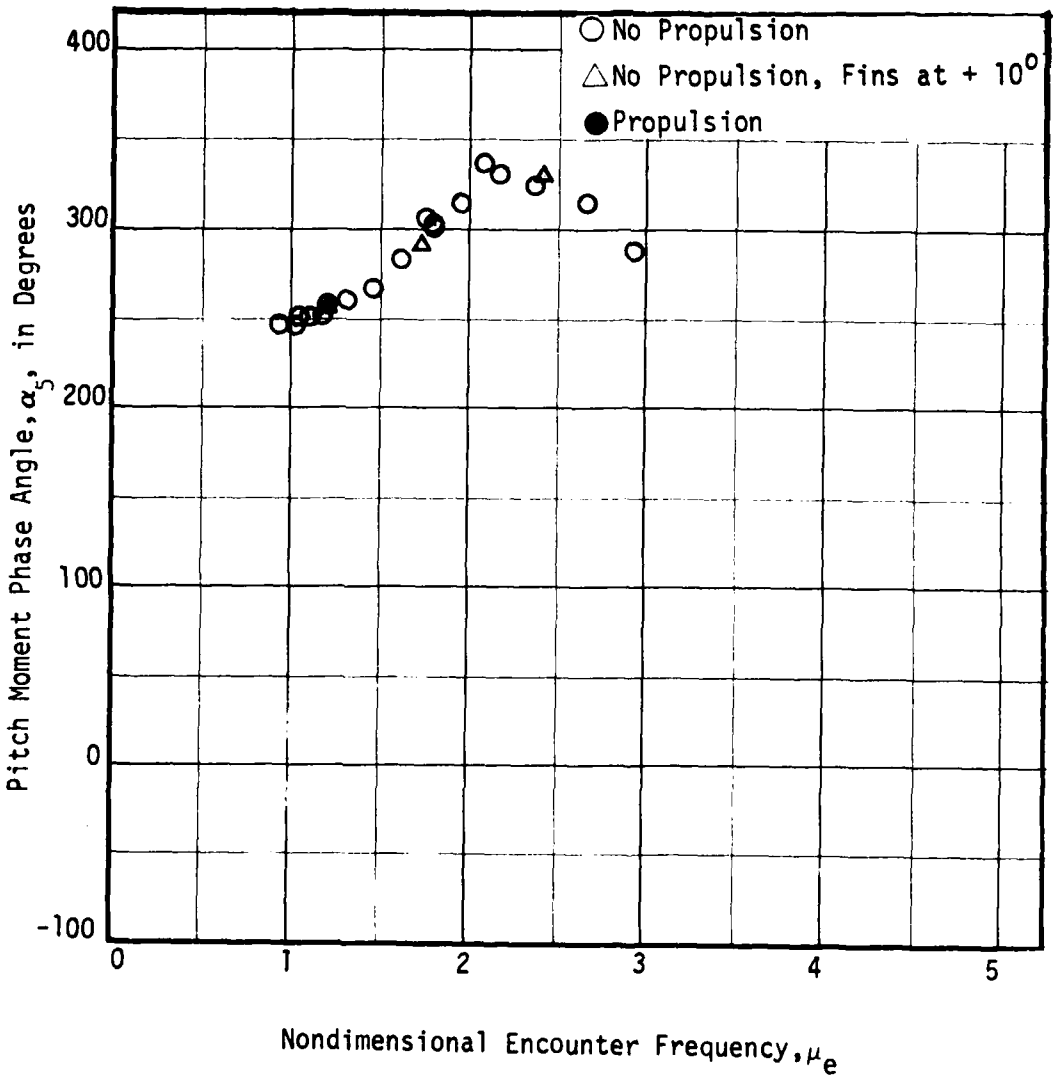

Figure 28 - Variation of Pitch Moment Phase Angle, α_5, with Nondimensional Encounter Frequency, μ_e, at Zero Speed for the SWATH 6D in Head Waves

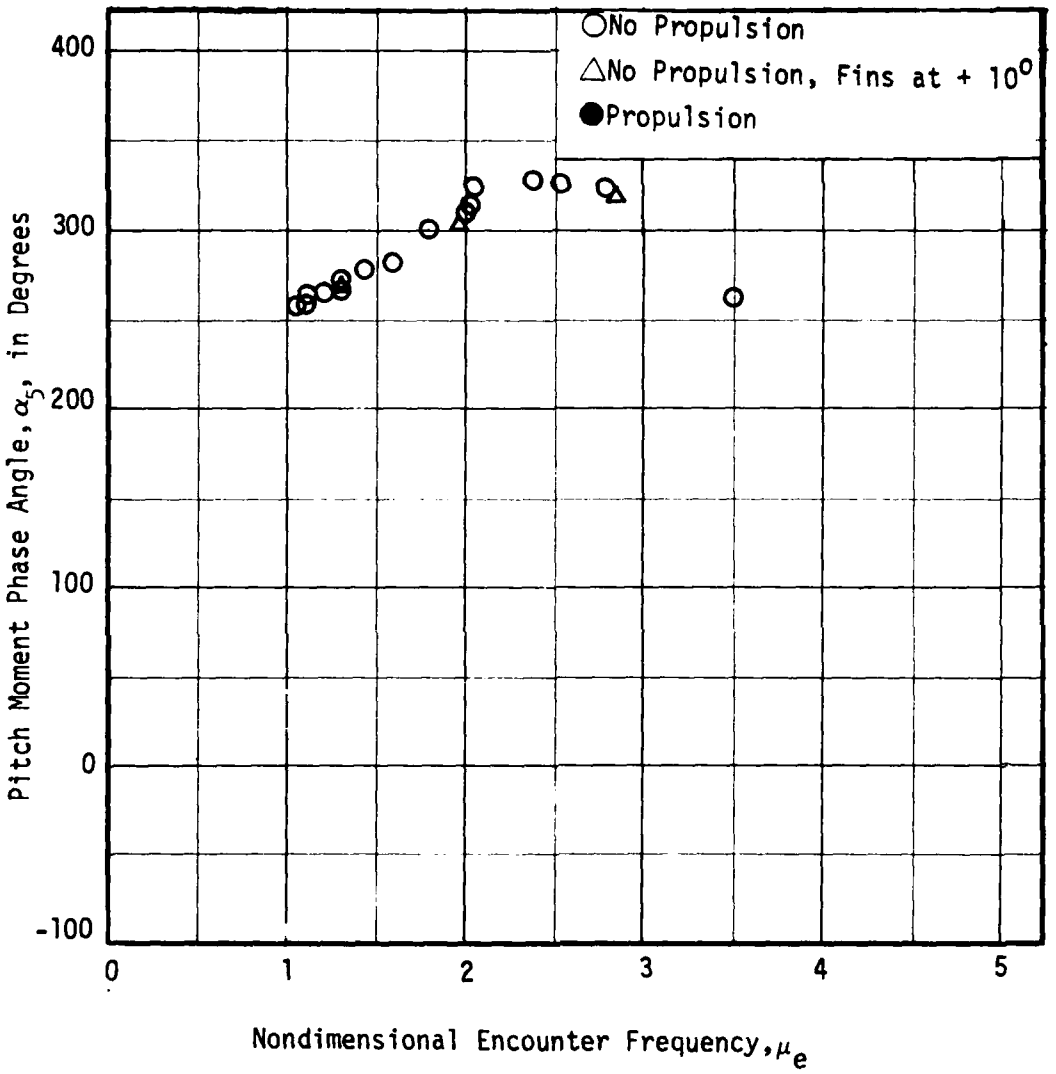

Figure 29 - Variation of Pitch Moment Phase Angle, α_5, with Nondimensional Encounter Frequency, μ_e, at a Full Scale Speed of 4 Knots for the SWATH 6D in Head Waves

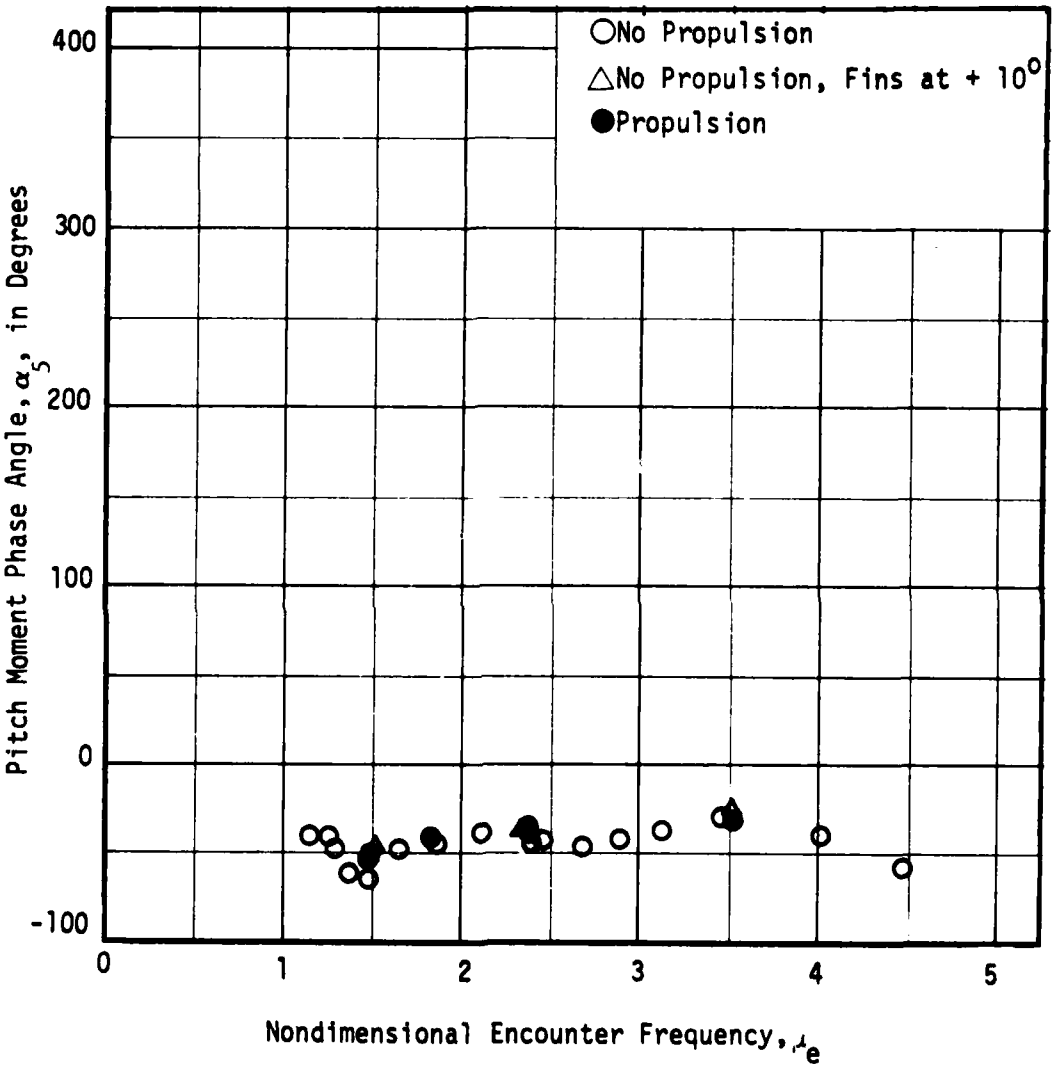

Figure 30 - Variation of Pitch Moment Phase Angle, $\alpha 5$, with Nondimensional Encounter Frequency, μ_e, at a Full Scale Speed of 10 knots for the SWATH 6D in Head Waves.

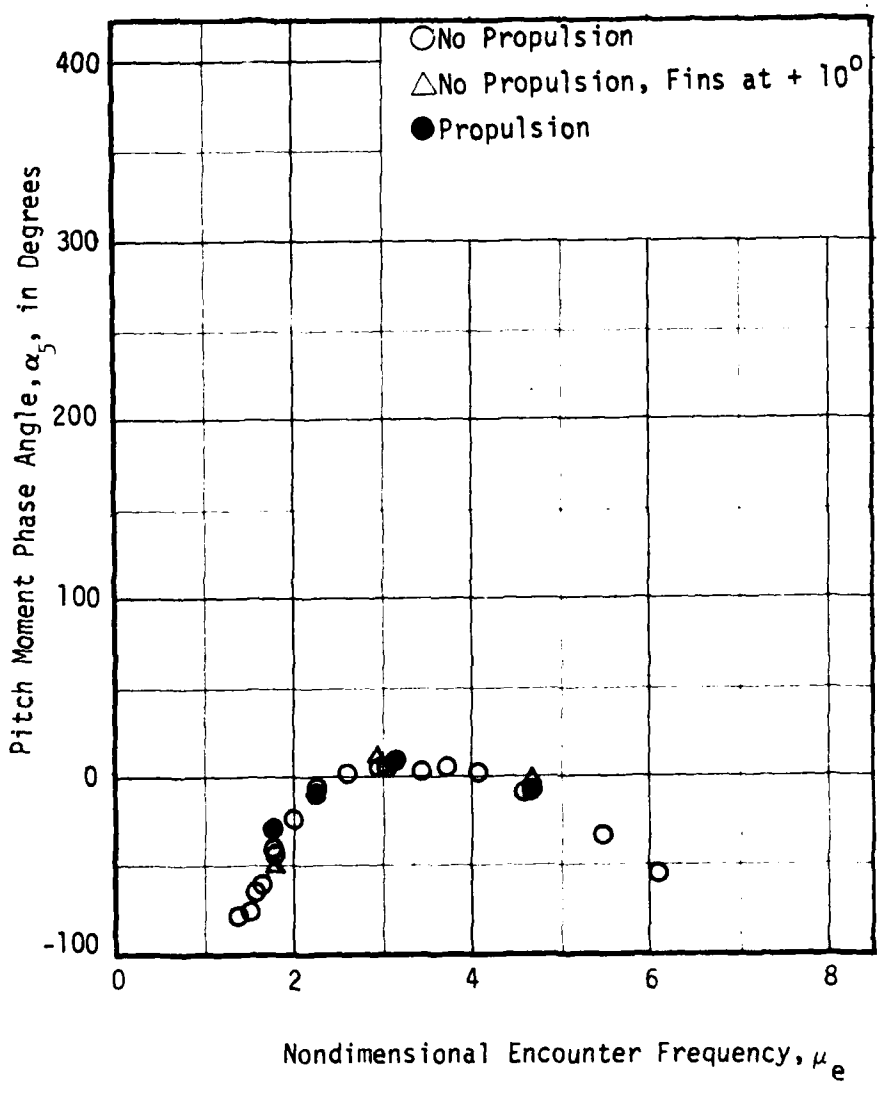

Figure 31 - Variation of Pitch Moment Phase Angle, α_5, with Nondimensional Encounter Frequency, μ_e, at a Full Scale Speed of 20 Knots for the SWATH 6D in Head Waves

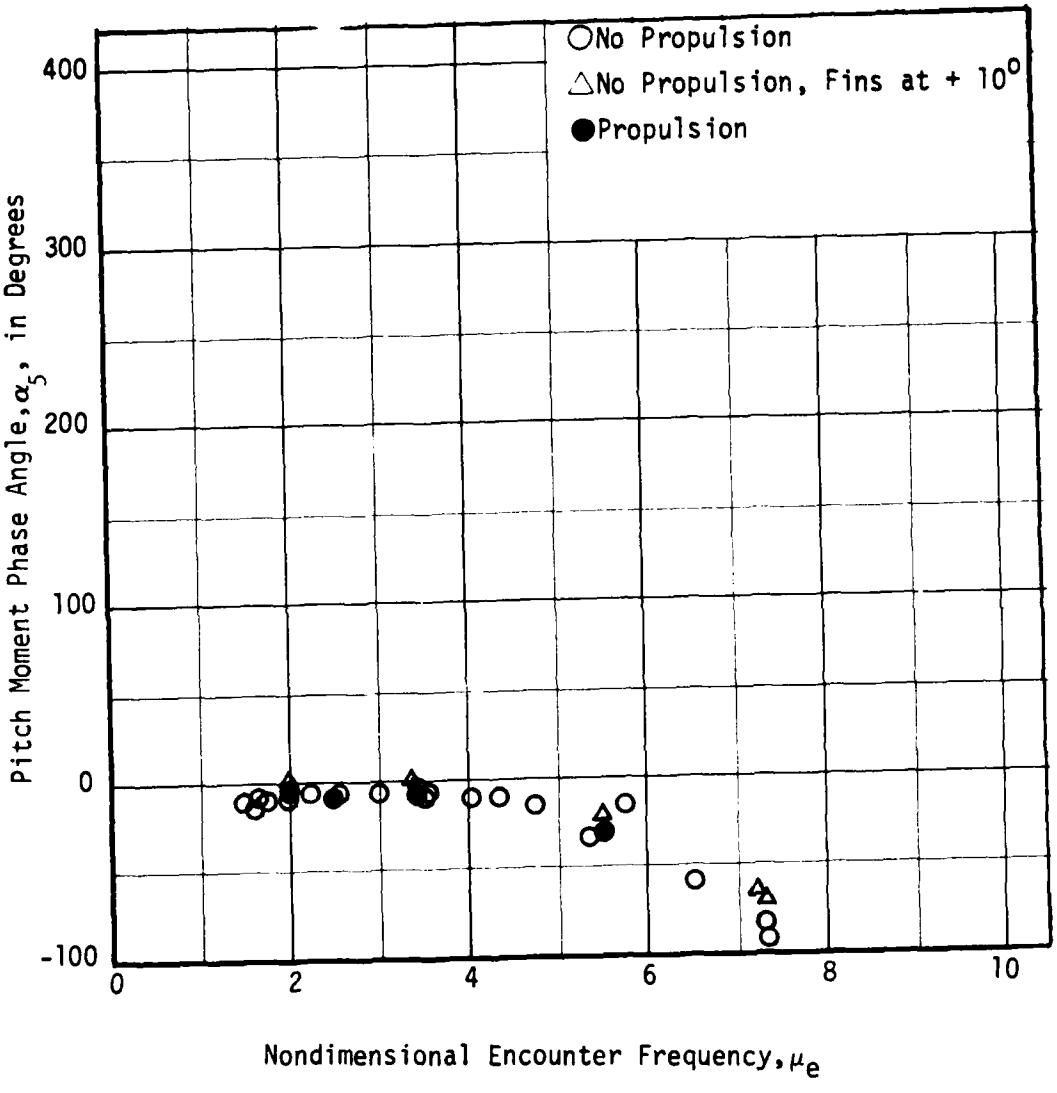

Figure 32 - Variation of Pitch Moment Phase Angle, α_5, with Nondimensional Encounter Frequency, μ_e, at a Full Scale Speed of 28 Knots for the SWATH 6D in Head Waves

APPENDIX B

SWATH 6D FOLLOWING SEA EXCITING FORCE EXPERIMENTAL DATA

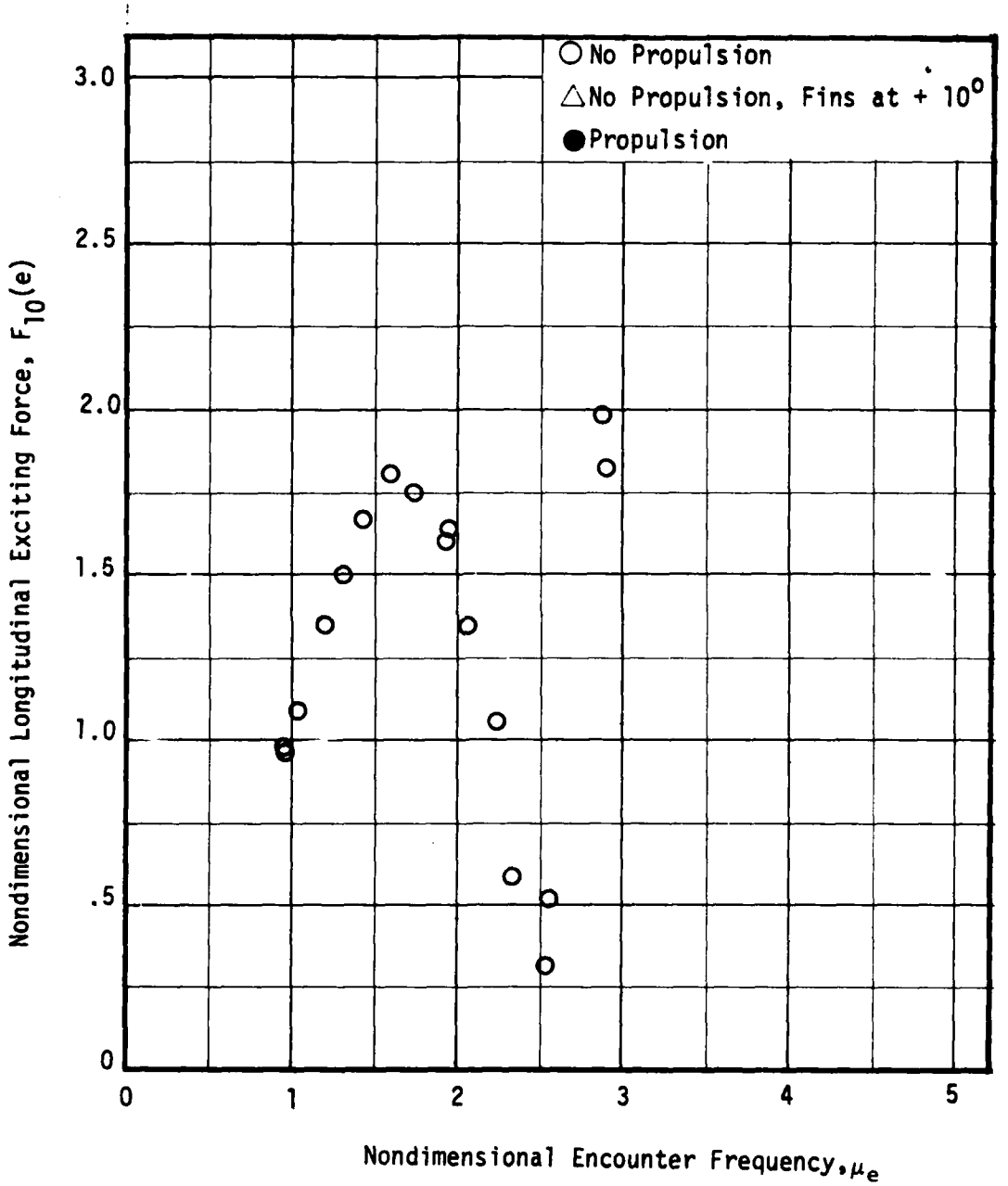

Figure 33 - Variation of Nondimensional Longitudinal Exciting Force, $F_{10}(e)$, with Nondimensional Encounter Frequency, μ_e, at Zero Speed for the SWATH 6D in Following Waves

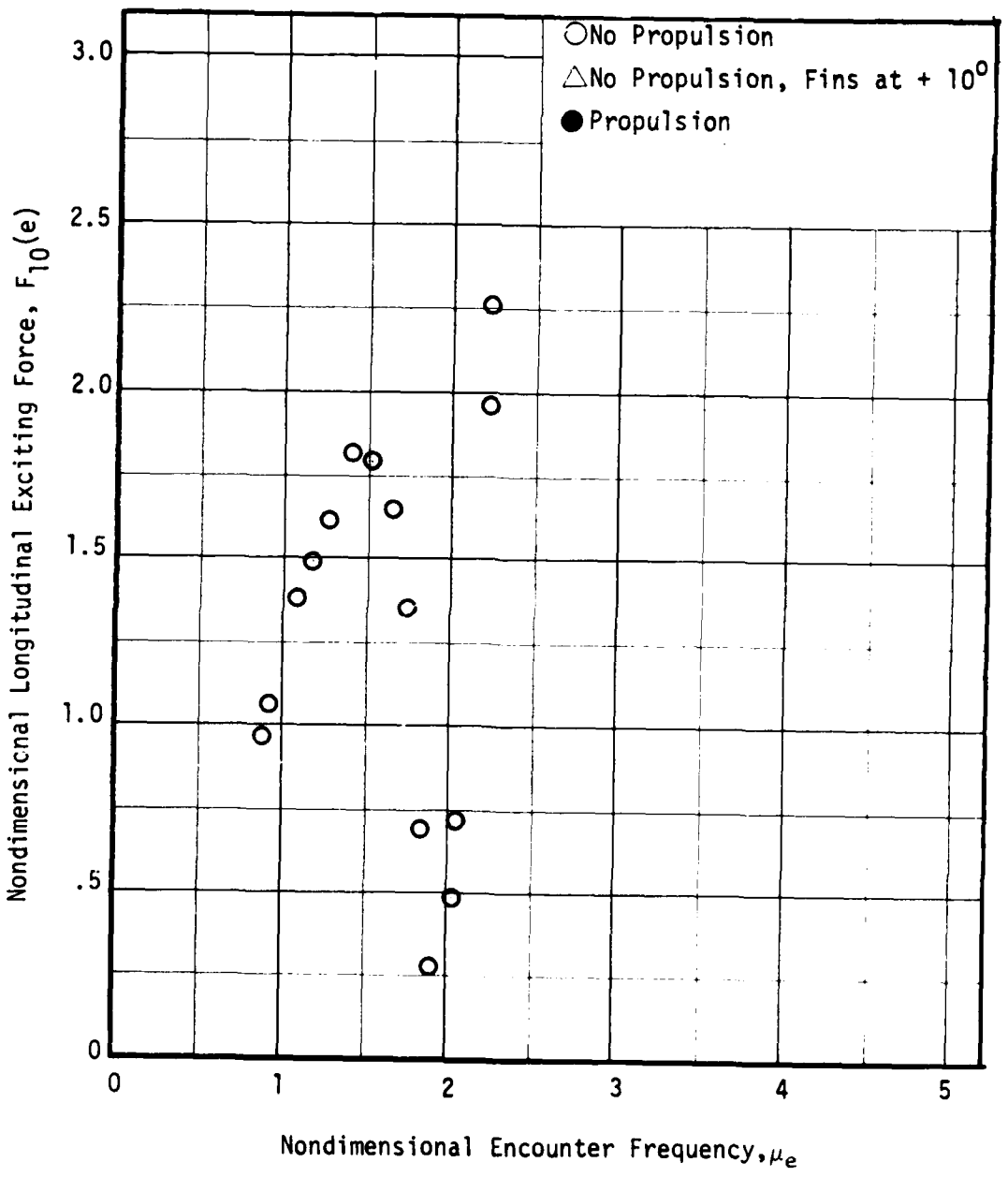

Figure 34 - Variation of Nondimensional Longitudinal Exciting Force, $F_{10}(e)$, with Nondimensional Encounter Frequency, μ_e, at a Full Scale Speed of 4 Knots for the SWATH 6D in Following Waves

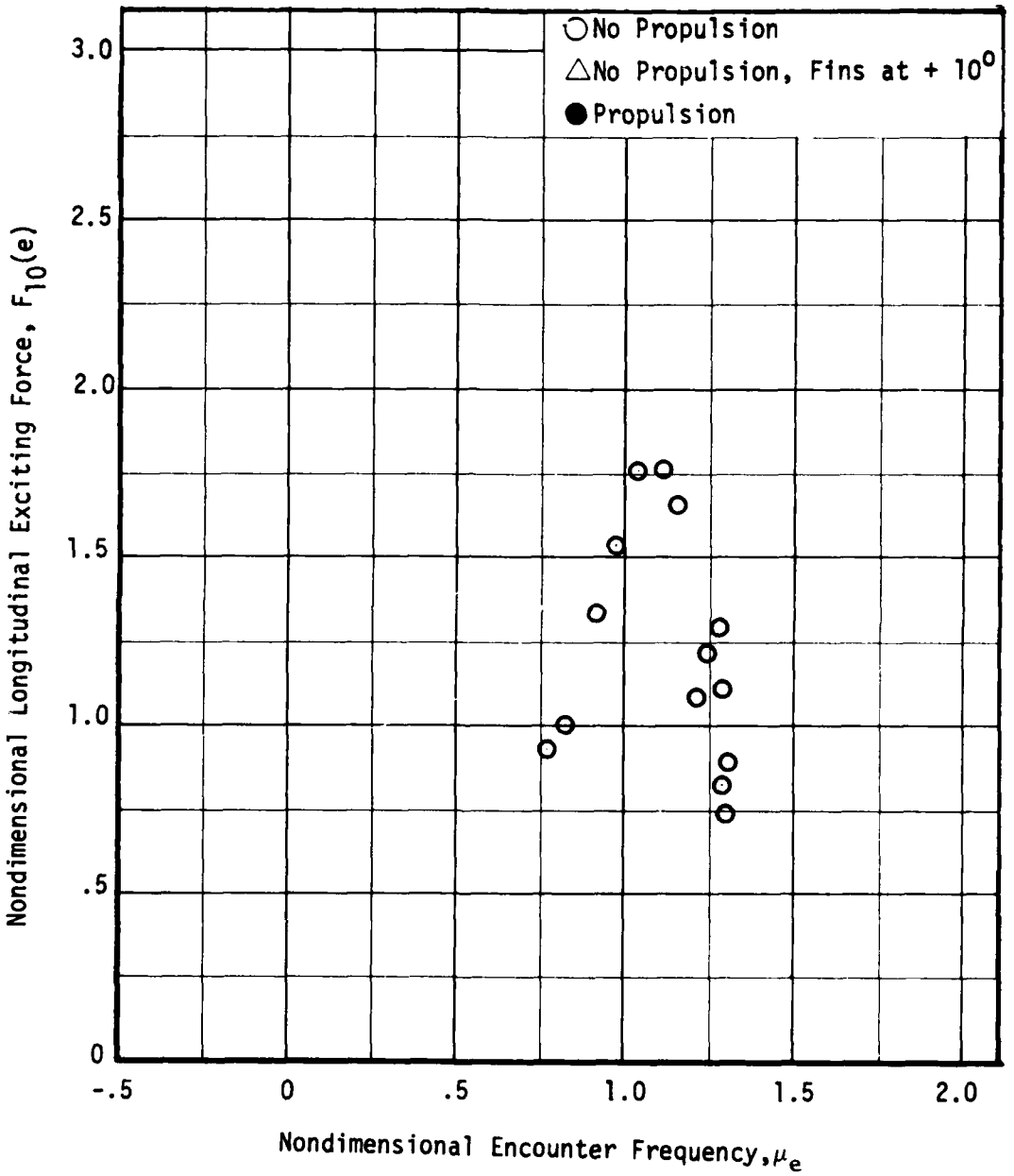

Figure 35 - Variation of Nondimensional Longitudinal Exciting Force, $F_{10}(e)$, with Nondimensional Encounter Frequency, μ_e, at a Full Scale Speed of 10 Knots for the SWATH 6D in Following Waves

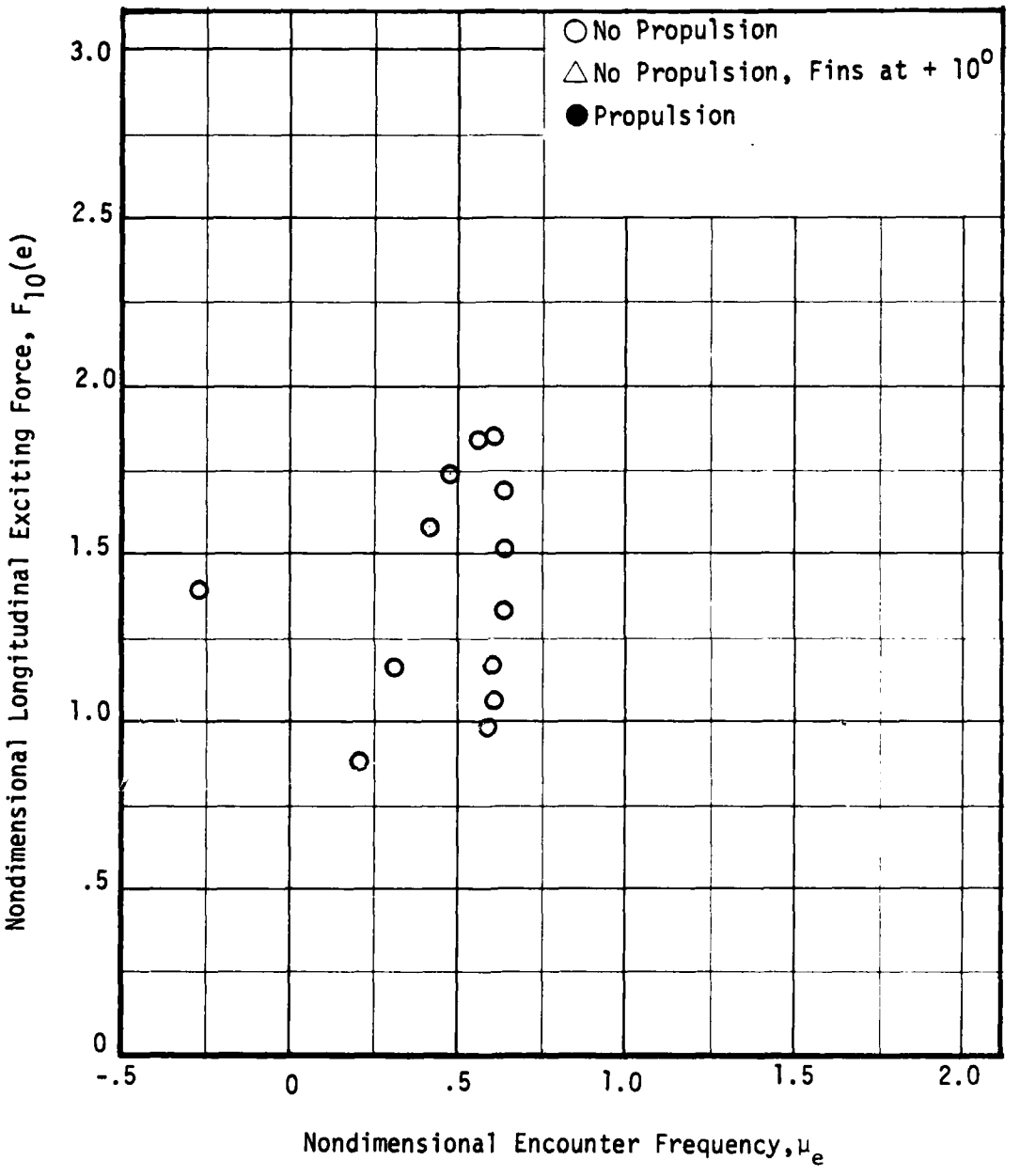

Figure 36 - Variation of Nondimensional Longitudinal Exciting Force, $F_{10}(e)$, with Nondimensional Encounter Frequency, μ_e, at a Full Scale Speed of 20 Knots for the SWATH 6D in Following Waves

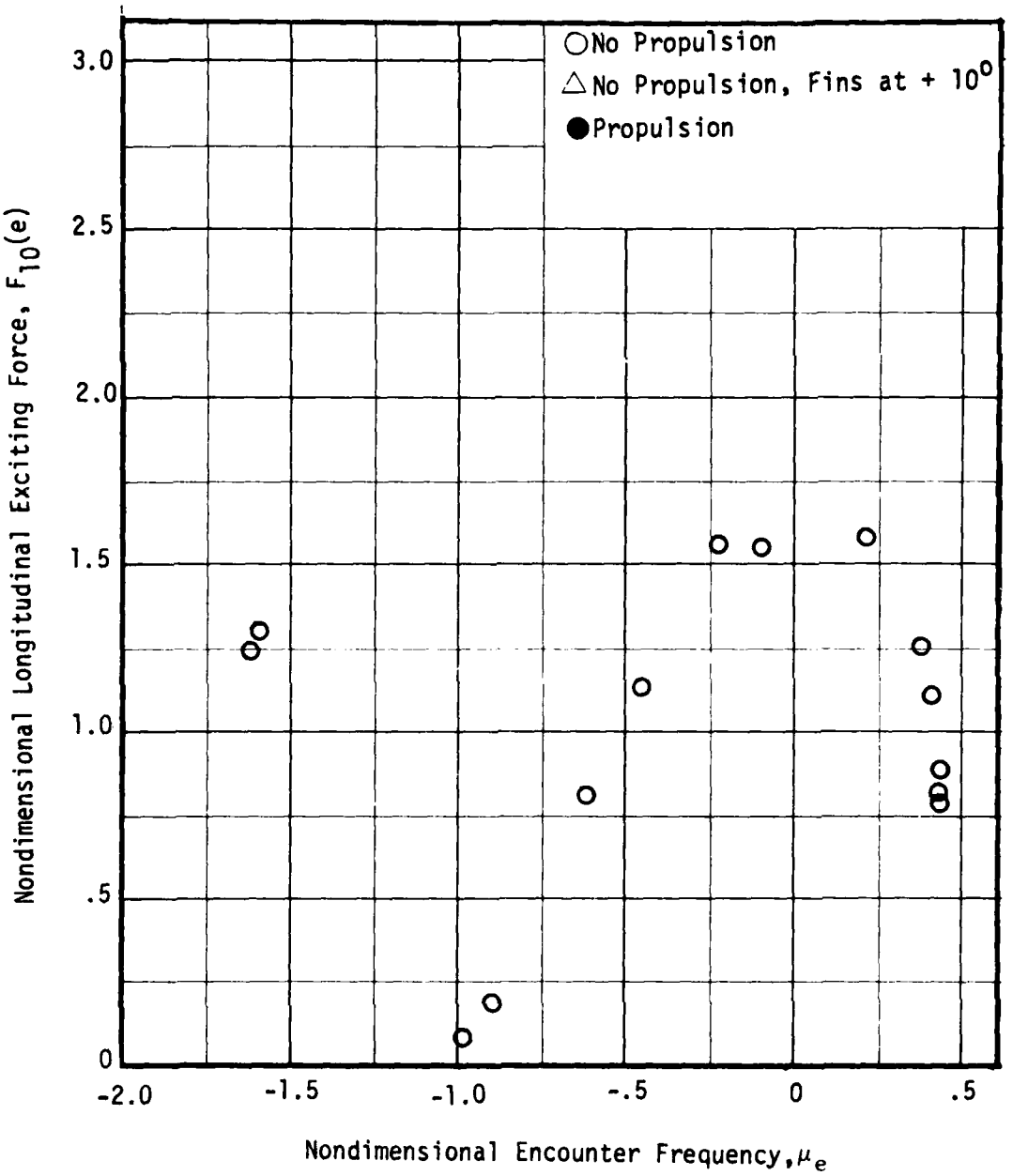

Figure 37 - Variation of Nondimensional Longitudinal Exciting Force, $F_{10}(e)$, with Nondimensional Encounter Frequency, μ_e, at a Full Scale Speed of 28 Knots for the SWATH 6D in Following Waves

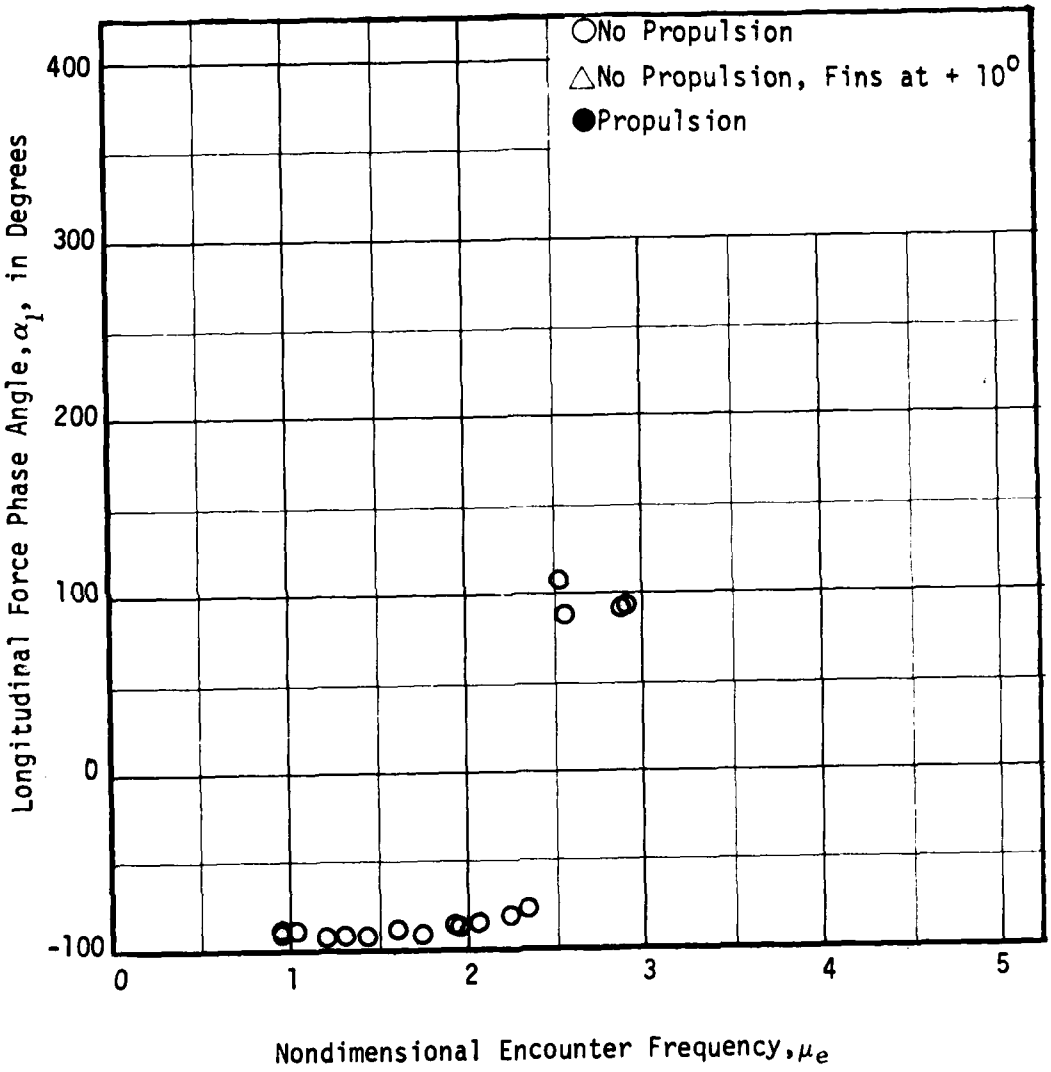

Figure 38 - Variation of Longitudinal Force Phase Angle, α_l, with Nondimensional Encounter Frequency, μ_e, at Zero Speed for the SWATH 6D in Following Waves

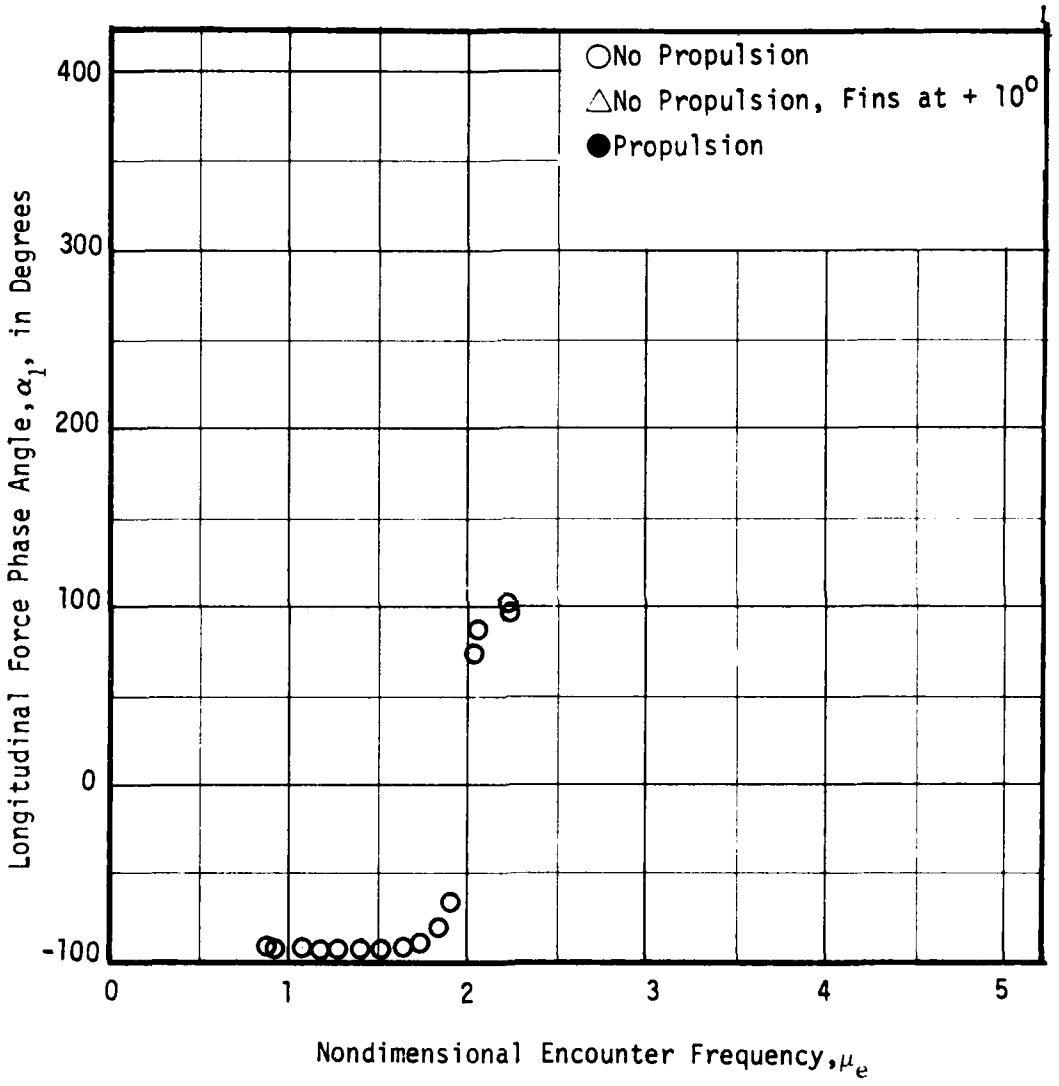

Figure 39 - Variation of Longitudinal Force Phase Angle, α_l, with Nondimensional Encounter Frequency, μ_e, at a Full Scale Speed of 4 Knots for the SWATH 6D in Following Waves

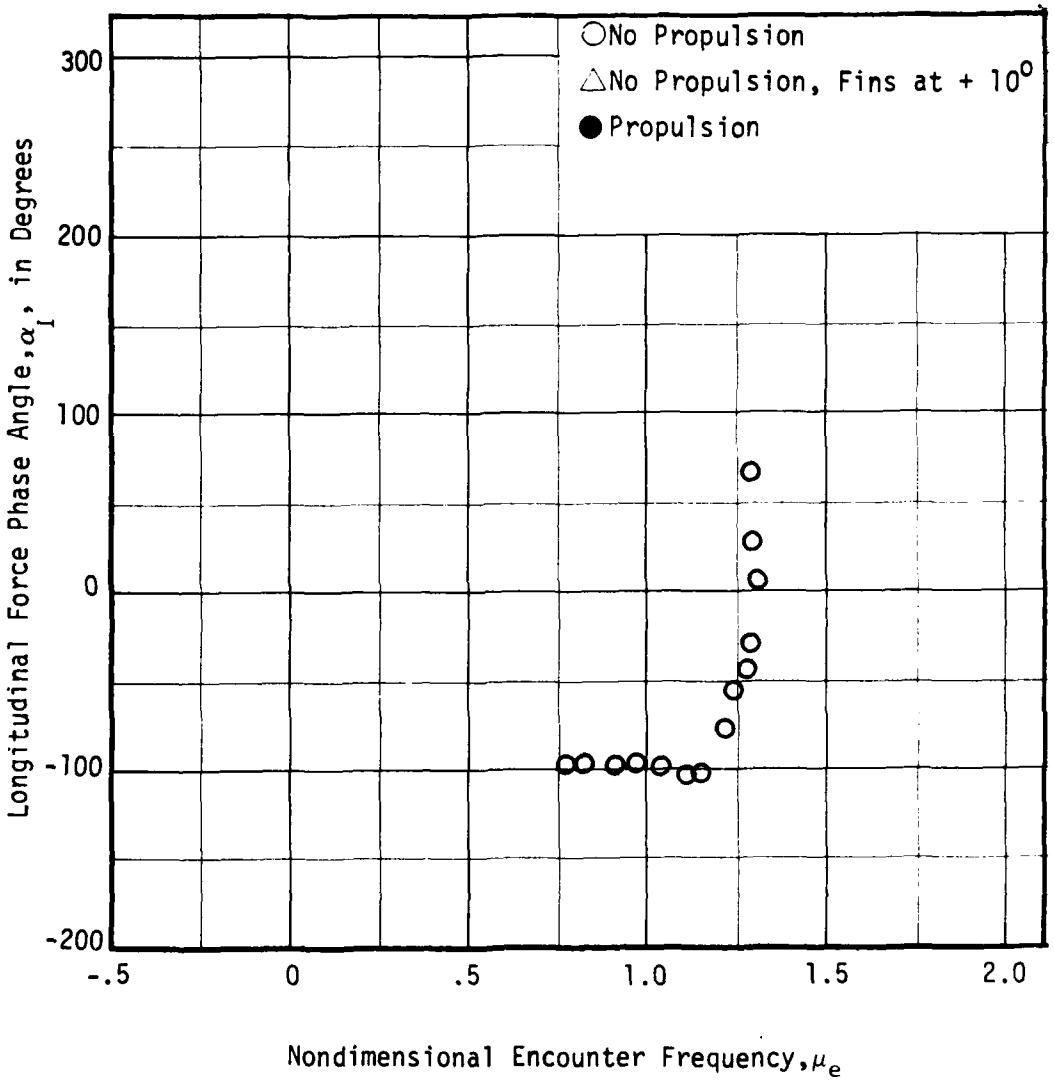

Figure 40 - Variation of Longitudinal Force Phase Angle, α_1, with Nondimensional Encounter Frequency, μ_e, at a Full Scale Speed of 10 Knots for the SWATH 6D in Following Waves

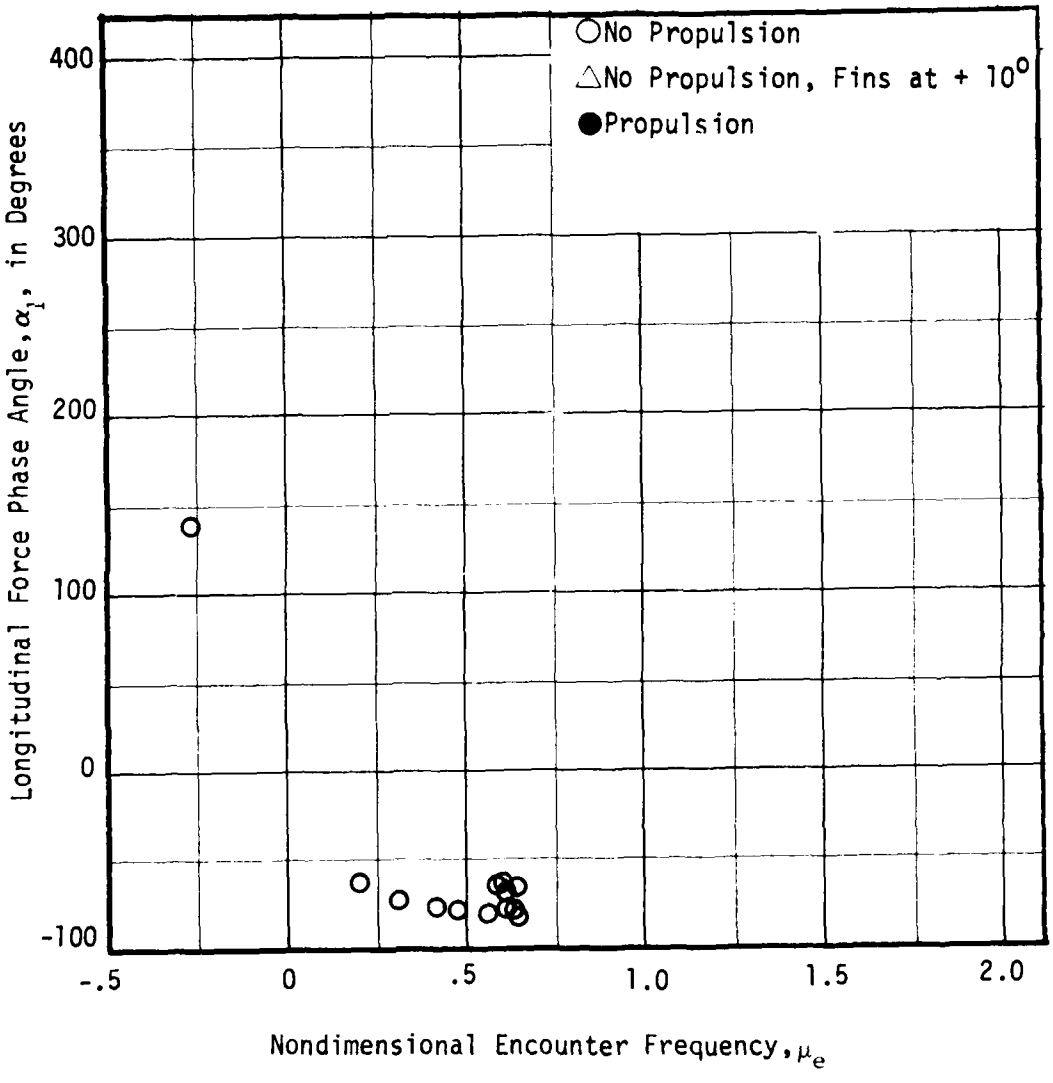

Figure 41 - Variation of Longitudinal Force Phase Angle, α_1, with Nondimensional Encounter Frequency, μ_e, at a Full Scale Speed of 20 Knots for the SWATH 6D in Following Waves

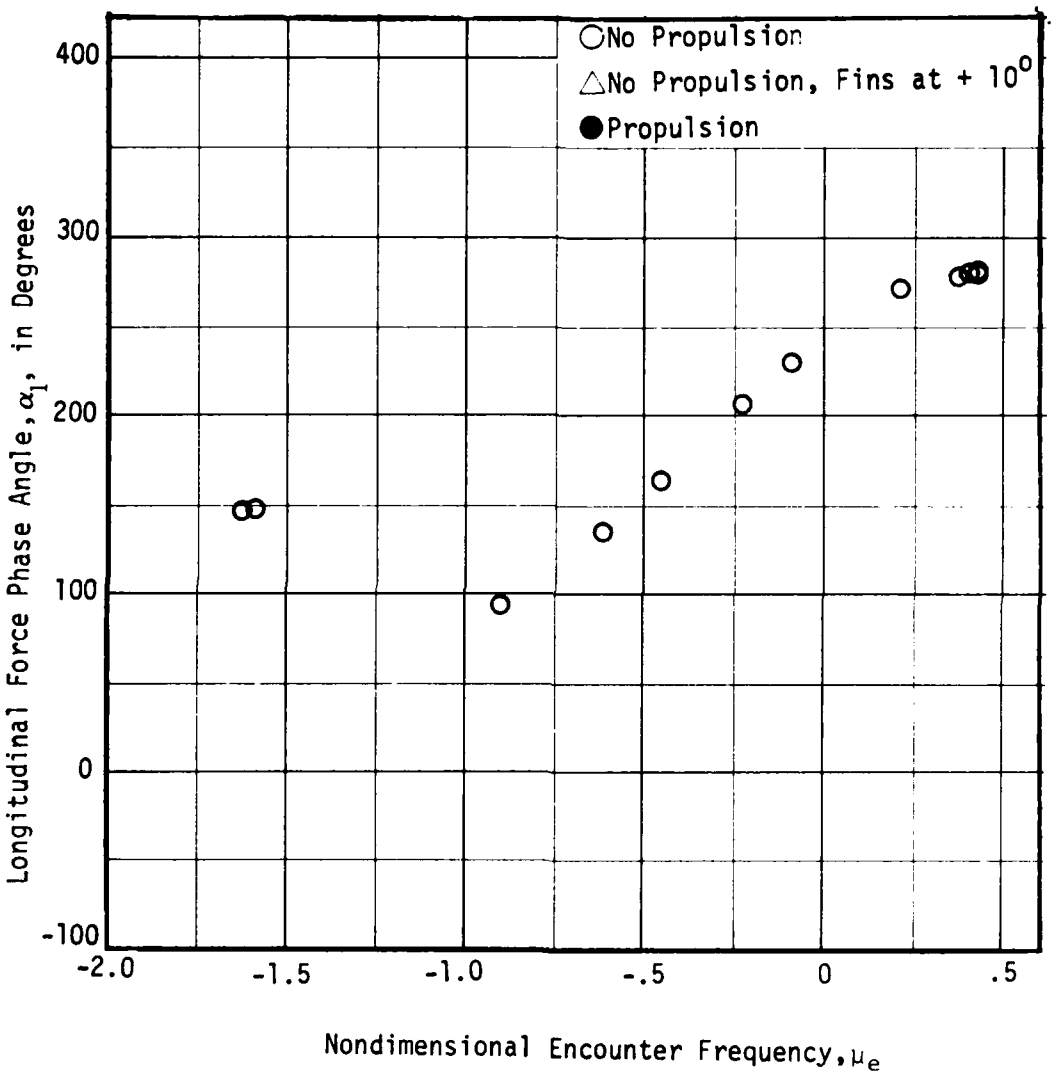

Figure 42 - Variation of Longitudinal Force Phase Angle, α_1, with Nondimensional Encounter Frequency, μ_e, at a Full Scale Speed of 28 Knots for the SWATH 6D in Following Waves

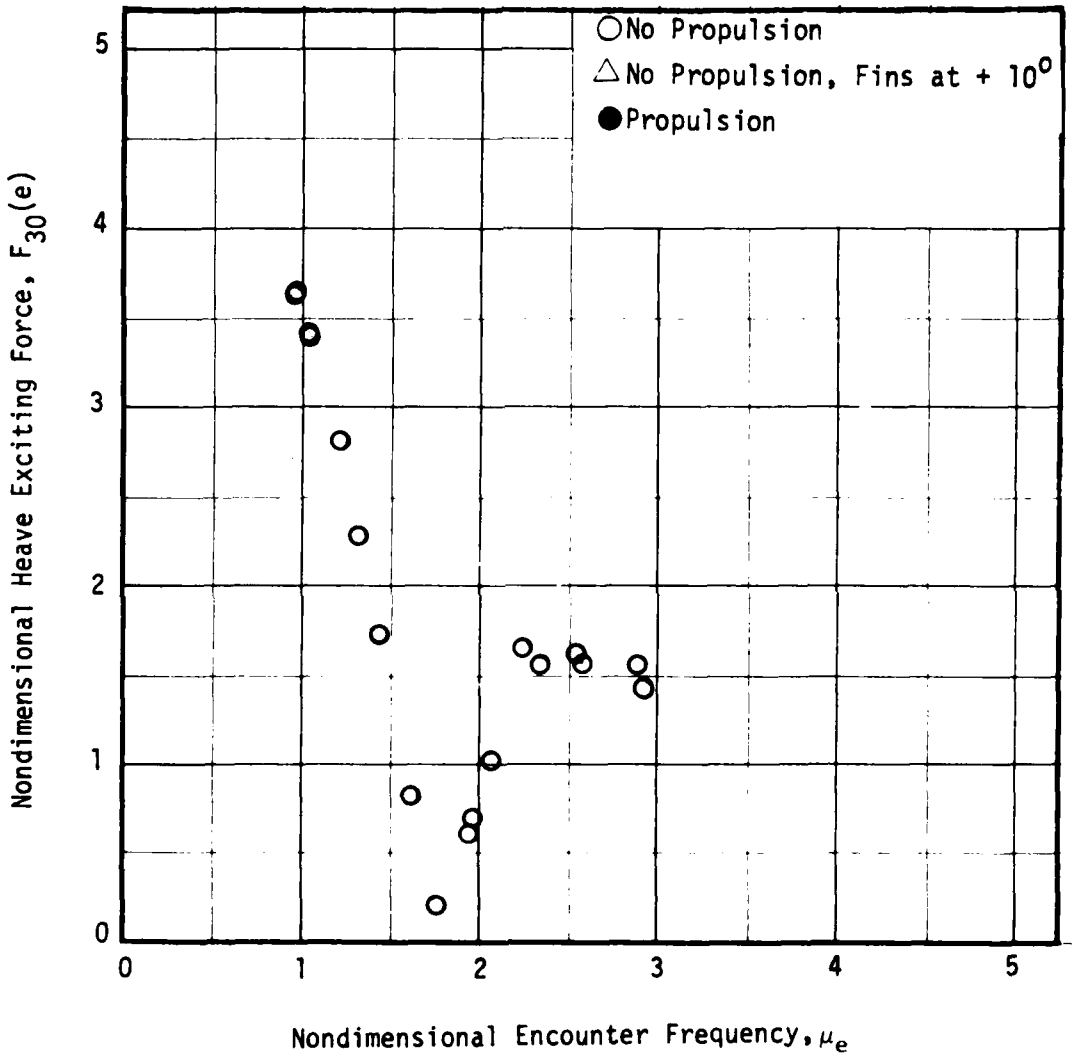

Figure 43 - Variation of Nondimensional Heave Exciting Force, $F_{30}(e)$, with Nondimensional Encounter Frequency, μ_e, at Zero Speed for the SWATH 6D in Following Waves

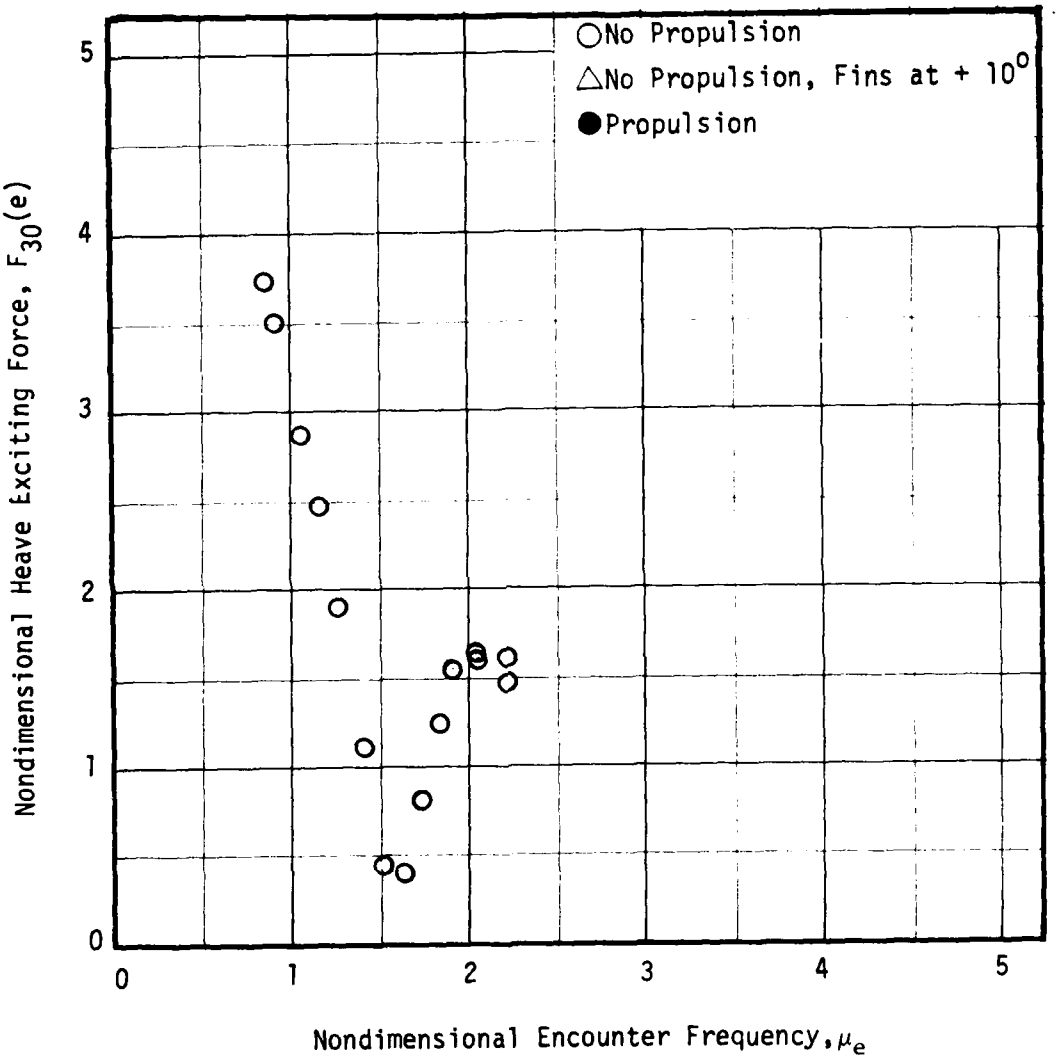

Figure 44 - Variation of Nondimensional Heave Exciting Force, $F_{30}(e)$, with Nondimensional Encounter Frequency, μ_e, at a Full Scale Speed of 4 Knots for the SWATH 6D in Following Waves

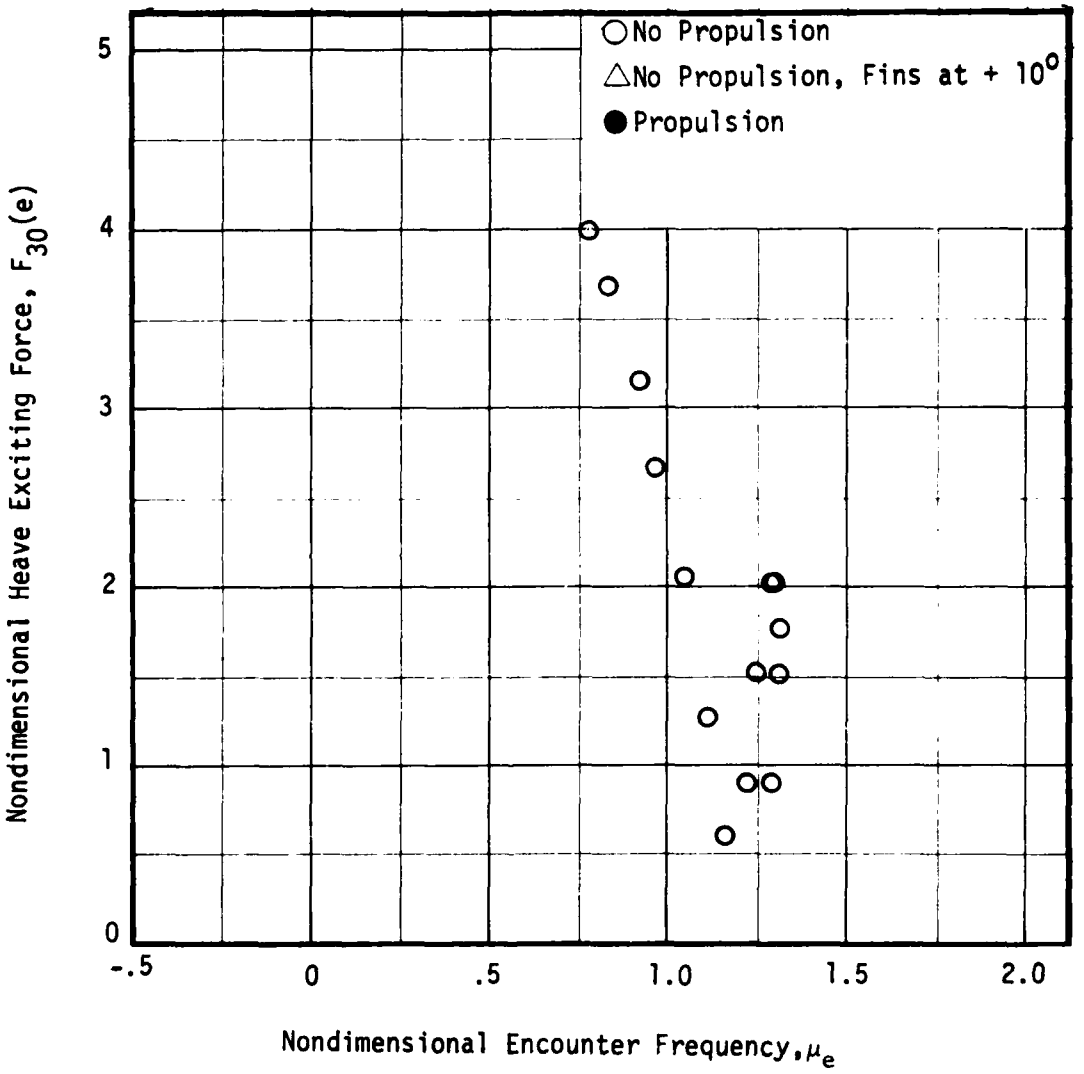

Figure 45 - Variation of Nondimensional Heave Exciting Force, $F_{30}(e)$, with Nondimensional Encounter Frequency, μ_e, at a Full Scale Speed of 10 Knots for the SWATH 6D in Following Waves

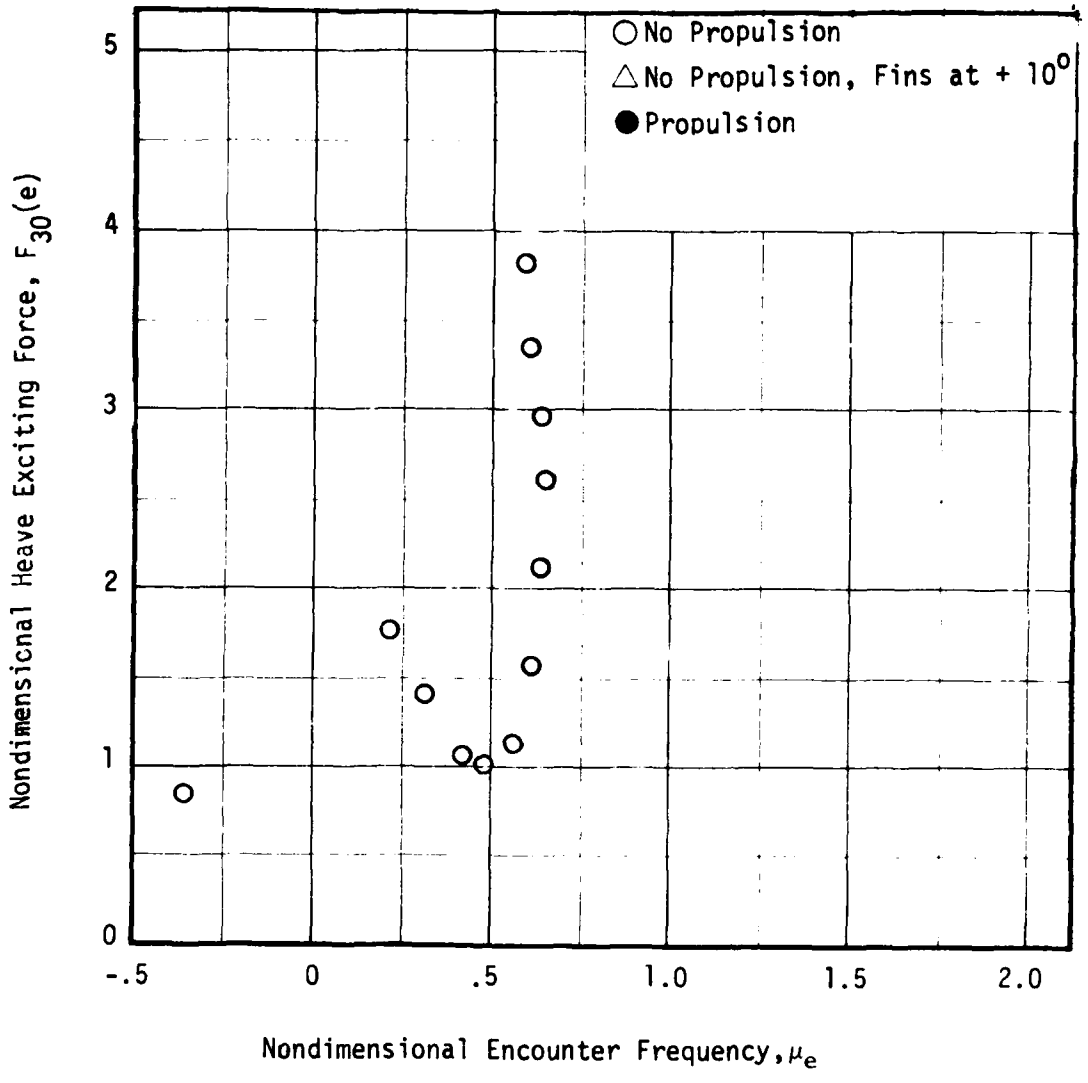

Figure 46 - Variation of Nondimensional Heave Exciting Force, $F_{30}(e)$, with Nondimensional Encounter Frequency, μ_e, at a Full Scale Speed of 20 Knots for the SWATH 6D in Following Waves

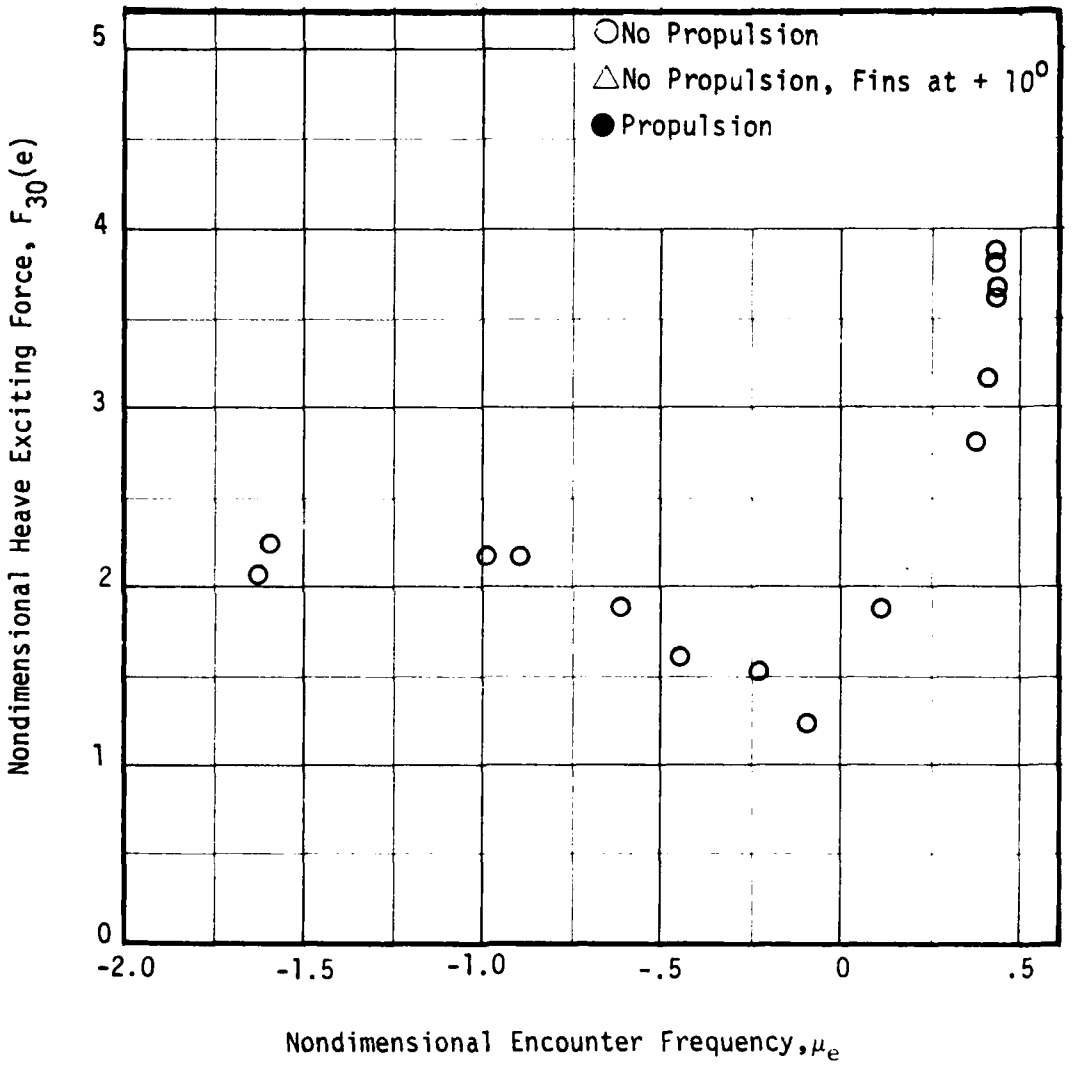

Figure 47 - Variation of Nondimensional Heave Exciting Force, $F_{30}(e)$, with Nondimensional Encounter Frequency, μ_e, at a Full Scale Speed of 28 Knots for the SWATH 6D in Following Waves

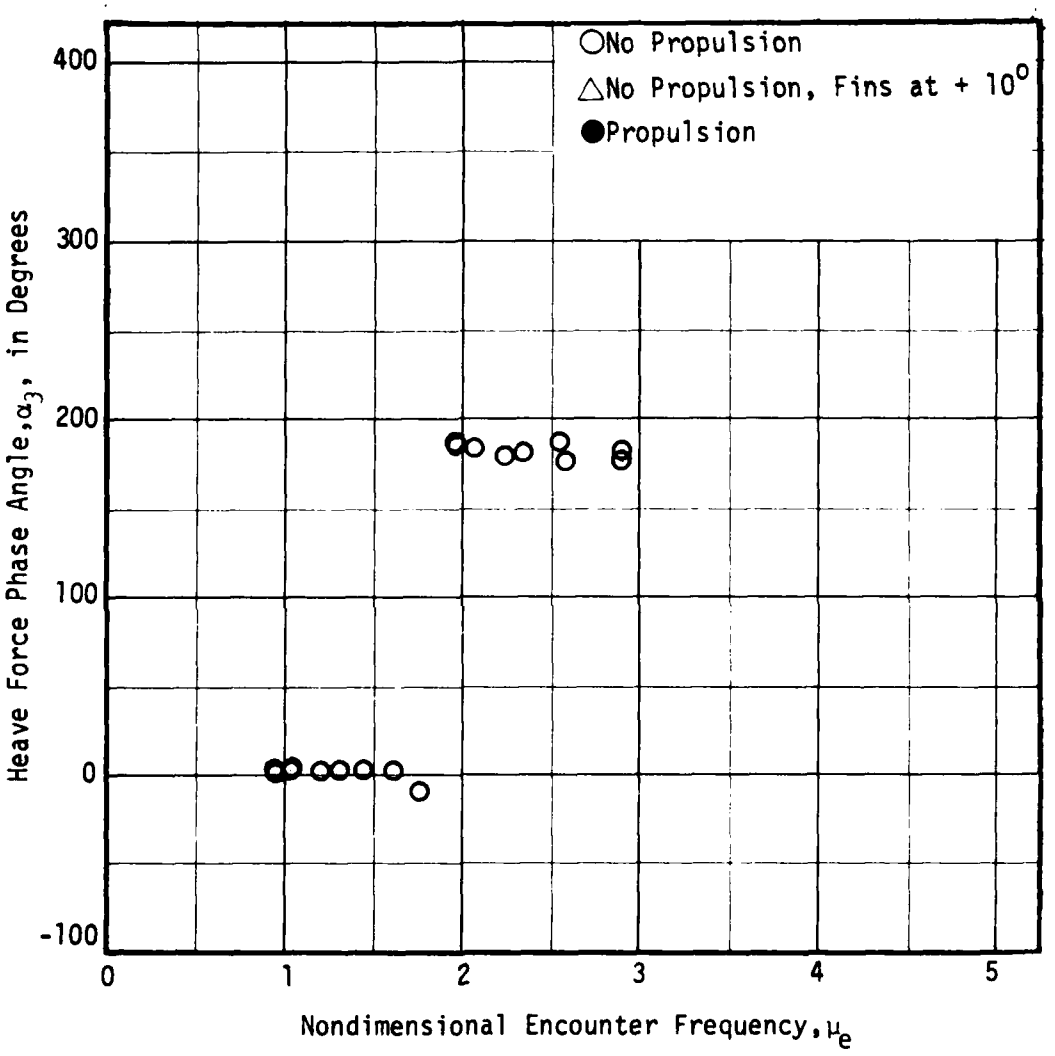

Figure 48 - Variation of Heave Force Phase Angle, α_3, with Nondimensional Encounter Frequency, μ_e, at Zero Speed for the SWATH 6D in Following Waves

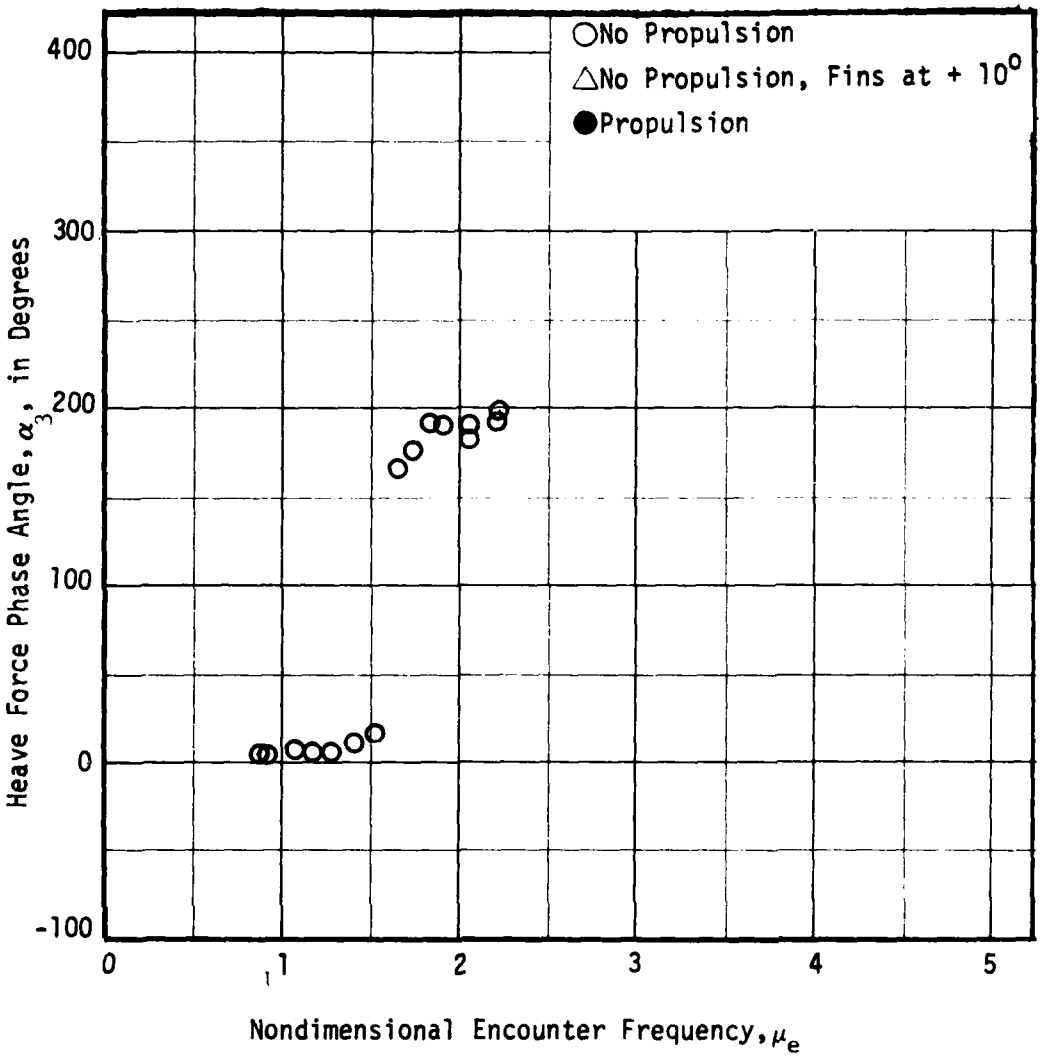

Figure 49 - Variation of Heave Force Phase Angle, α_3, with Nondimensional Encounter Frequency, μ_e, at a Full Scale Speed of 4 Knots for the SWATH 6D in Following Waves

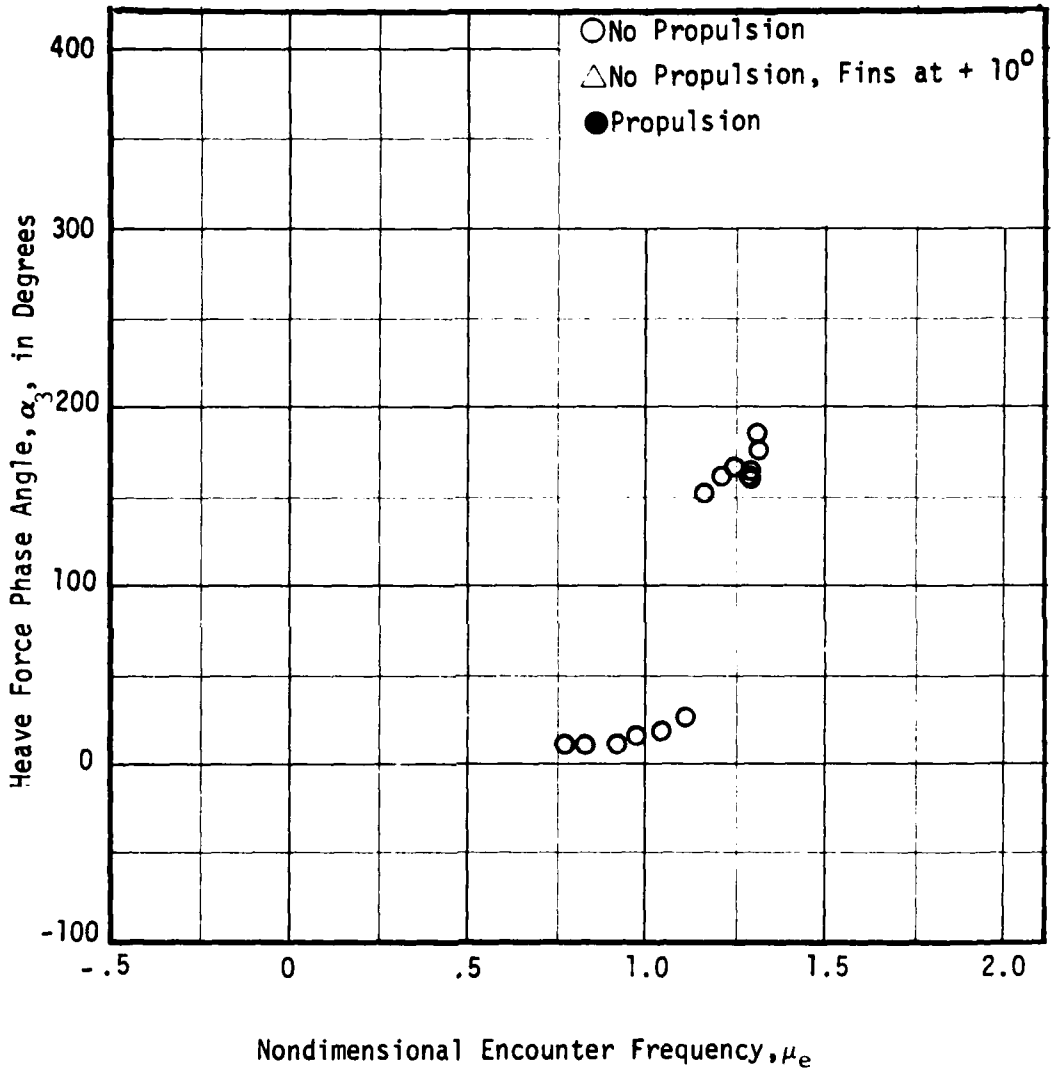

Figure 50 - Variation of Heave Force Phase Angle, α_3, with Nondimensional Encounter Frequency, μ_e, at a Full Scale Speed of 10 Knots for the SWATH 6D in Following Waves

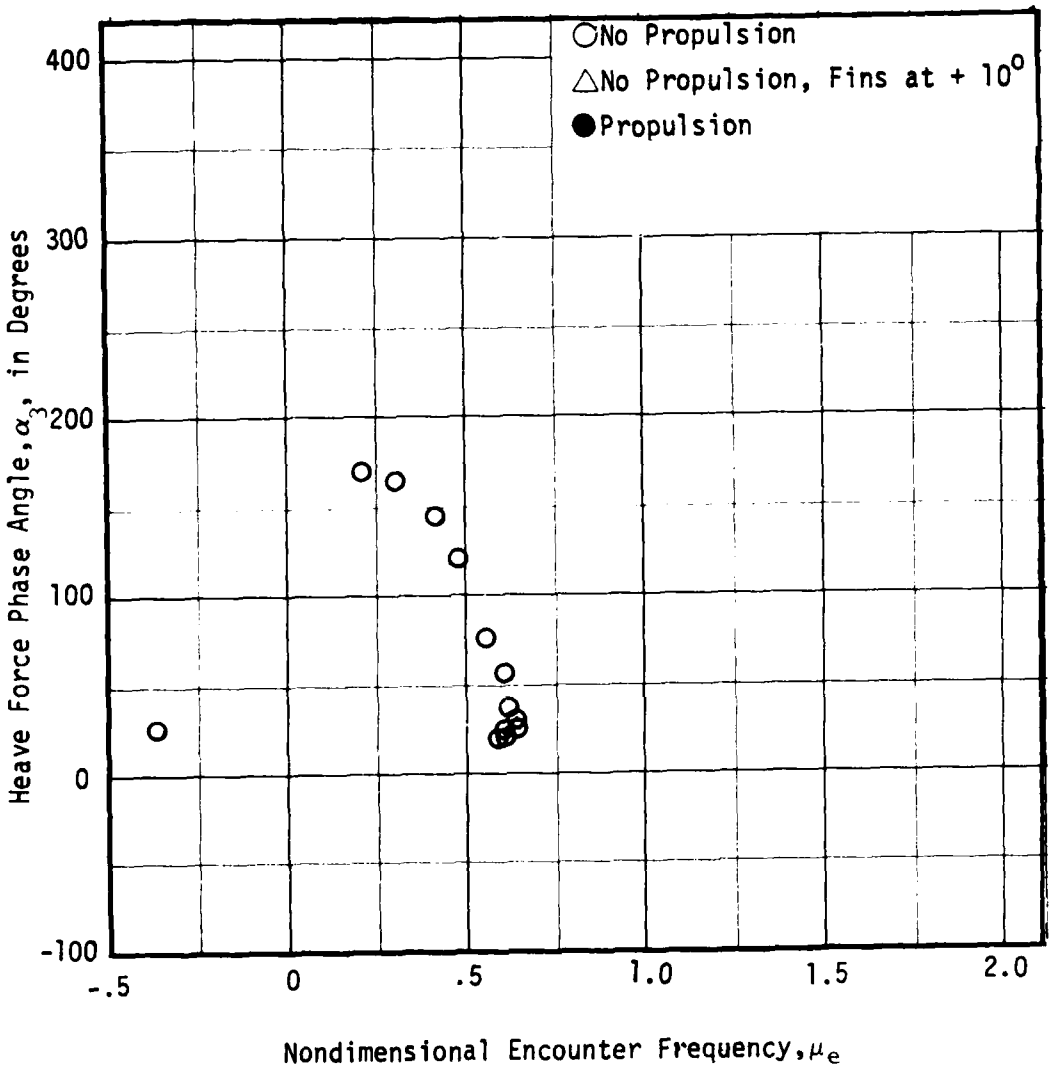

Figure 51 - Variation of Heave Force Phase Angle, α_3, with Nondimensional Encounter Frequency, μ_e, at a Full Scale Speed of 20 Knots for the SWATH 6D in Following Waves

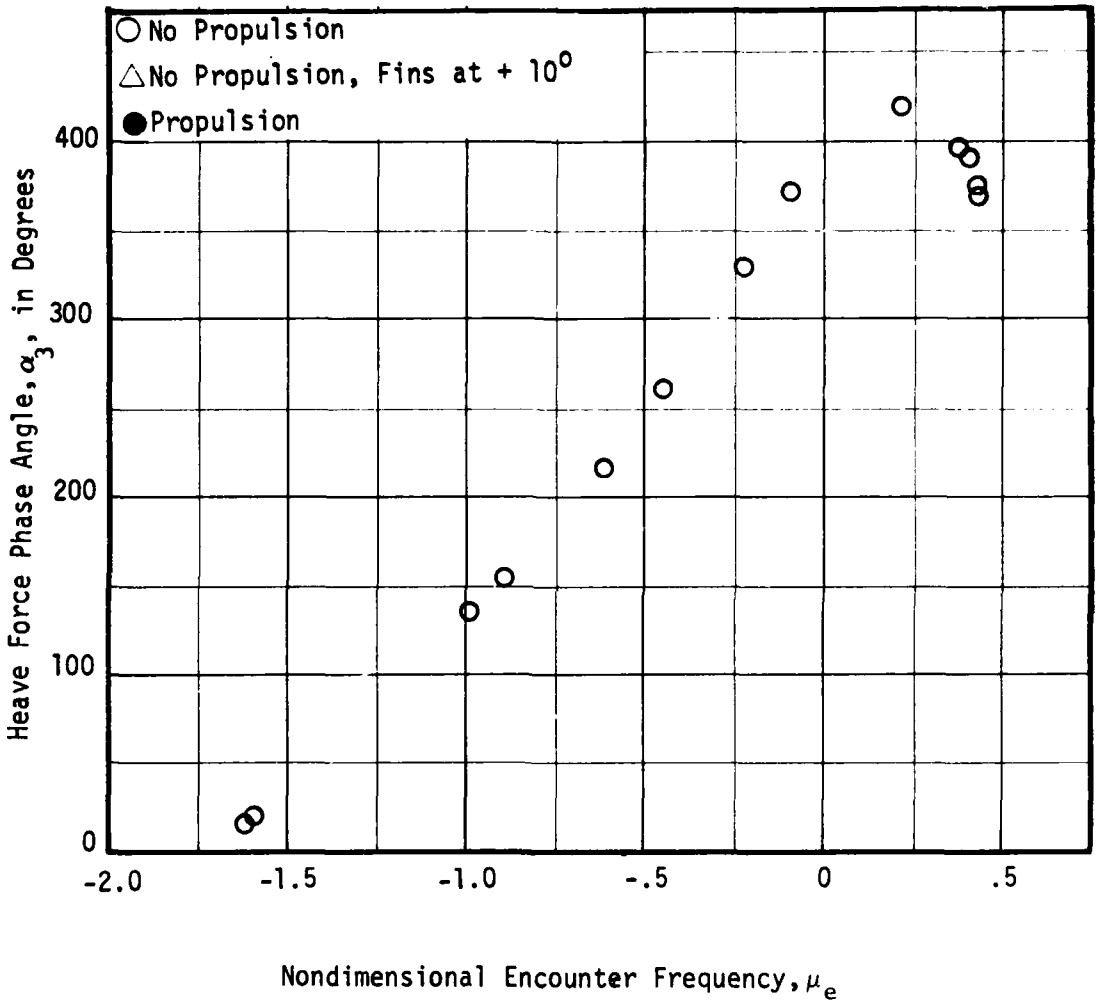

Figure 52 - Variation of Heave Force Phase Angle, α_3, with Nondimensional Encounter Frequency, μe, at a Full Scale Speed of 28 Knots for the SWATH 6D in Following Waves

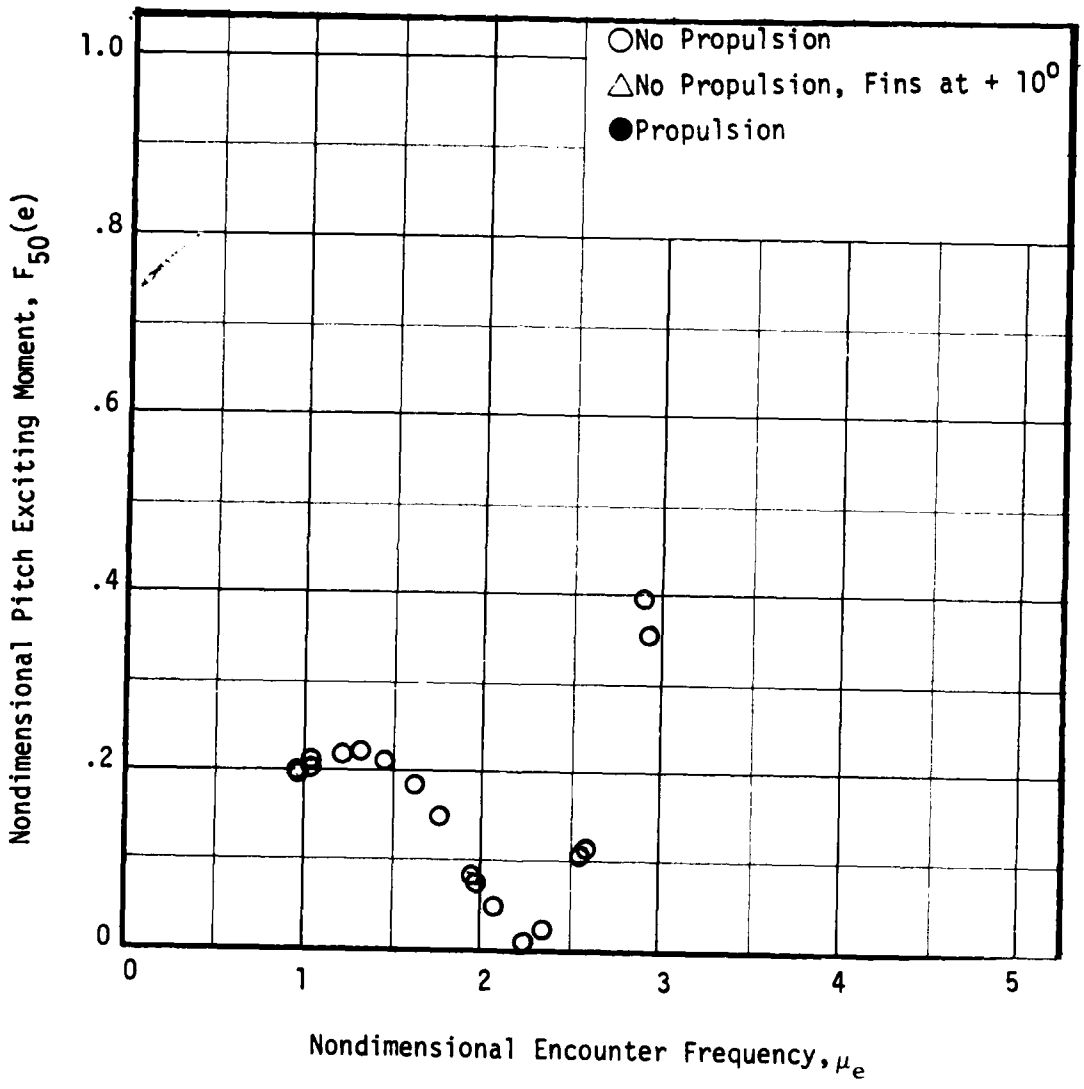

Figure 53 - Variation of Nondimensional Pitch Exciting Force, $F_{50}(e)$ with Nondimensional Encounter Frequency, μ_e, at Zero Speed for the SWATH 6D in Following Waves

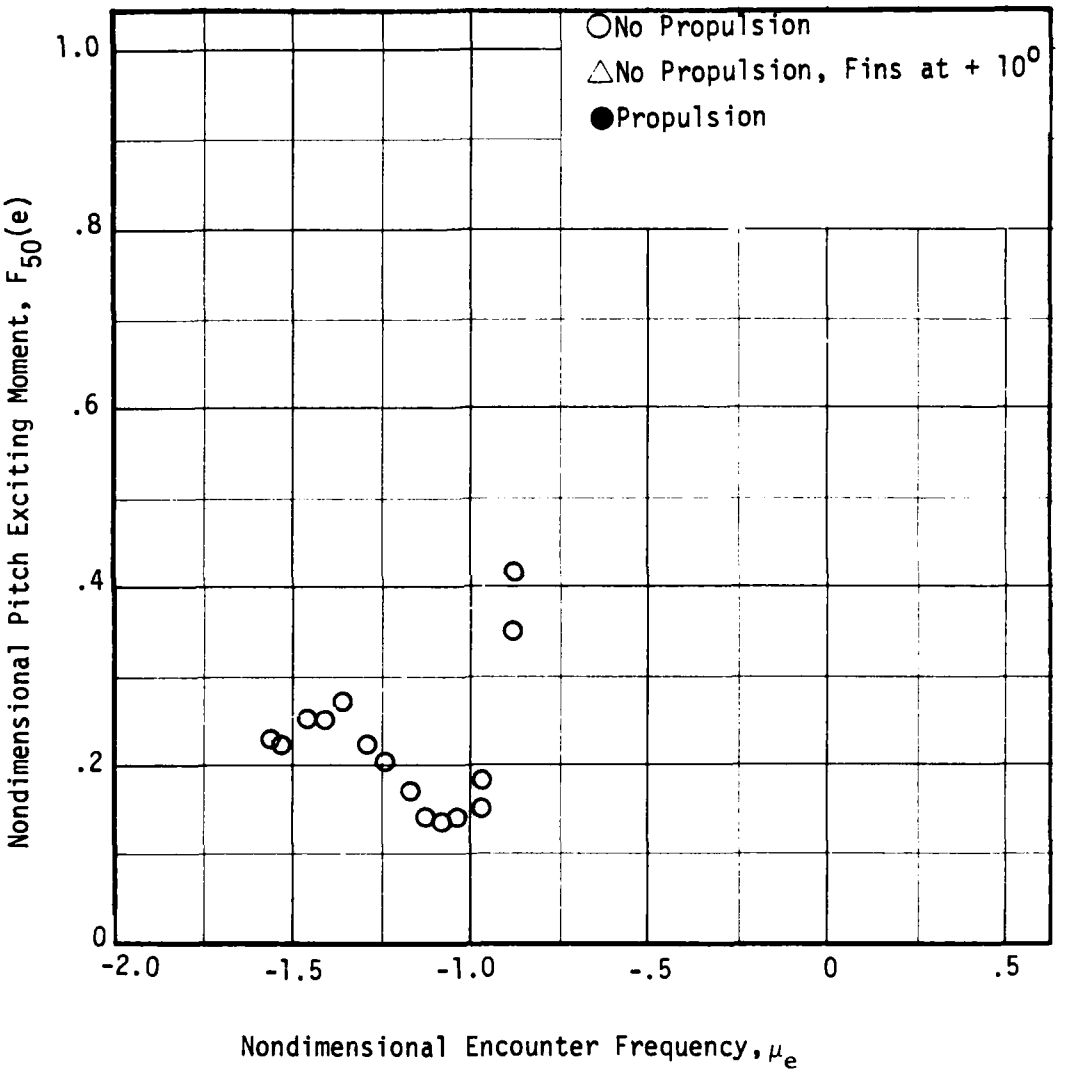

Figure 54 - Variation of Nondimensional Pitch Exciting Moment, $F_{50}(e)$, with Nondimensional Encounter Frequency, μ_e, at a Full Scale Speed of 4 Knots for the SWATH 6D in Following Waves

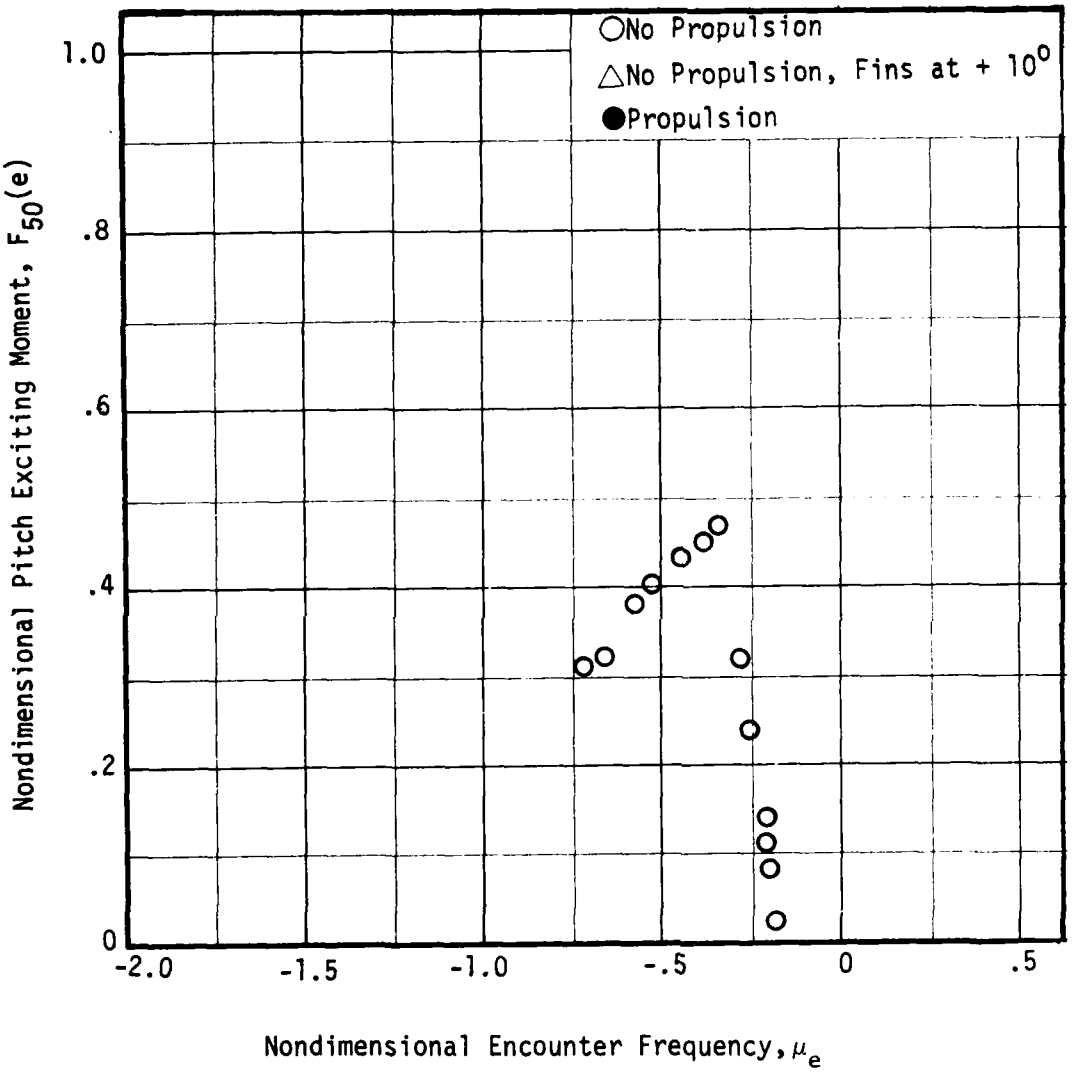

Figure 55 - Variation of Nondimensional Pitch Exciting Force, $F_{50}(e)$, with Nondimensional Encounter Frequency, μ_e at a Full Scale Speed of 10 Knots for the SWATH 6D in Following Waves

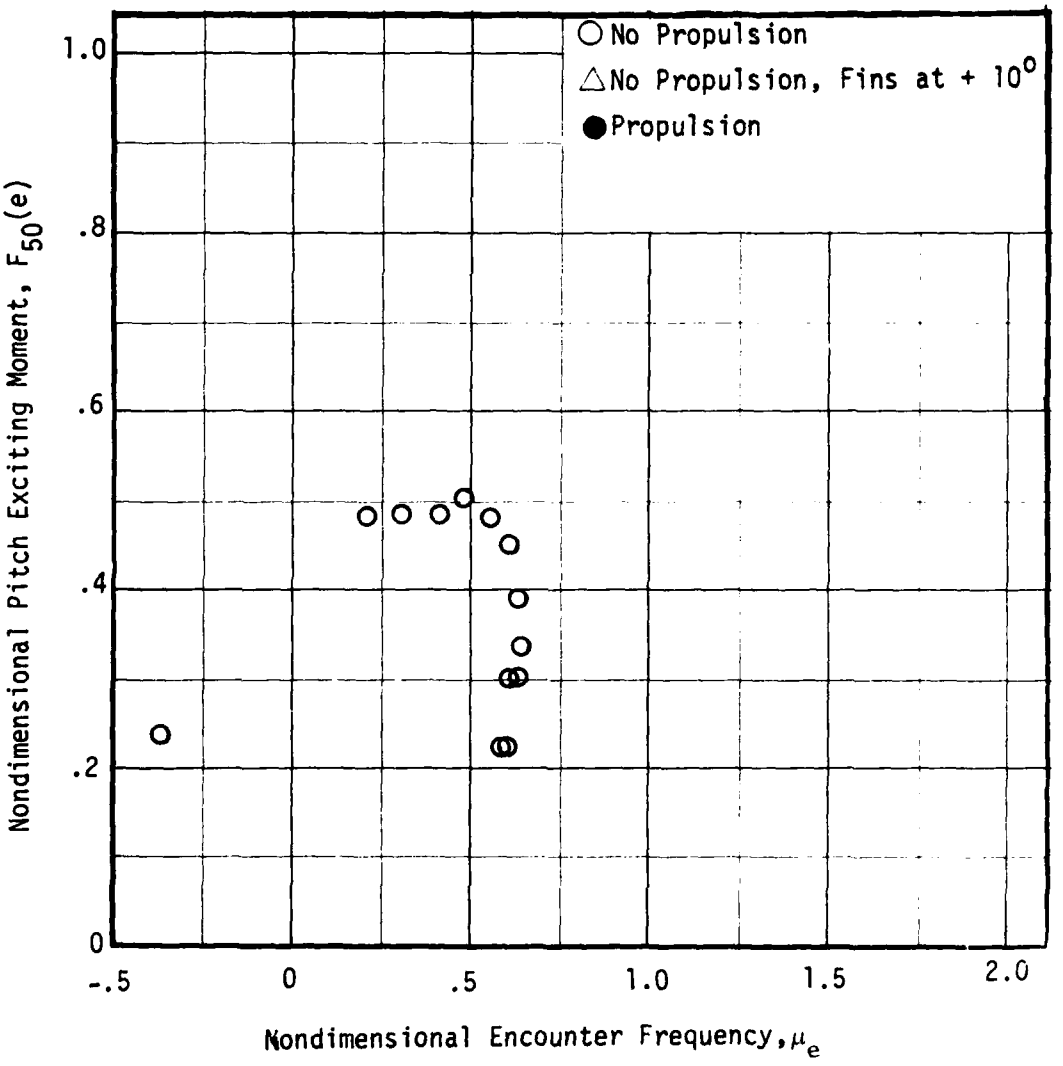

Figure 56 - Variation of Nondimensional Pitch Exciting Moment, $F_{50}(e)$, with Nondimensional Encounter Frequency, μ_e, at a Full Scale Speed of 20 Knots for the SWATH 6D in Following Waves

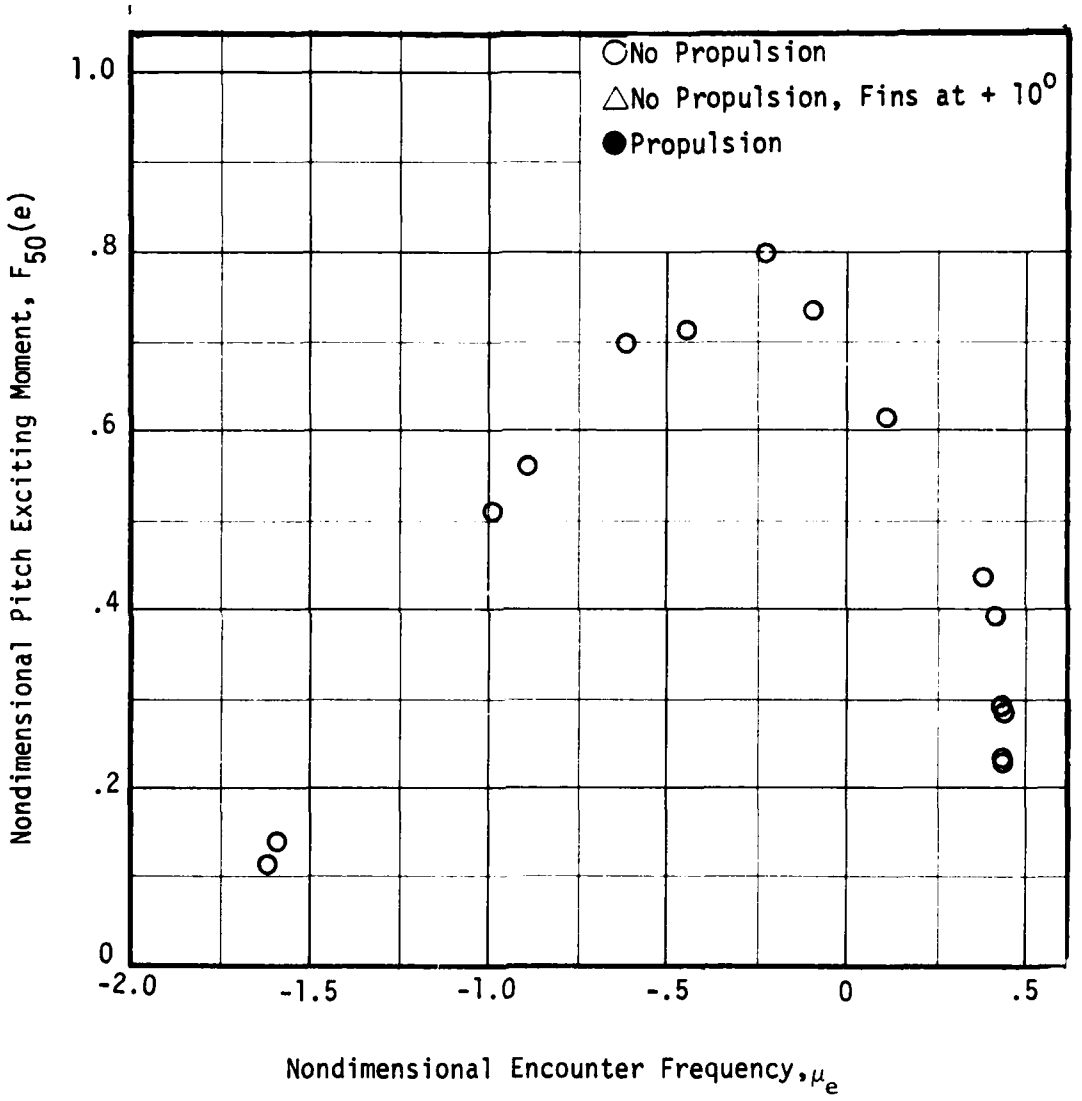

Figure 57 - Variation of Nondimensional Pitch Exciting Moment, $F_{50}(e)$, with Nondimensional Encounter Frequency, μ_e, at a Full Scale Speed of 28 Knots for the SWATH 6D in Following Waves

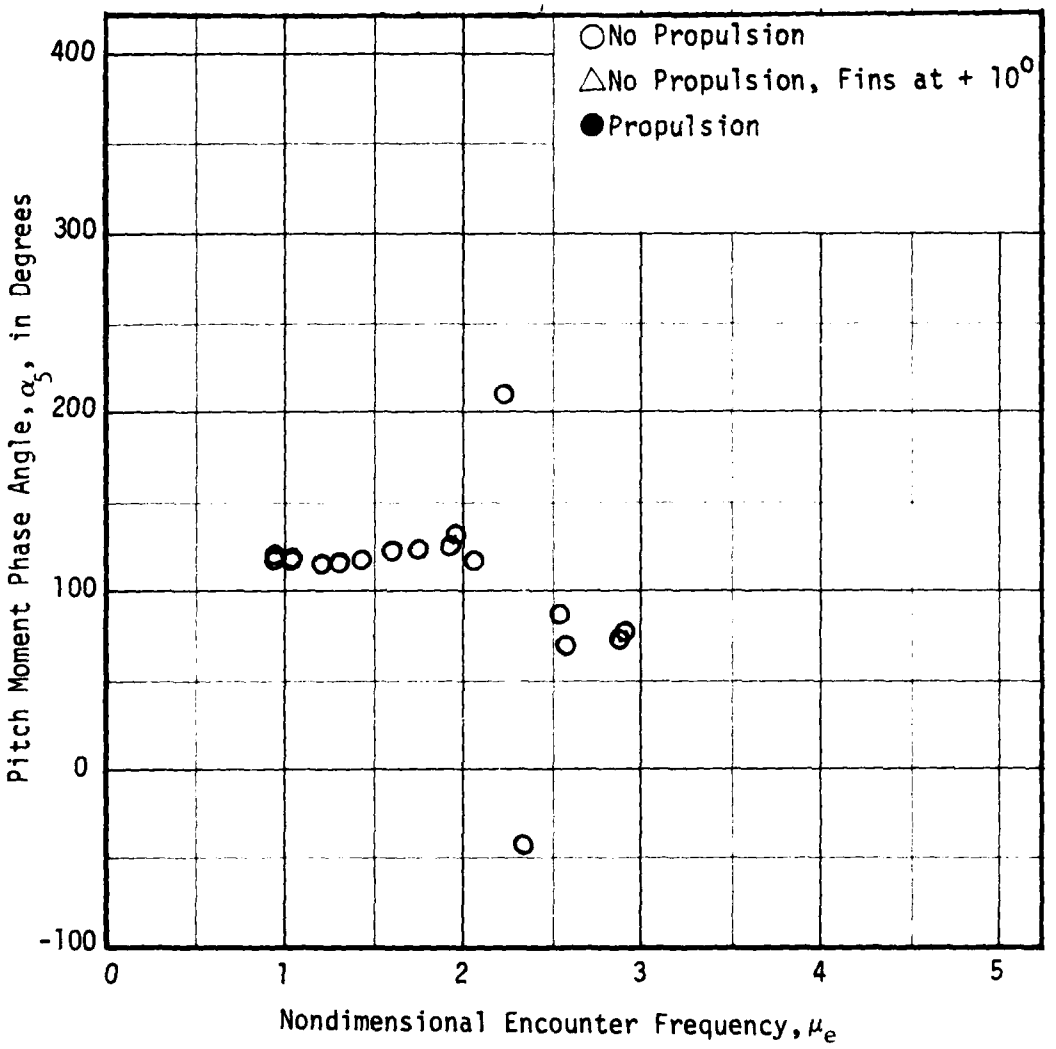

Figure 58 - Variation of Pitch Moment Phase Angle, α_5, with Nondimensional Encounter Frequency, μ_e, at Zero Speed for the SWATH 6D in Following Waves

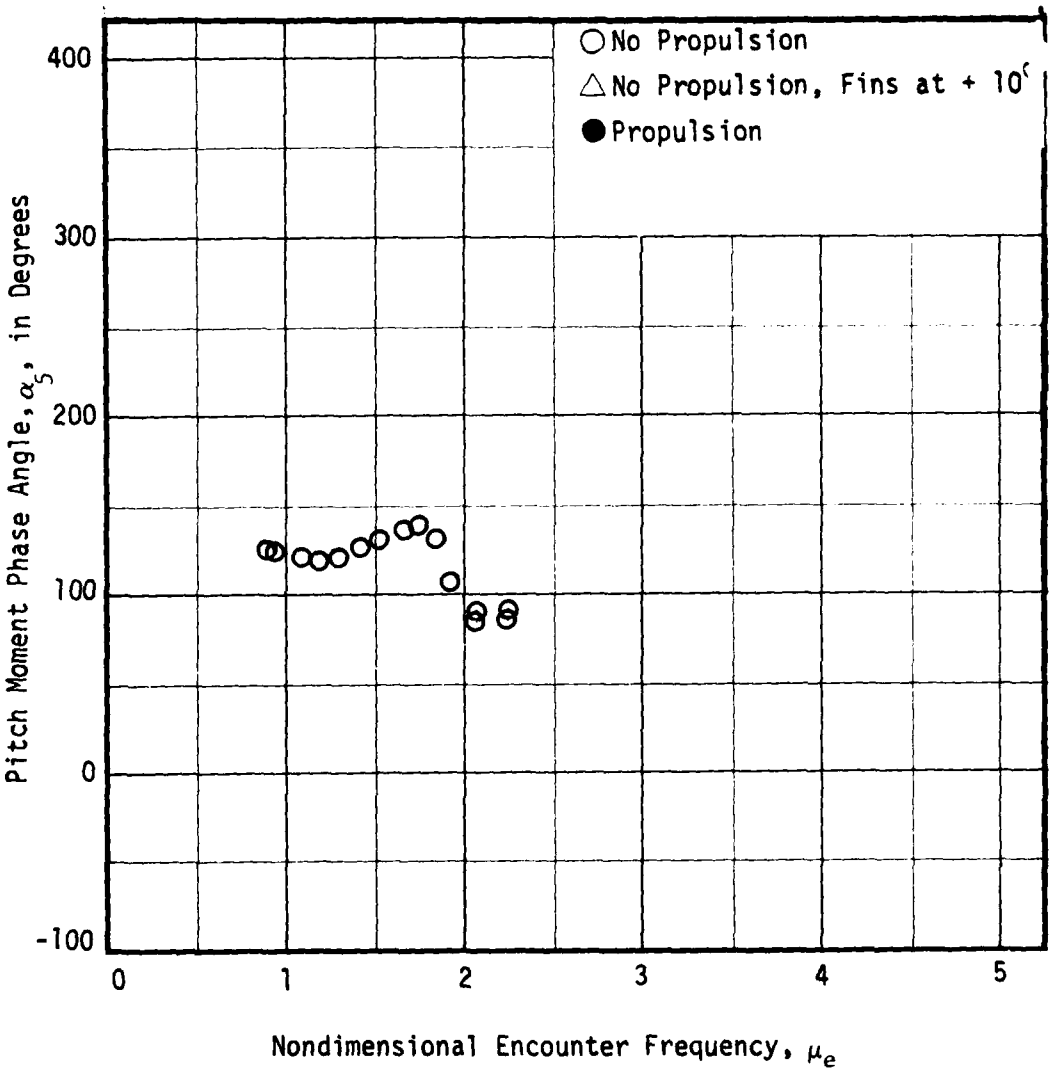

Figure 59 - Variation of Pitch Moment Phase Angle, α_5, with Nondimensional Encounter Frequency, μ_e, at a Full Scale Speed of 4 Knots for the SWATH 6D in Following Waves

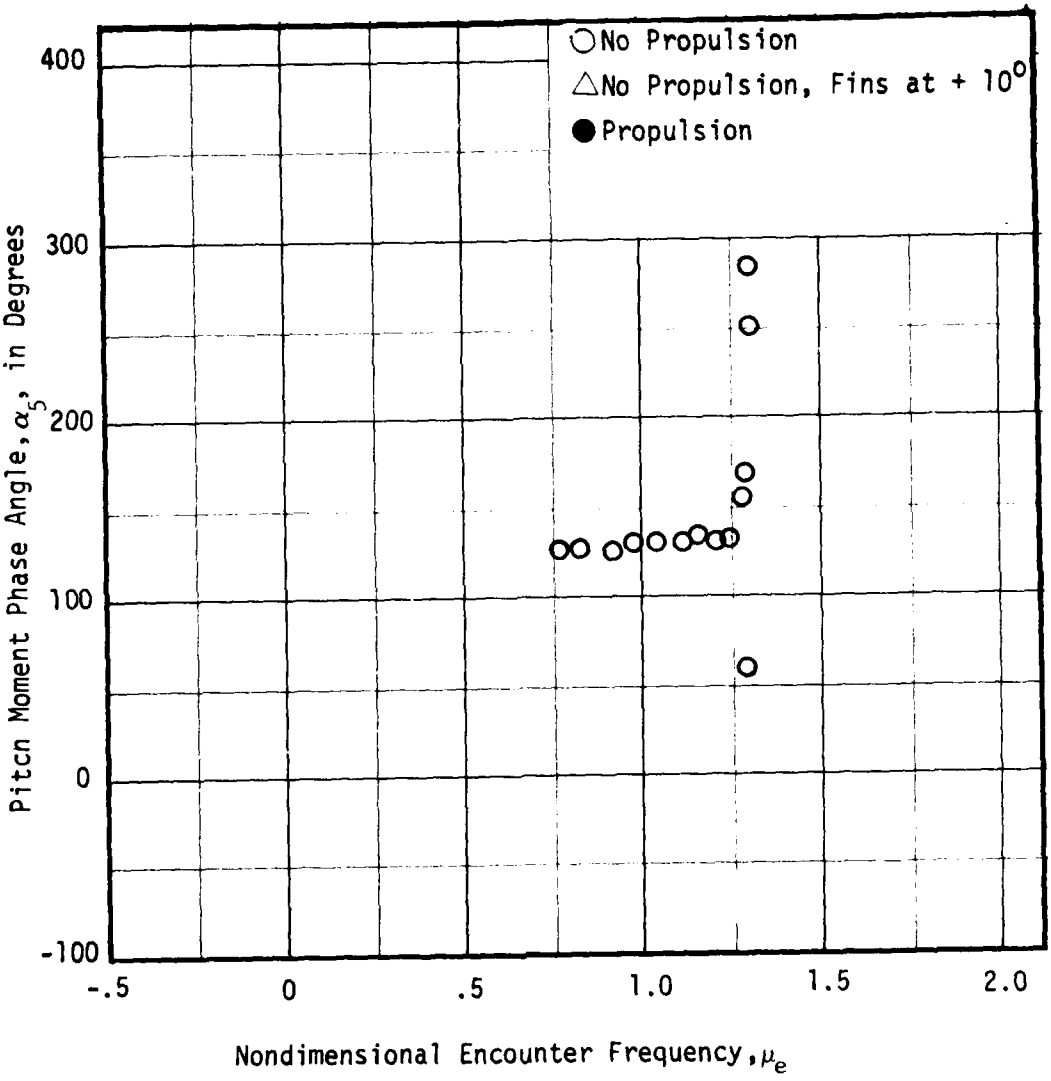

Figure 60 - Variation of Pitch Moment Phase Angle, α_5, with Nondimensional Encounter Frequency, μ_e, at a Full Scale Speed of 10 Knots for the SWATH 6D in Following Waves

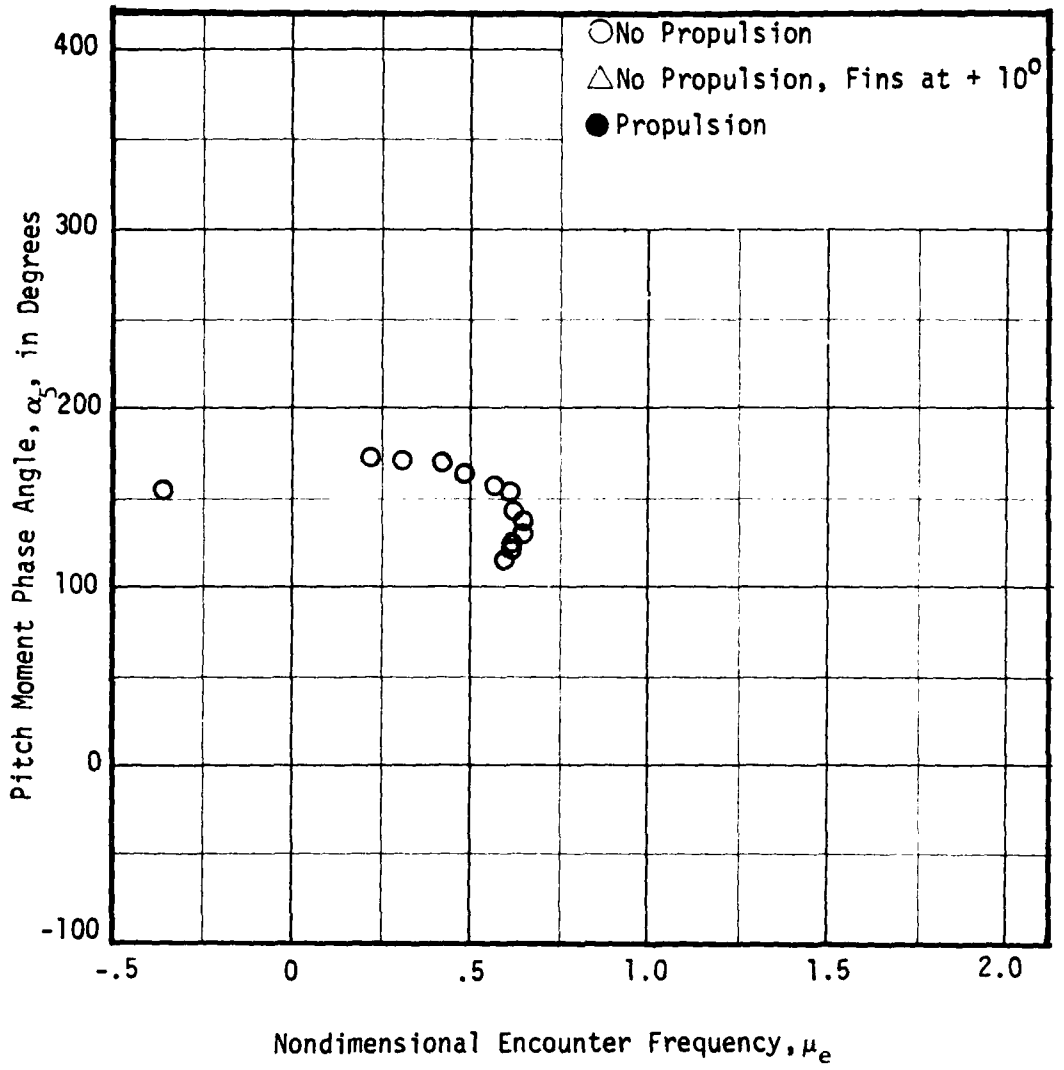

Figure 61 - Variation of Pitch Moment Phase Angle, α_5, with Nondimensional Encounter Frequency, μ_e, at a Full Scale Speed of 20 Knots for the SWATH 6D in Following Waves

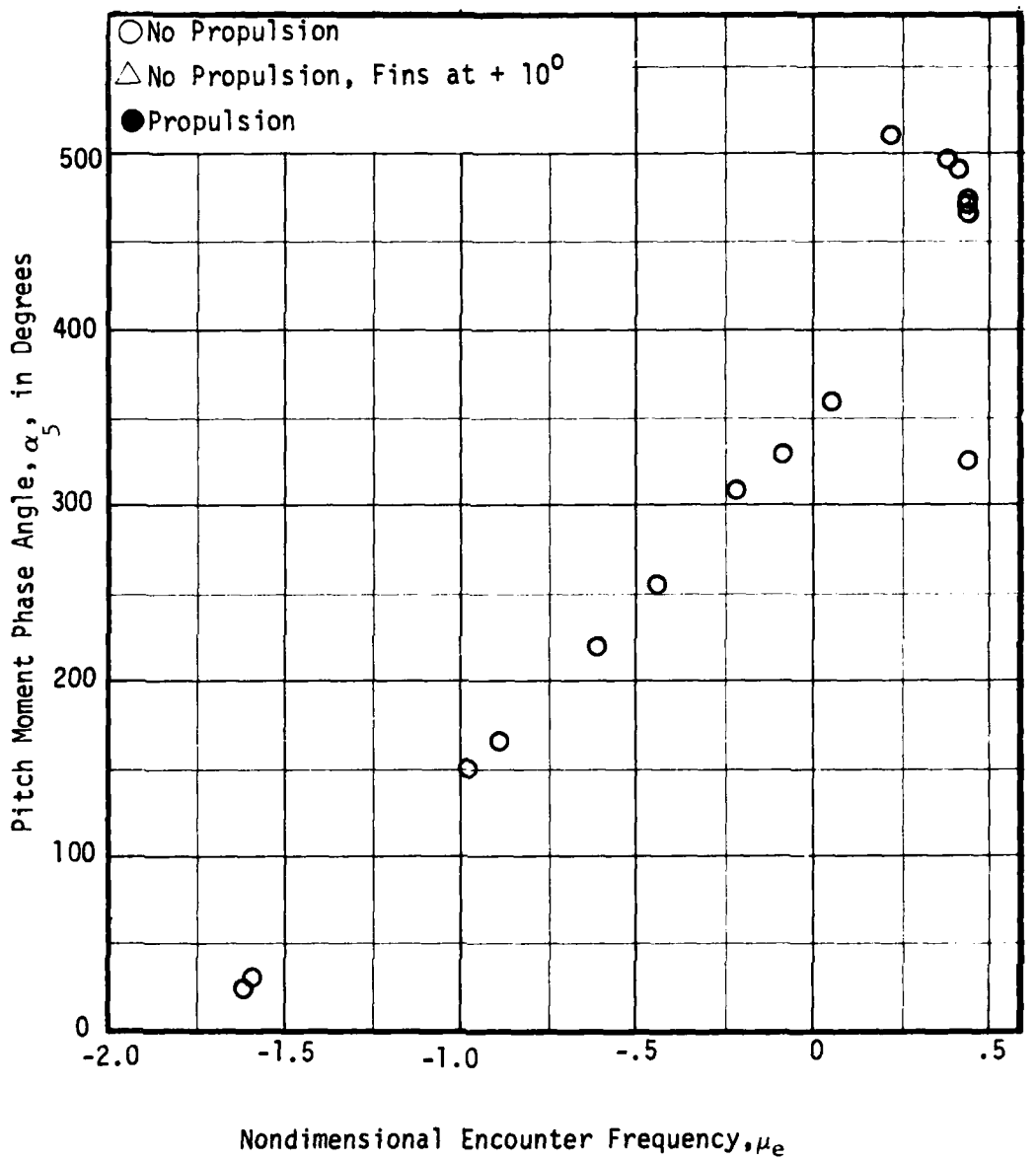

Figure 62 - Variation of Pitch Moment Phase Angle, α_5, with Nondimensional Encounter Frequency, μ_e, at a Full Scale Speed of 28 Knots for the SWATH 6D in Following Waves

APPENDIX C

SSP HEAD SEA EXCITING FORCE EXPERIMENTAL DATA

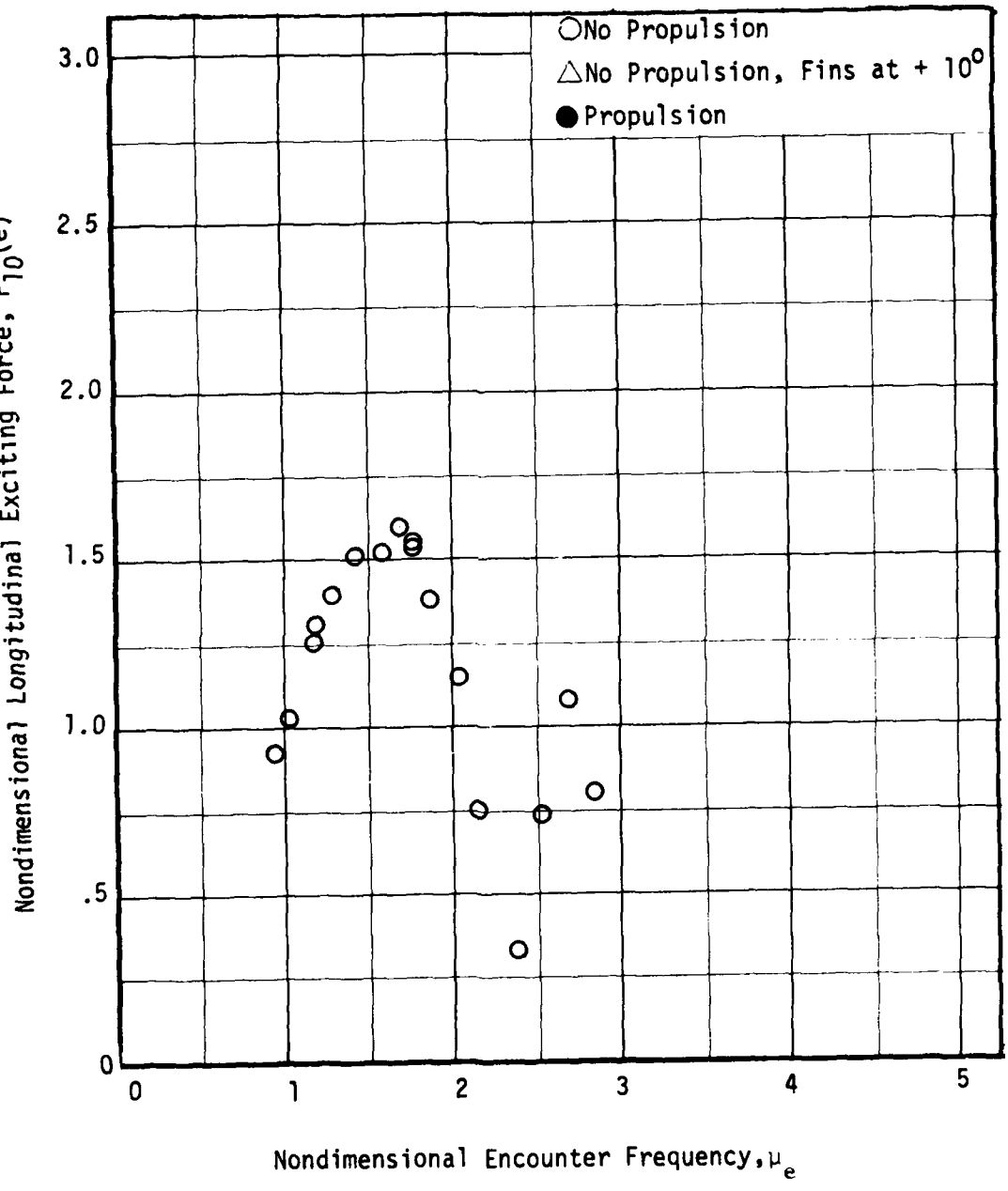

Figure 63 - Variation of Nondimensional Longitudinal Exciting Force, $F_{10}(e)$, with Nondimensional Encounter Frequency, μ_e, at Zero Speed for the SSP in Head Waves

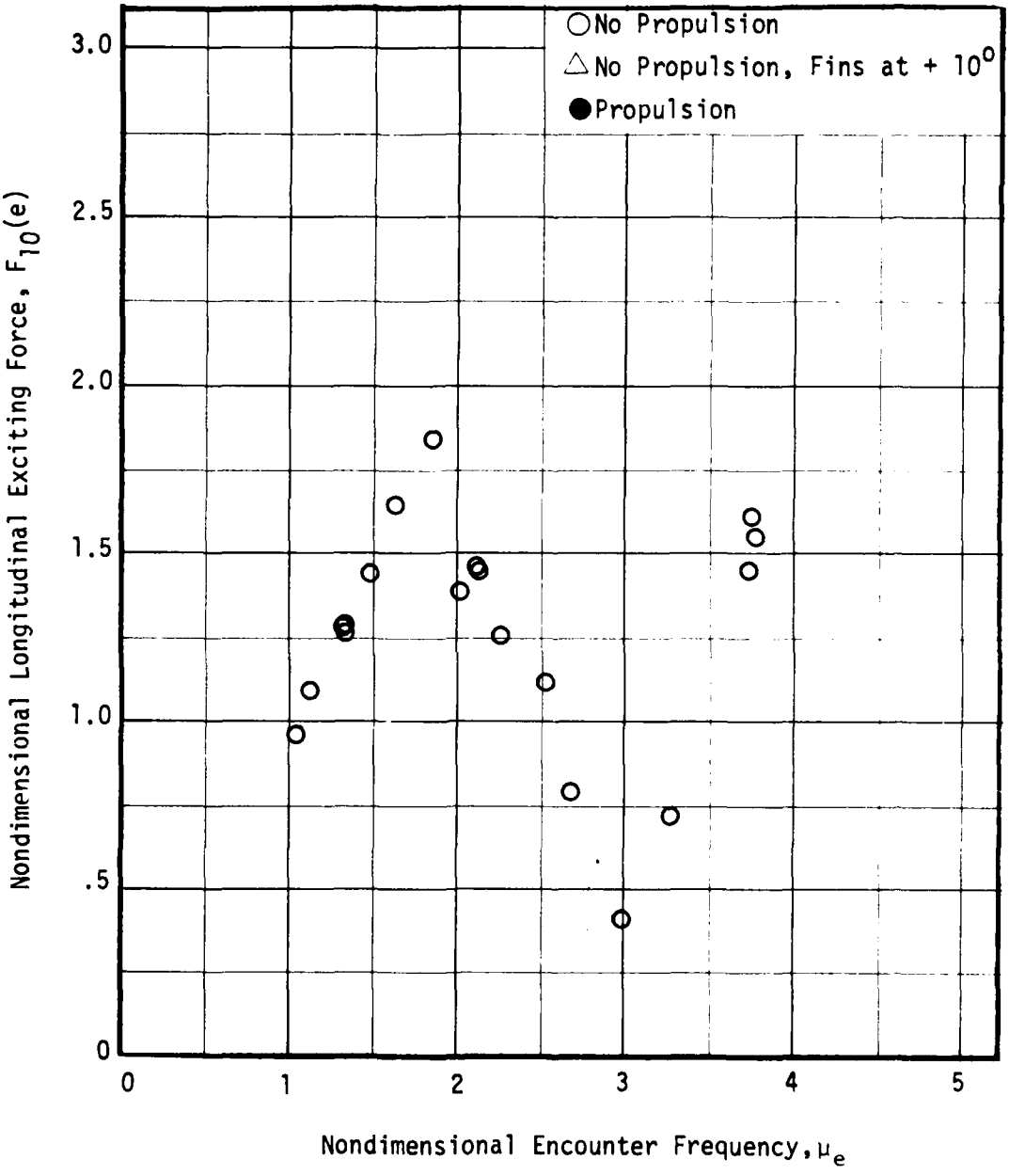

Figure 64 - Variation of Nondimensional Longitudinal Exciting Force, $F_{10}(e)$, with Nondimensional Encounter Frequency, μ_e, at a Full Scale Speed of 3 Knots for the SSP in Head Waves

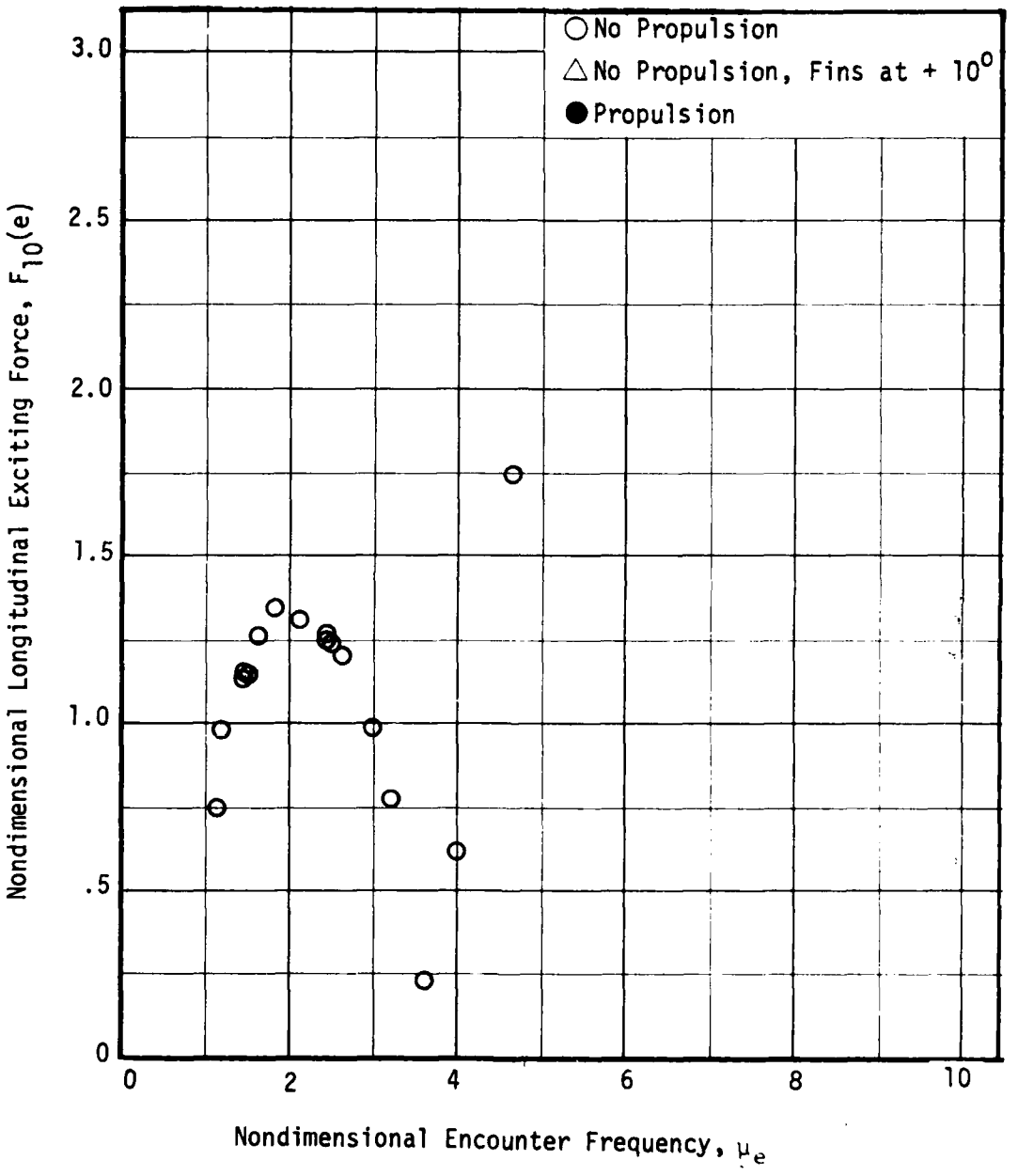

Figure 65 - Variation of Nondimensional Longitudinal Exciting Force, $F_{10}(e)$, with Nondimensional Encounter Frequency, μ_e, at a Full Scale Speed of 7 Knots for the SSP in Head Waves

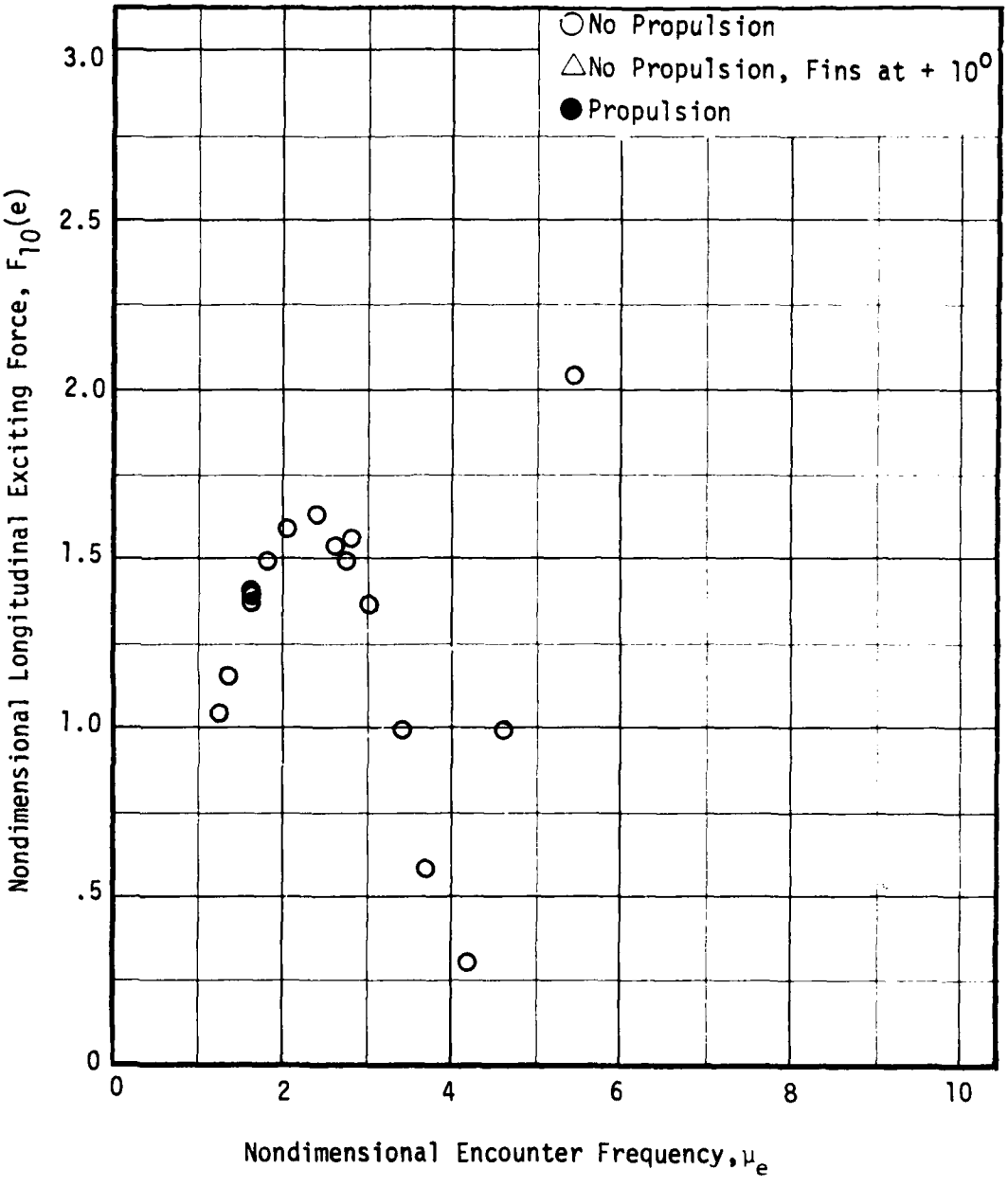

Figure 66 - Variation of Nondimensional Longitudinal Exciting Force, $F_{10}(e)$, with Nondimensional Encounter Frequency, μ_e, at a Full Scale Speed of 10 Knots for the SSP in Head Waves

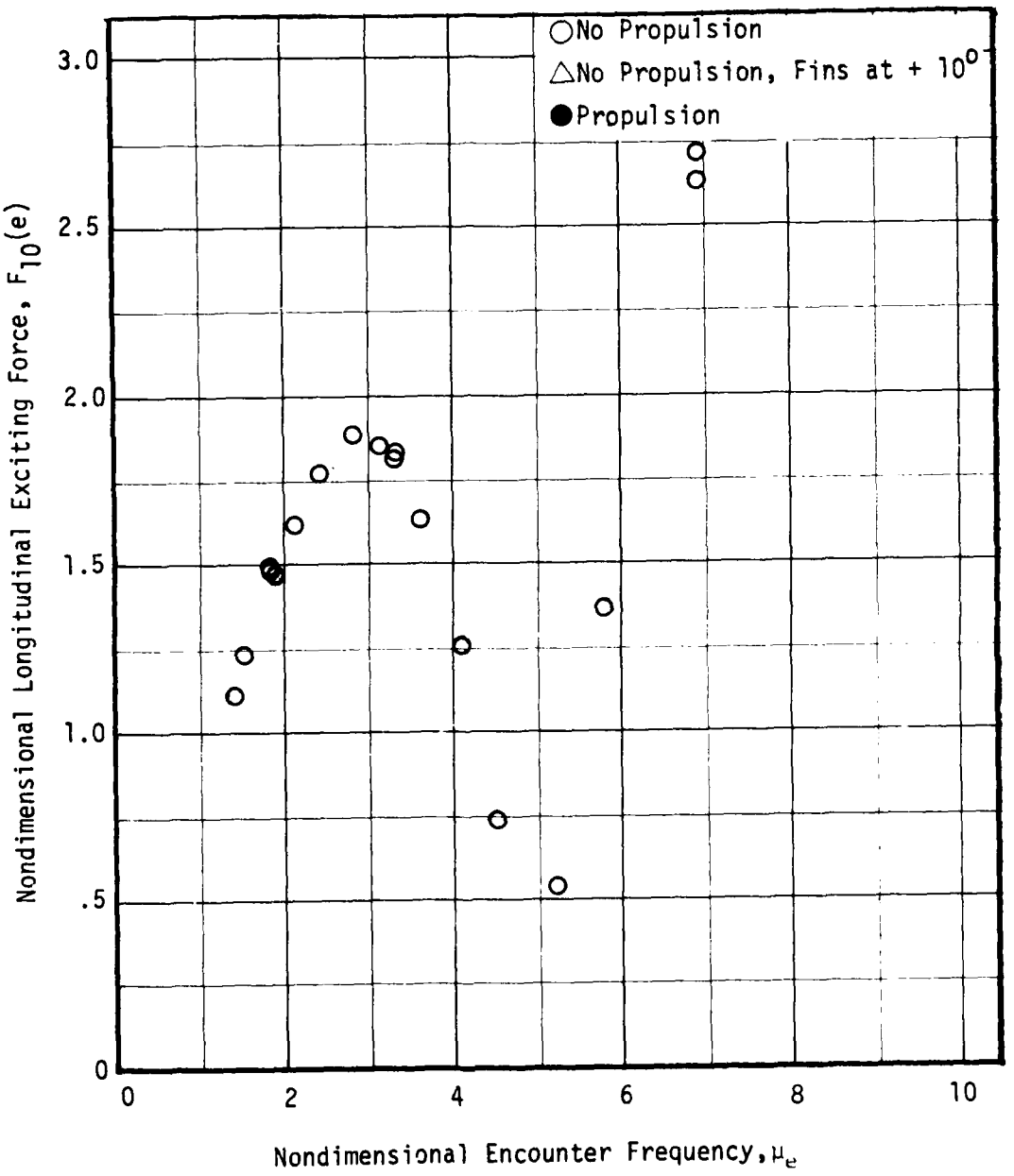

Figure 67 - Variation of Nondimensional Longitudinal Exciting Force, $F_{10}(e)$, with Nondimensional Encounter Frequency, μ_e, at a Full Scale Speed of 15.5 Knots for the SSP in Head Waves

AD-A087 335 DAVID W TAYLOR NAVAL SHIP RESEARCH AND DEVELOPMENT CE--ETC F/G 13/10
HEAD AND FOLLOWING WAVE EXCITING FORCE EXPERIMENTS ON TWO SWATH--ETC(U)
JUN 80 J A FEIN, R STAHL

UNCLASSIFIED DTNSRDC/SPD-0928-01 NL

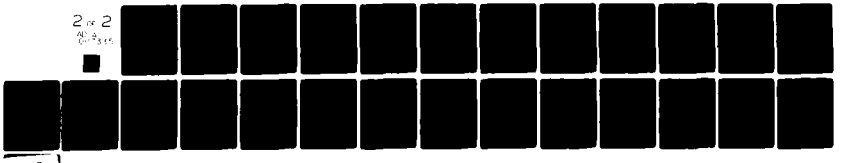

END
DATE FILMED
9-80
DTIC

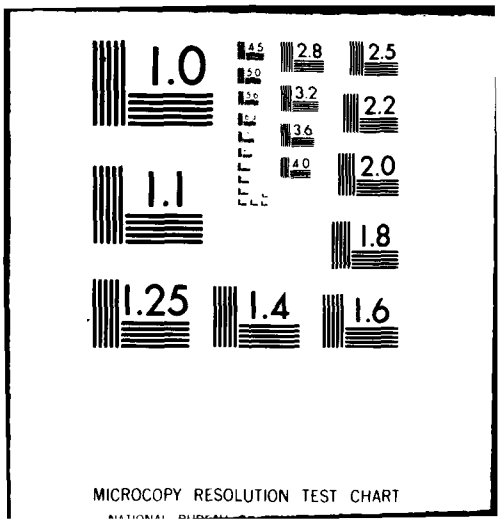
1.0
1.1
1.25
1.4
1.6
1.8
2.0
2.2
2.5
2.8
3.2
3.6
4.0
4.5
5.0
5.6
MICROCOPY RESOLUTION TEST CHART

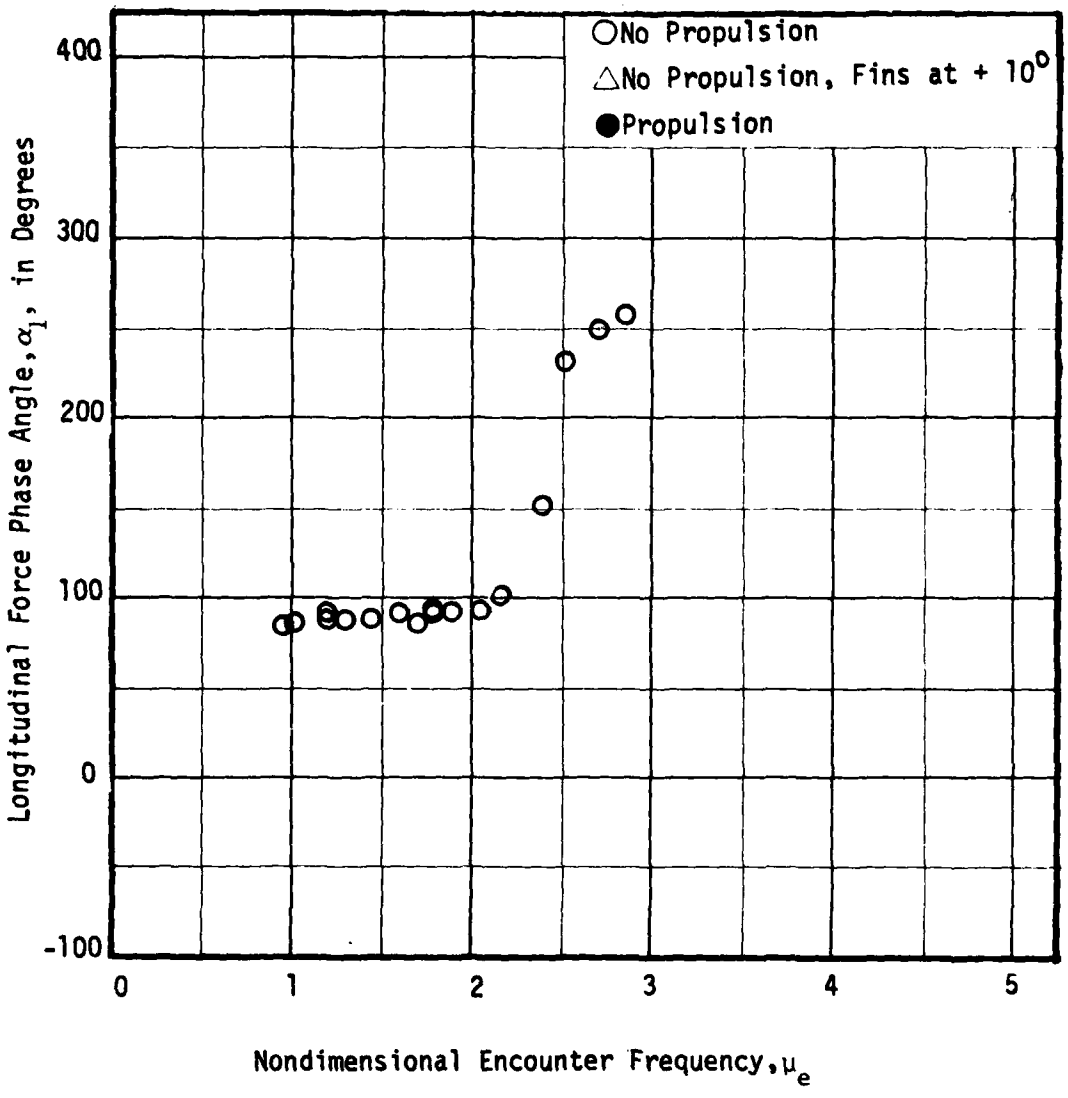

Figure 68 - Variation of Longitudinal Force Phase Angle, α_1, with Nondimensional Encounter Frequency, μ_e, at Zero Speed for the SSP in Head Waves

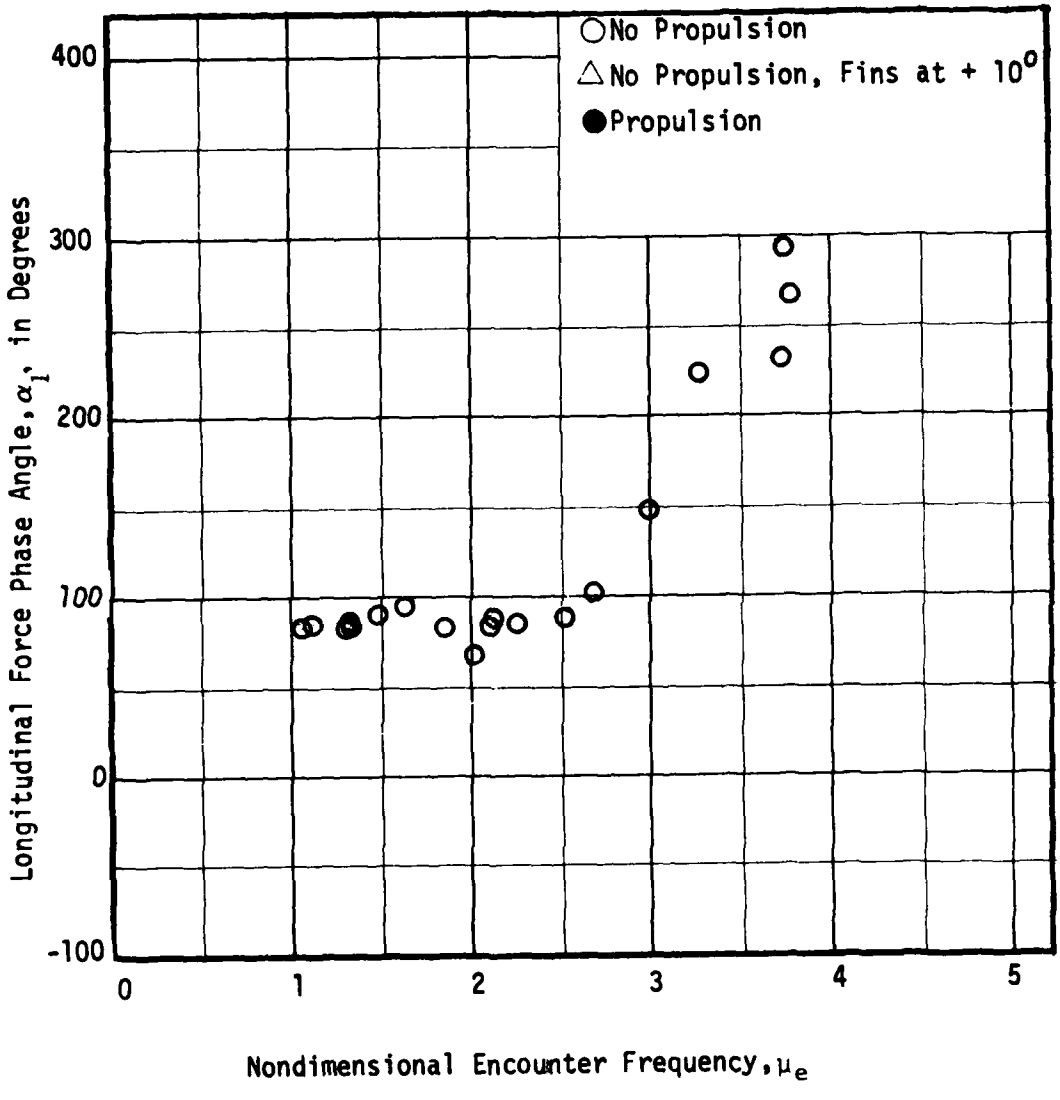

Figure 69 - Variation of Longitudinal Force Phase Angle, α_1, with Nondimensional Encounter Frequency, μ_e, at a Full Scale Speed of 3 Knots for the SSP in Head Waves

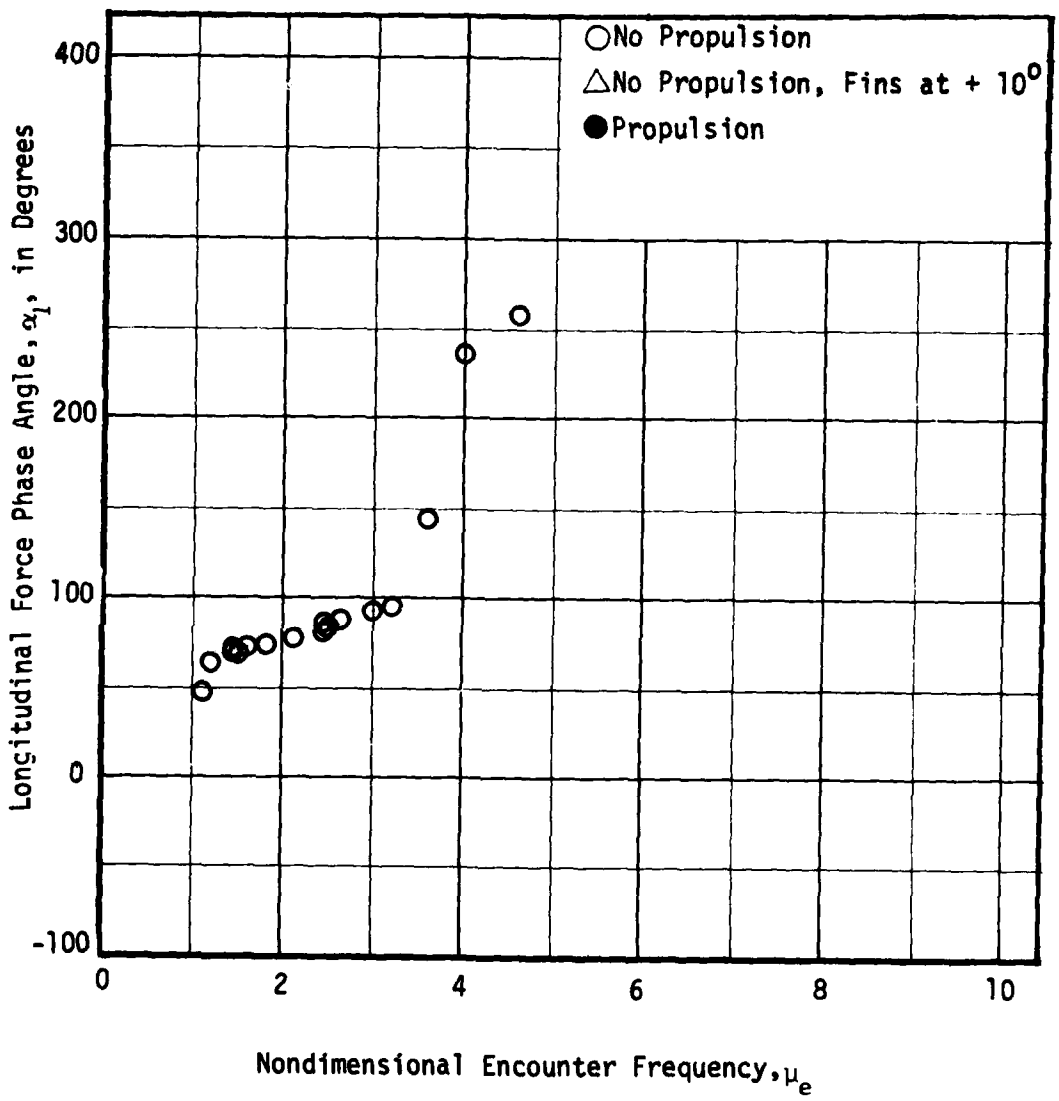

Figure 70 - Variation of Longitudinal Force Phase Angle, α_1, with Nondimensional Encounter Frequency, μ_e, at a Full Scale Speed of 7 Knots for the SSP in Head Waves

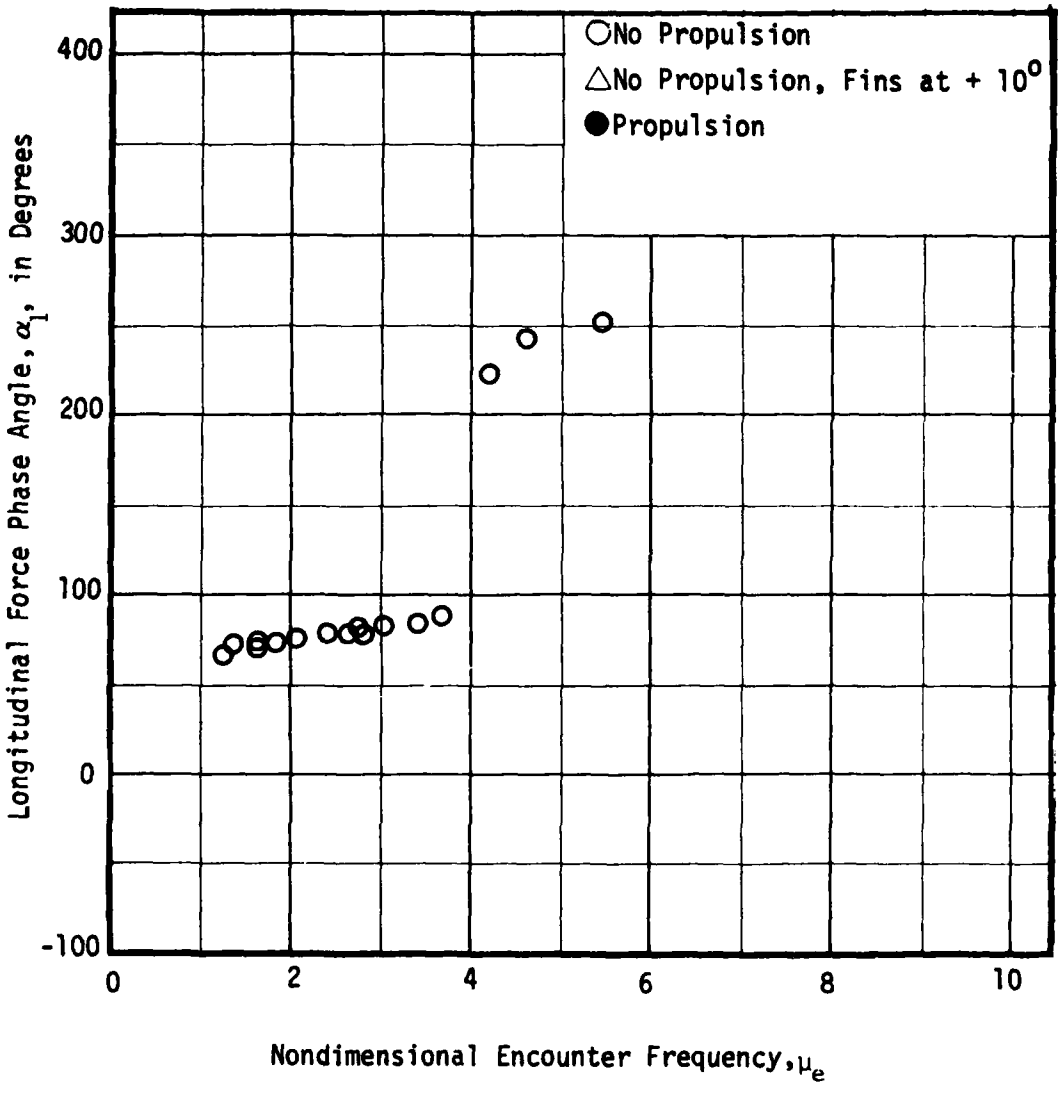

Figure 71 - Variation of Longitudinal Force Phase Angle, α_1, with Nondimensional Encounter Frequency, μ_e, at a Full Scale Speed of 10 Knots for the SSP in Head Waves

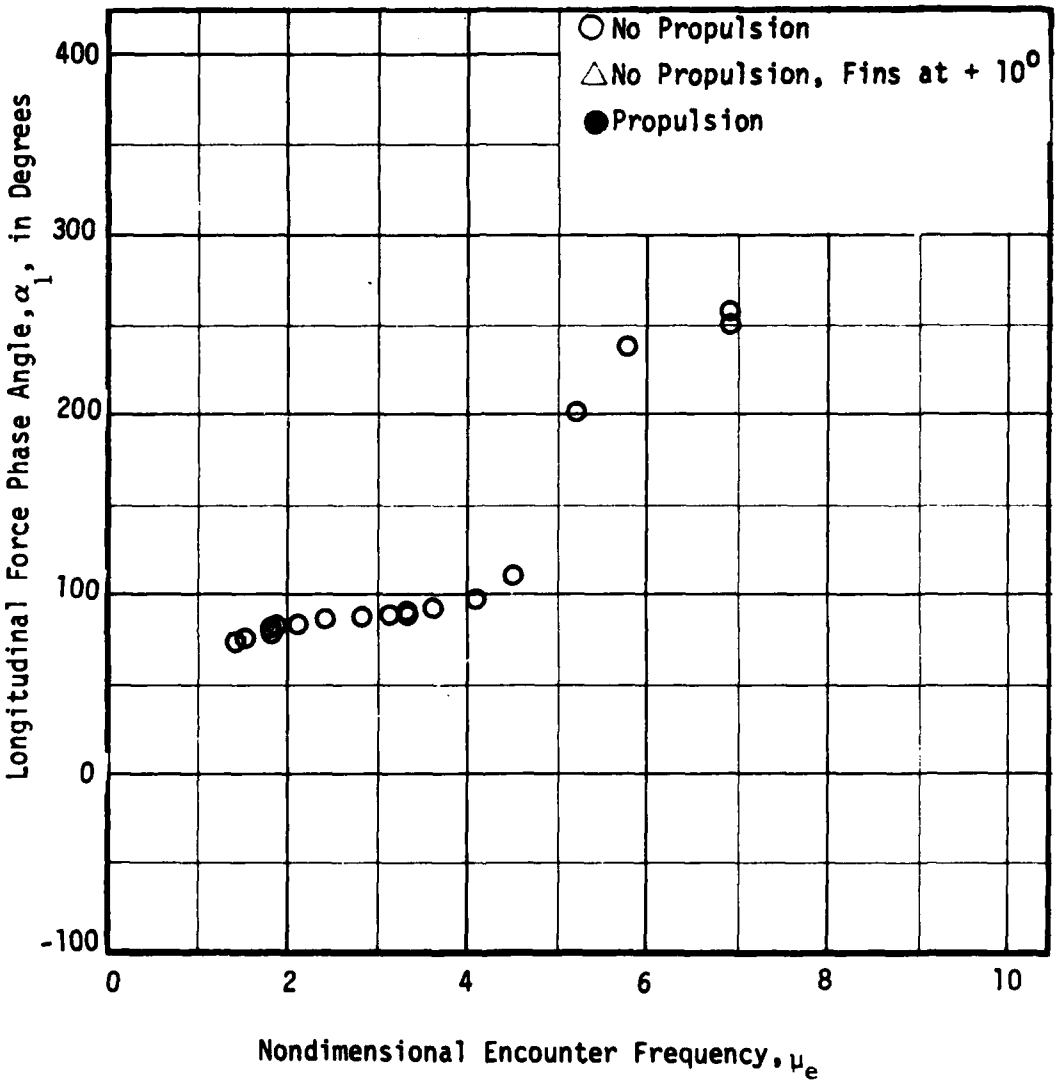

Figure 72 - Variation of Longitudinal Force Phase Angle, α_1, with Nondimensional Encounter Frequency, μ_e, at a Full Scale Speed of 15.5 Knots for the SSP in Head Waves

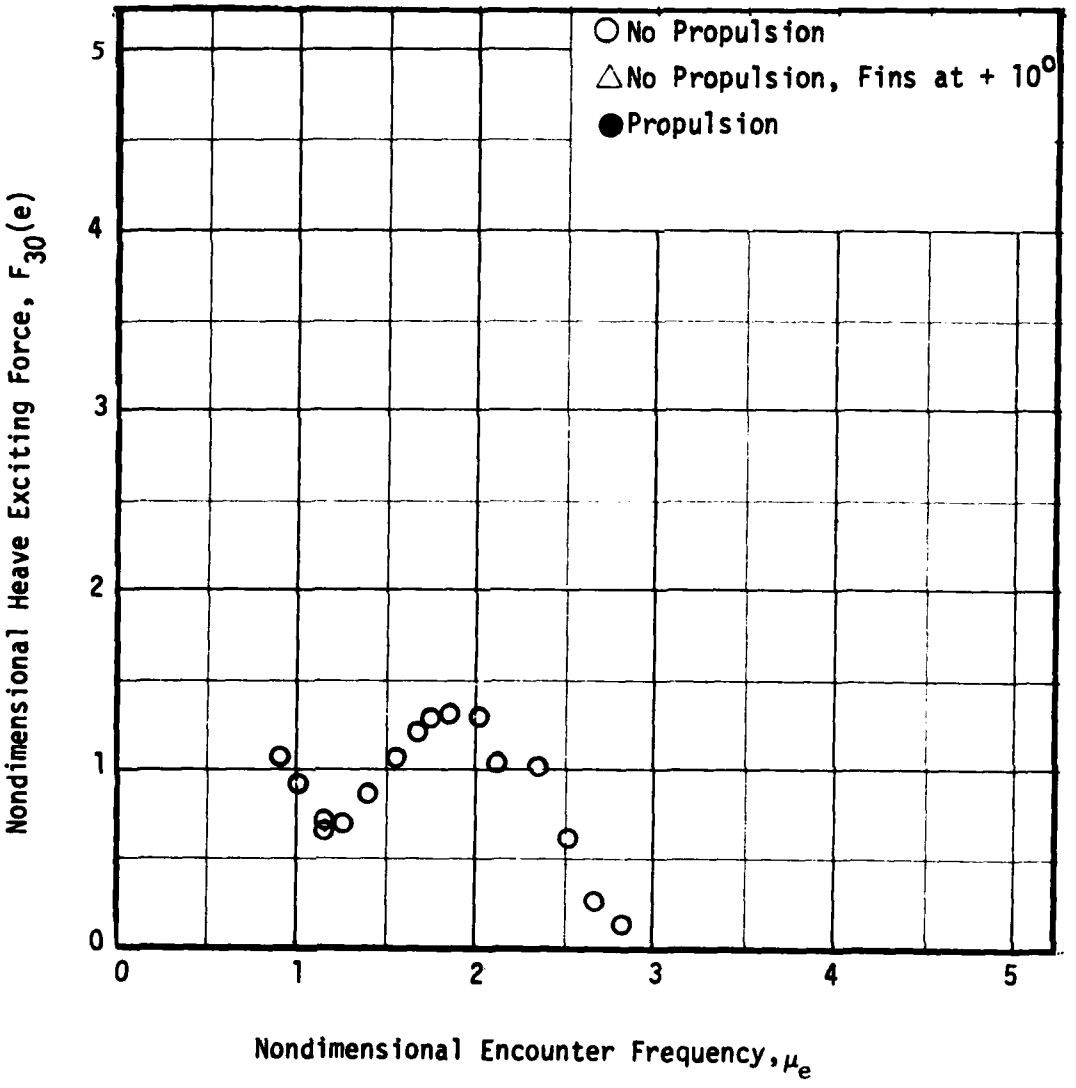

Figure 73 - Variation of Nondimensional Heave Exciting Force, $F_{30}(e)$, with Nondimensional Encounter Frequency, μ_e, at Zero Speed for the SSP in Head Waves

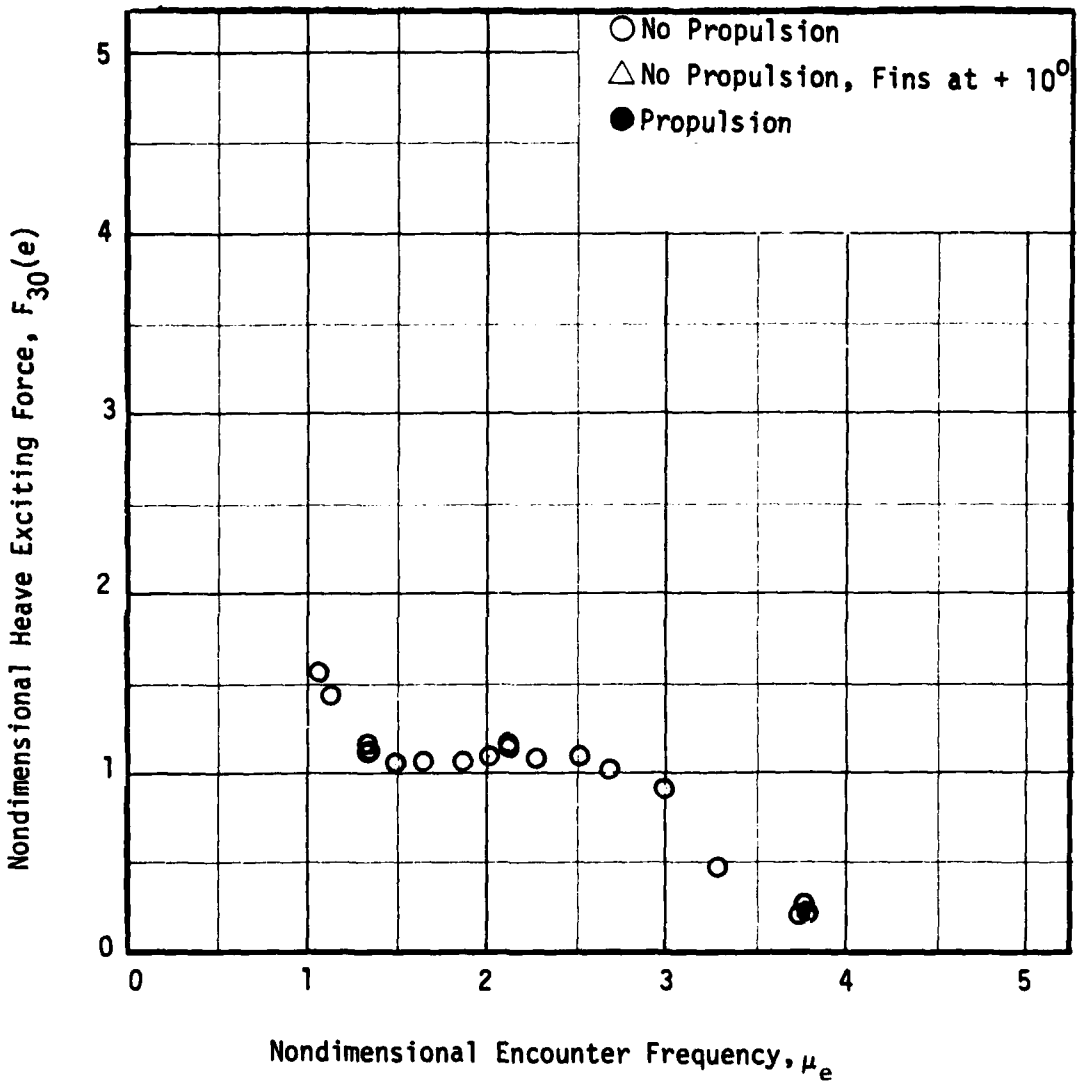

Figure 74 - Variation of Nondimensional Heave Exciting Force, $F_{30}(e)$, with Nondimensional Encounter Frequency, μ_e, at a Full Scale Speed of 3 Knots for the SSP in Head Waves

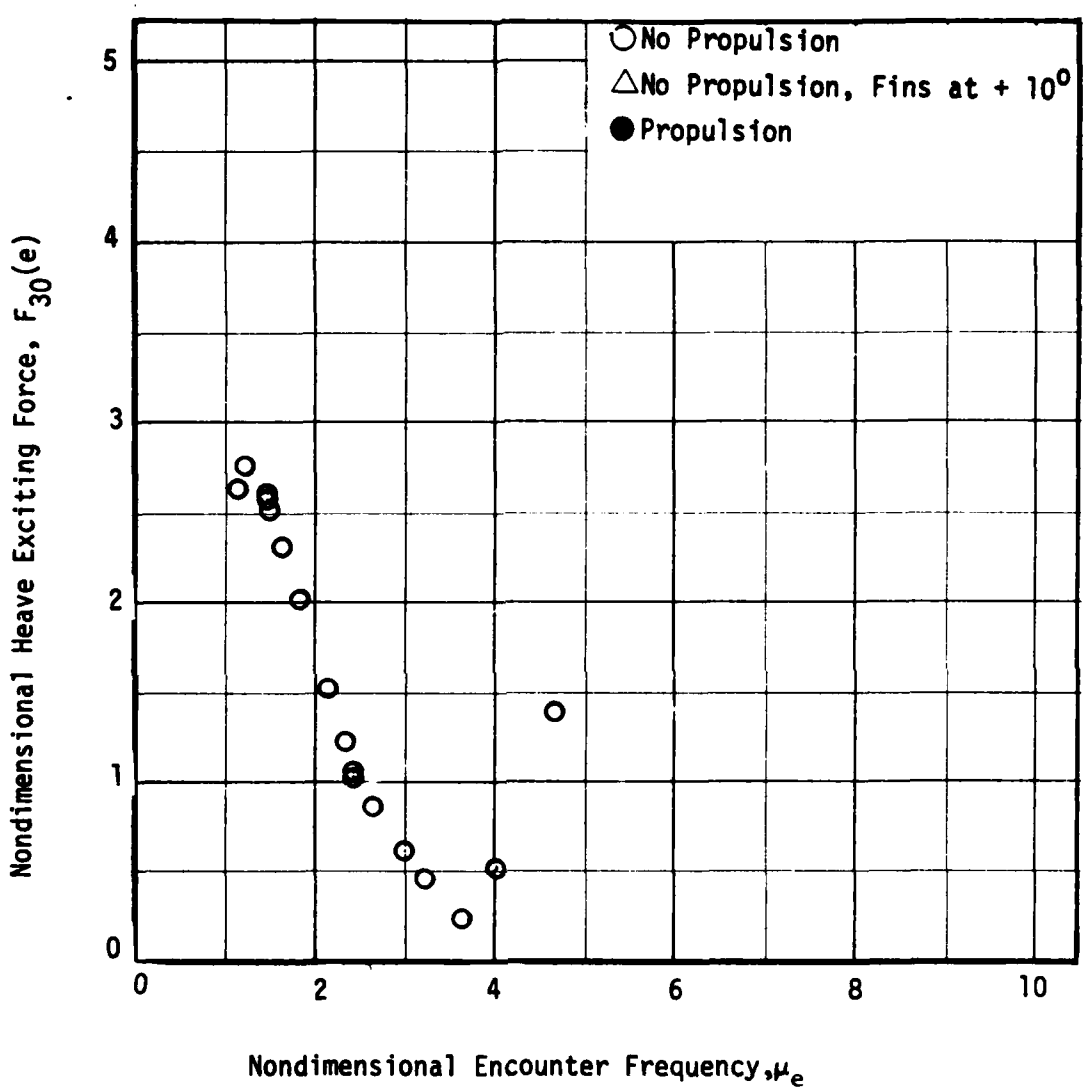

Figure 75 - Variation of Nondimensional Heave Exciting Force, $F_{30}(e)$, with Nondimensional Encounter Frequency, μ_e, at a Full Scale Speed of 7 Knots for the SSP in Head Waves

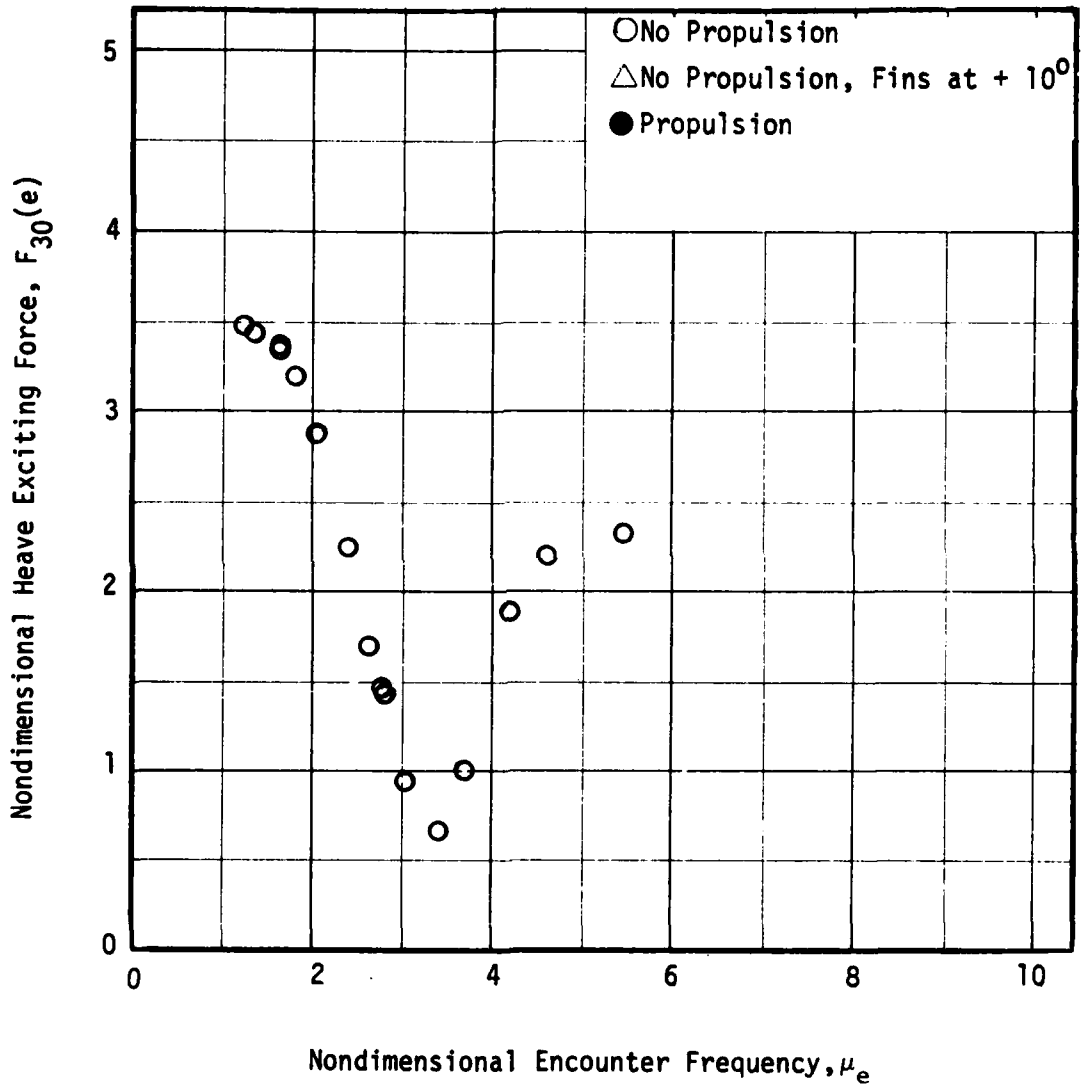

Figure 76 - Variation of Nondimensional Heave Exciting Force, $F_{30}(e)$, with Nondimensional Encounter Frequency, μ_e, at a Full Scale Speed of 10 Knots for the SSP in Head Waves

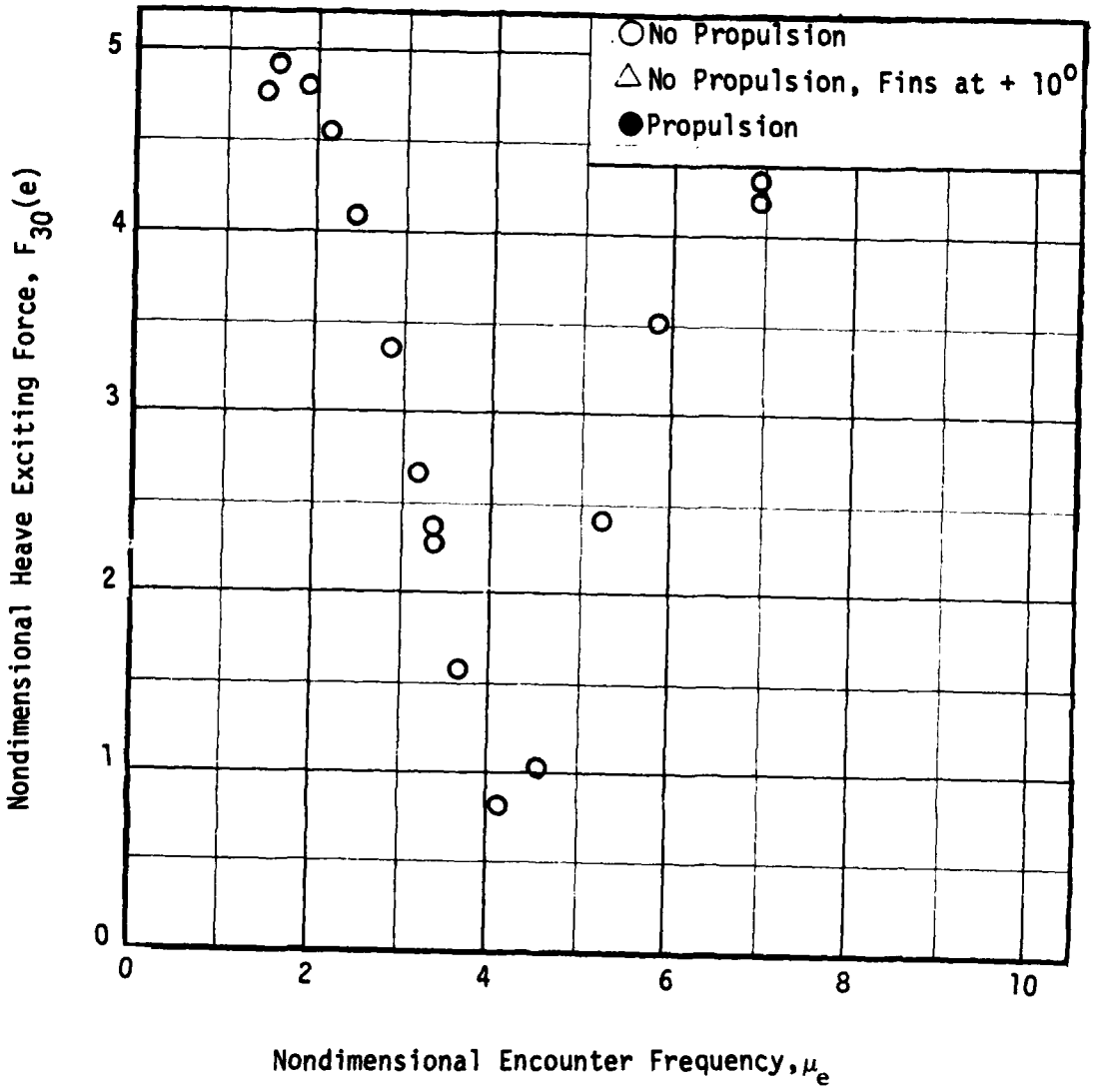

Figure 77 - Variation of Nondimensional Heave Exciting Force, $F_{30}(e)$, with Nondimensional Encounter Frequency, μ_e, at a Full Scale Speed of 15.5 Knots for the SSP in Head Waves

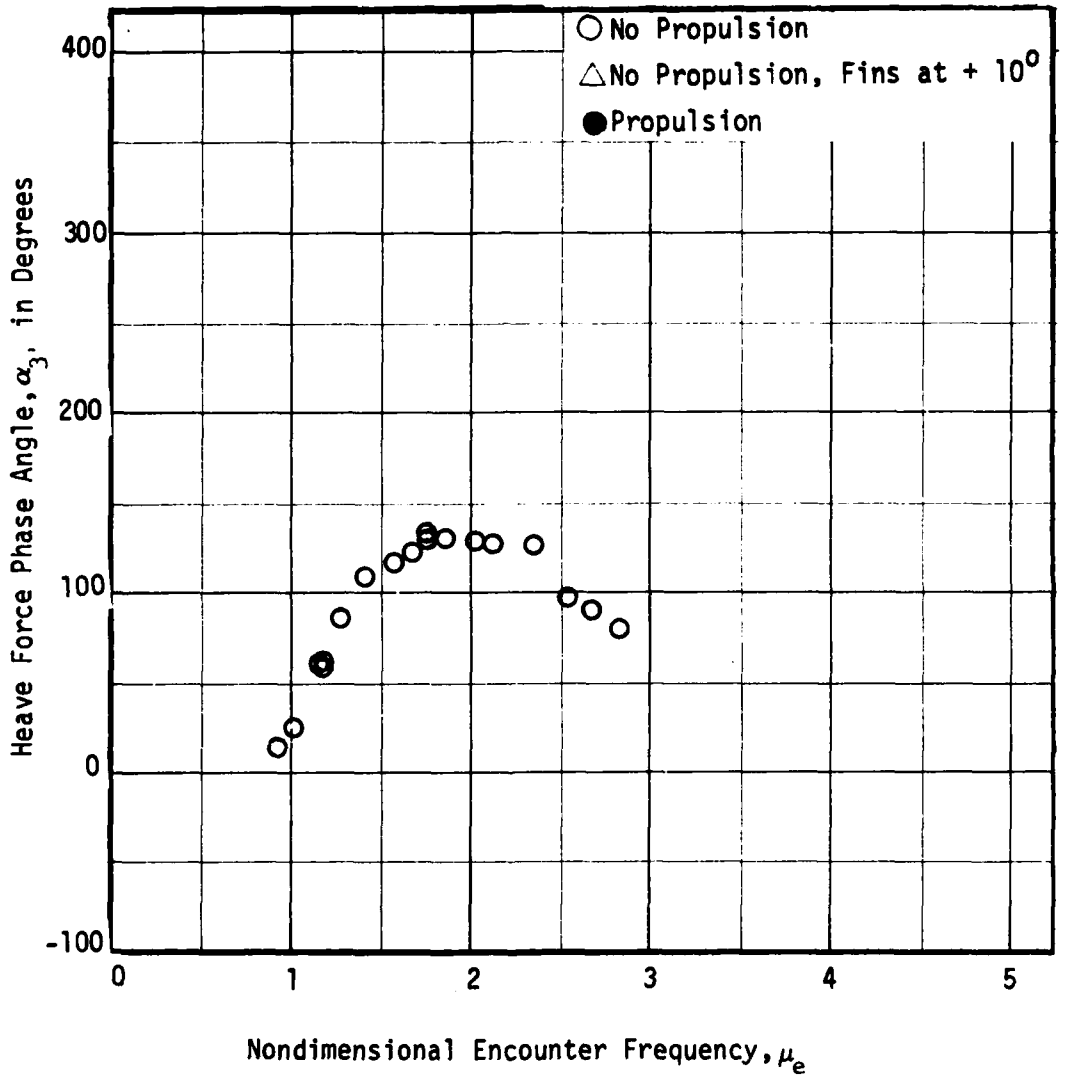

Figure 78 - Variation of Heave Force Phase Angle, α_3, with Nondimensional Encounter Frequency, μ_e, at Zero Speed for the SSP in Head Waves

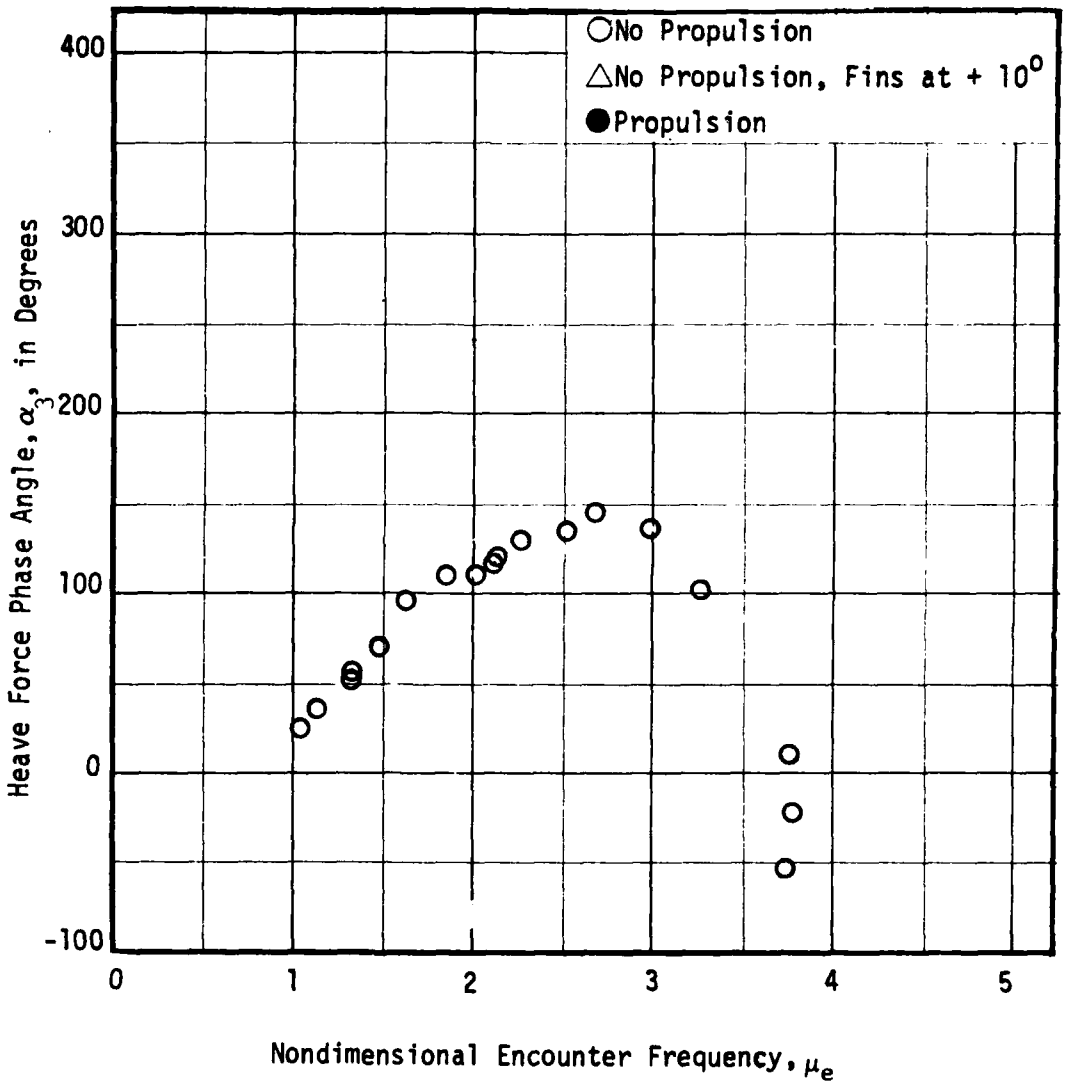

Figure 79 - Variation of Heave Force Phase Angle, α_3, with Nondimensional Encounter Frequency, μ_e, at a Full Scale Speed of 3 Knots for the SSP in Head Waves

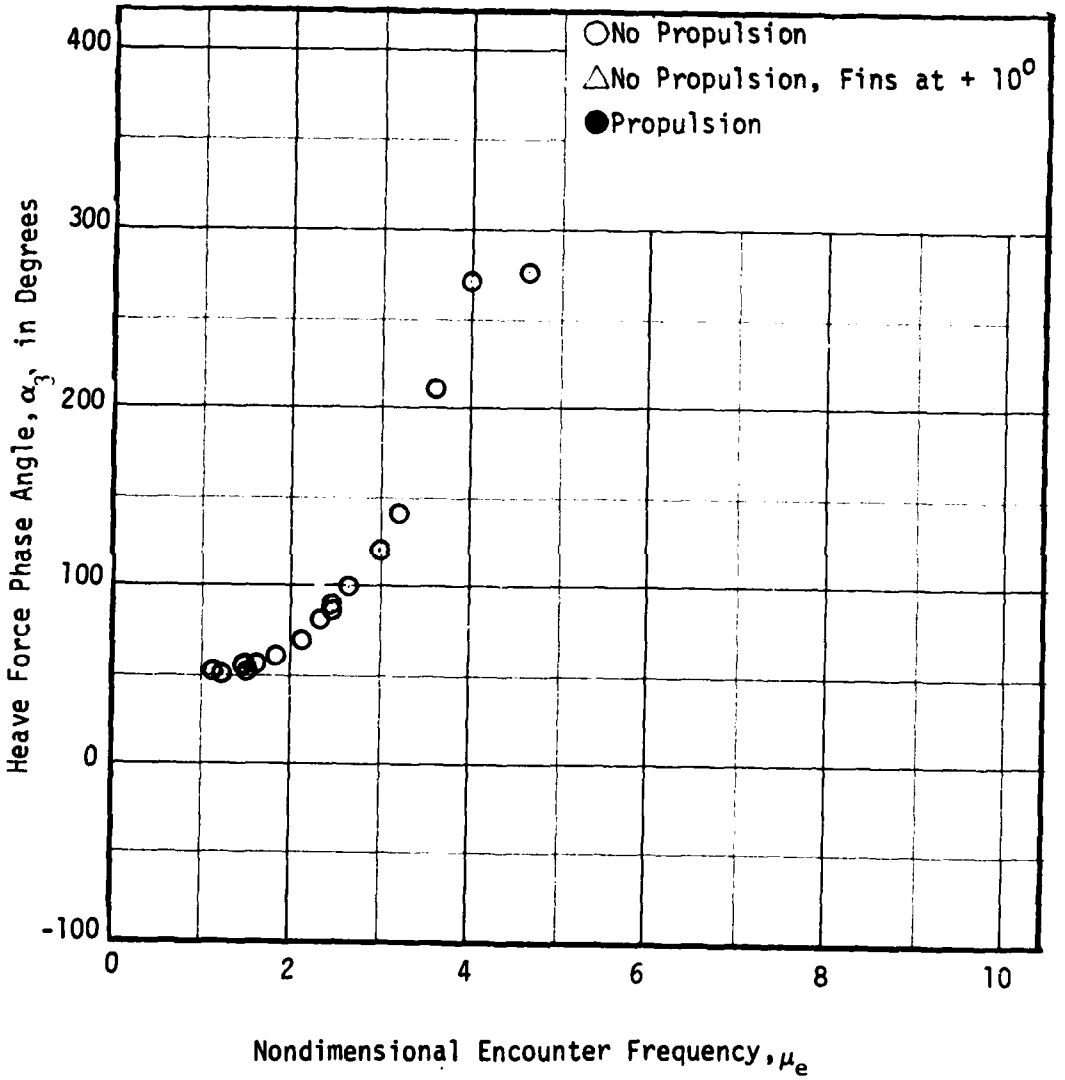

Figure 80 - Variation of Heave Force Phase Angle, α_3, with Nondimensional Encounter Frequency, μ_e, at a Full Scale Speed of 7 Knots for the SSP in Head Waves

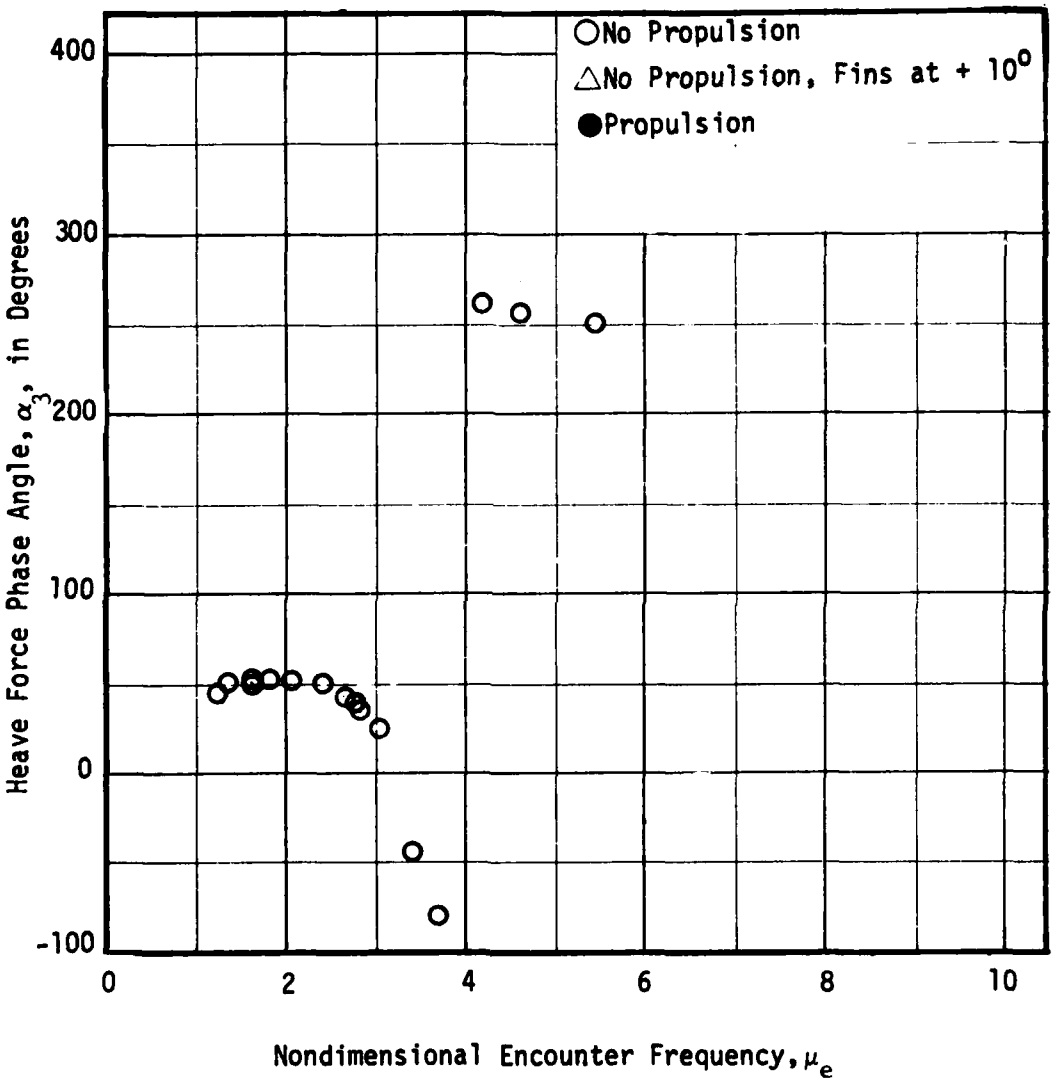

Figure 81 - Variation of Heave Force Phase Angle, α_3, with Nondimensional Encounter Frequency, μ_e, at a Full Scale Speed of 10 Knots for the SSP in Head Waves

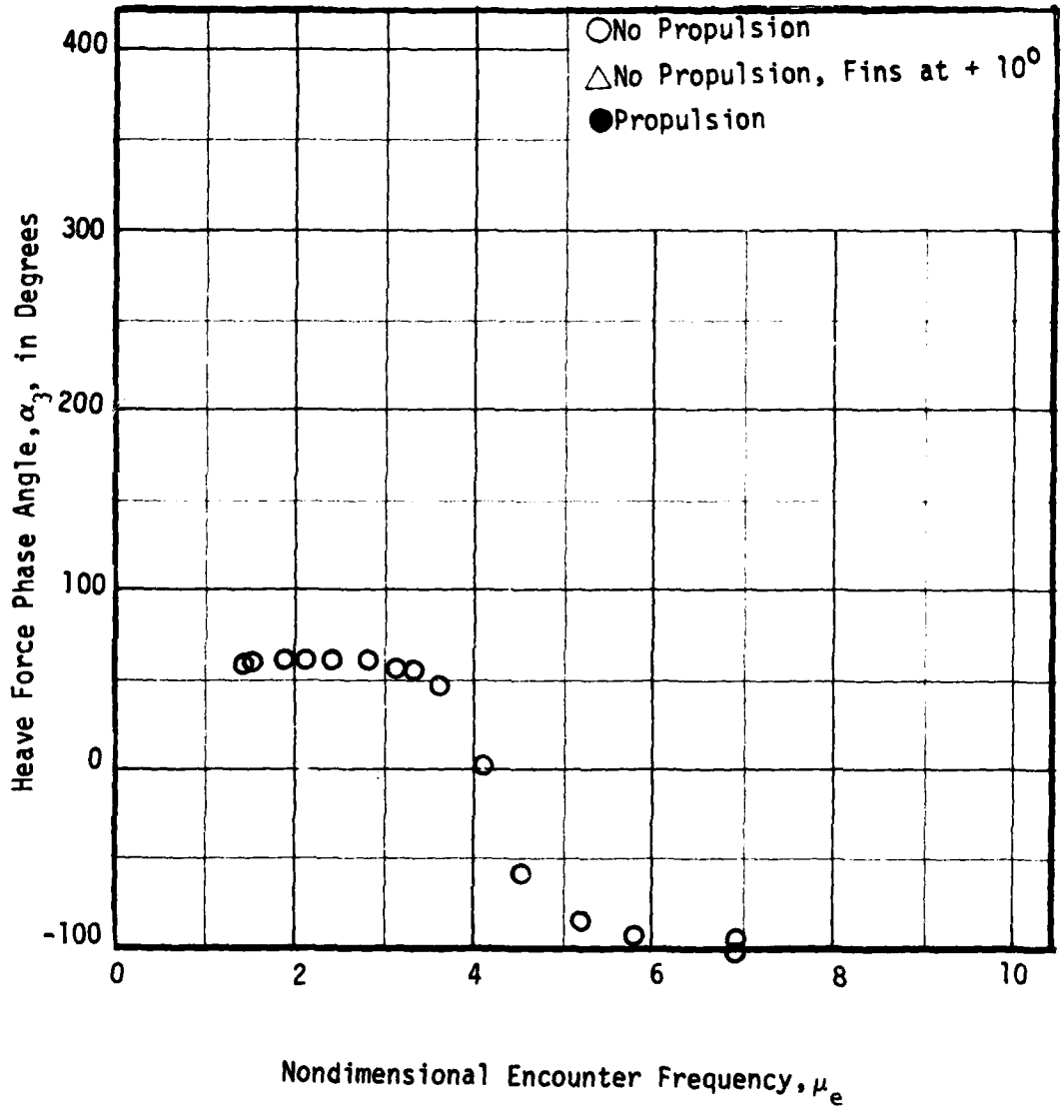

Figure 82 - Variation of Heave Force Phase Angle, α_3, with Nondimensional Encounter Frequency, μ_e, at a Full Scale Speed of 15.5 Knots for the SSP in Head Waves

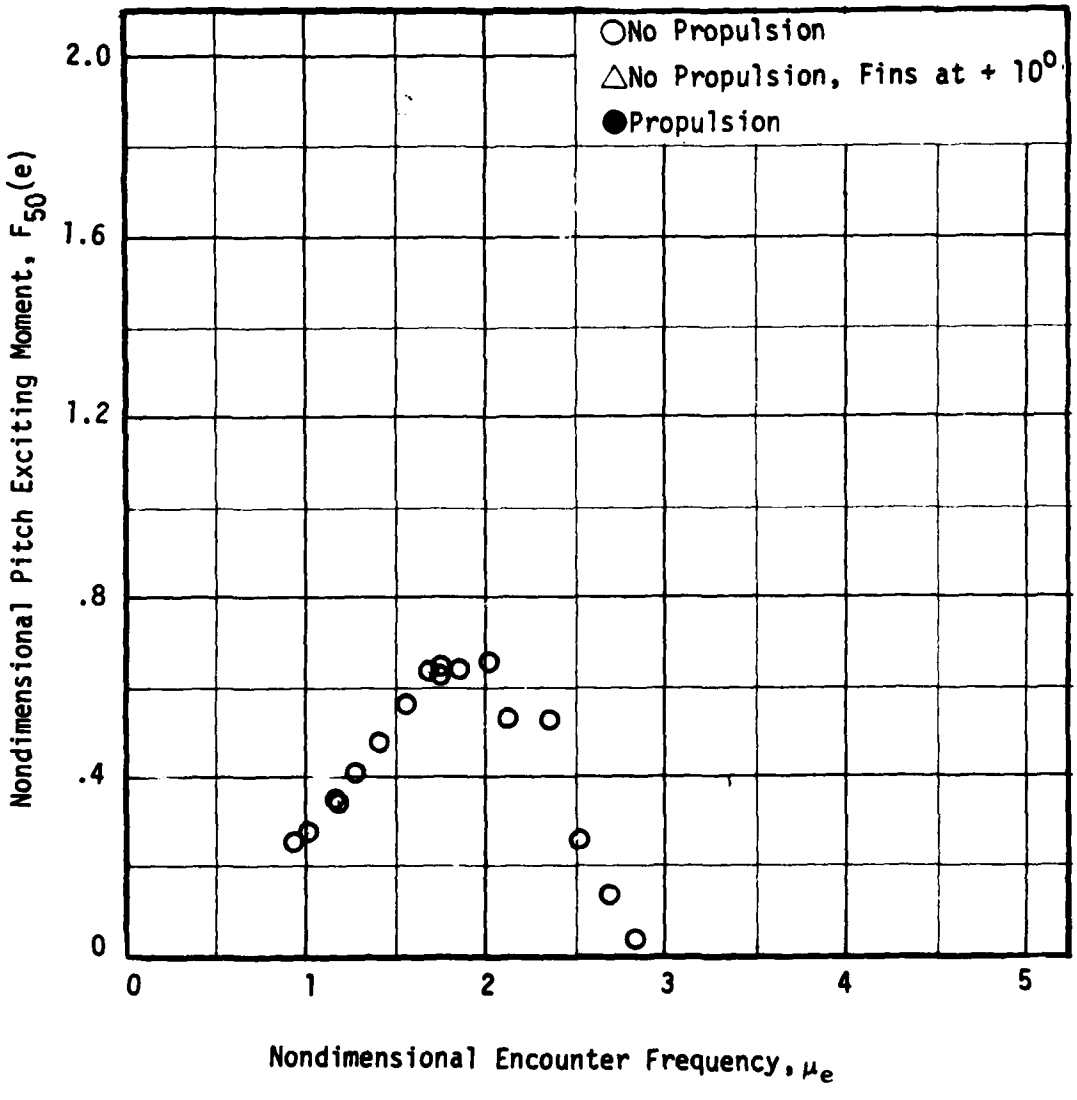

Figure 83 - Variation of Nondimensional Pitch Exciting Moment, $F_{50}(e)$, with Nondimensional Encounter Frequency, μ_e, at Zero Speed for the SSP in Head Waves

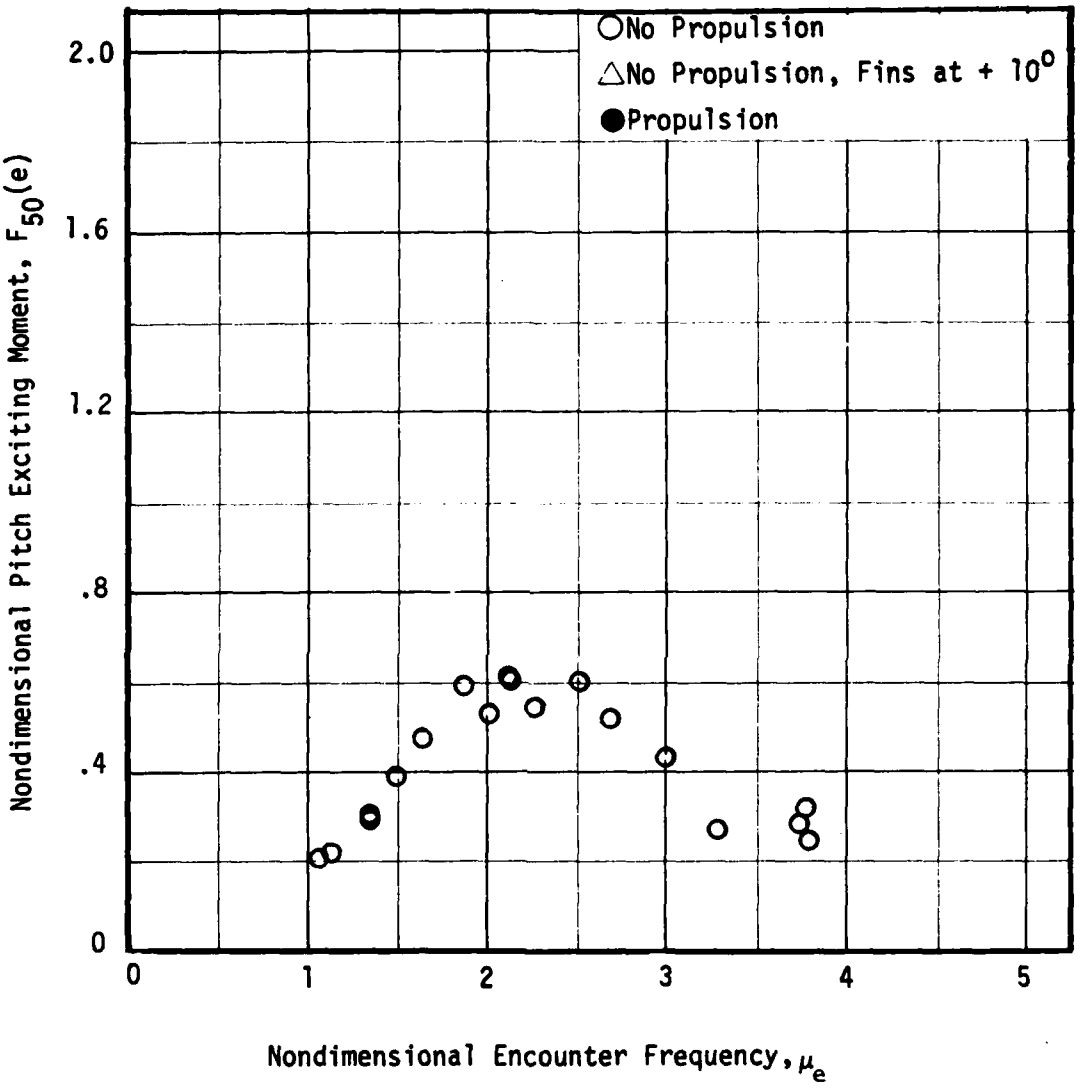

Figure 84 - Variation of Nondimensional Pitch Exciting Moment, $F_{50}(e)$, with Nondimensional Encounter Frequency, μ_e, at a Full Scale Speed of 3 Knots for the SSP in Head Waves

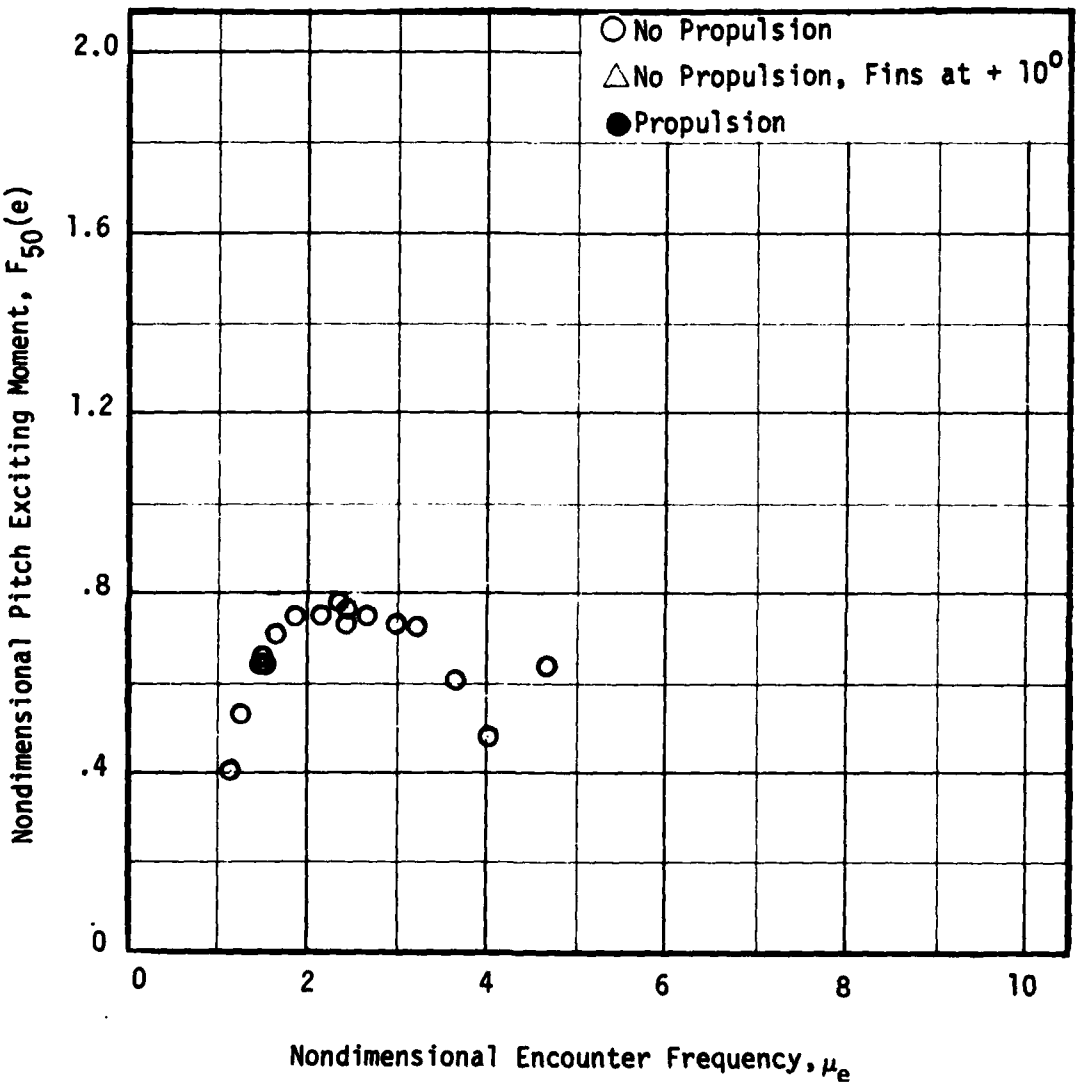

Figure 85 - Variation of Nondimensional Pitch Exciting Moment, $F_{50}(e)$, with Nondimensional Encounter Frequency, μ_e, at a Full Scale Speed of 7 Knots for the SSP in Head Waves

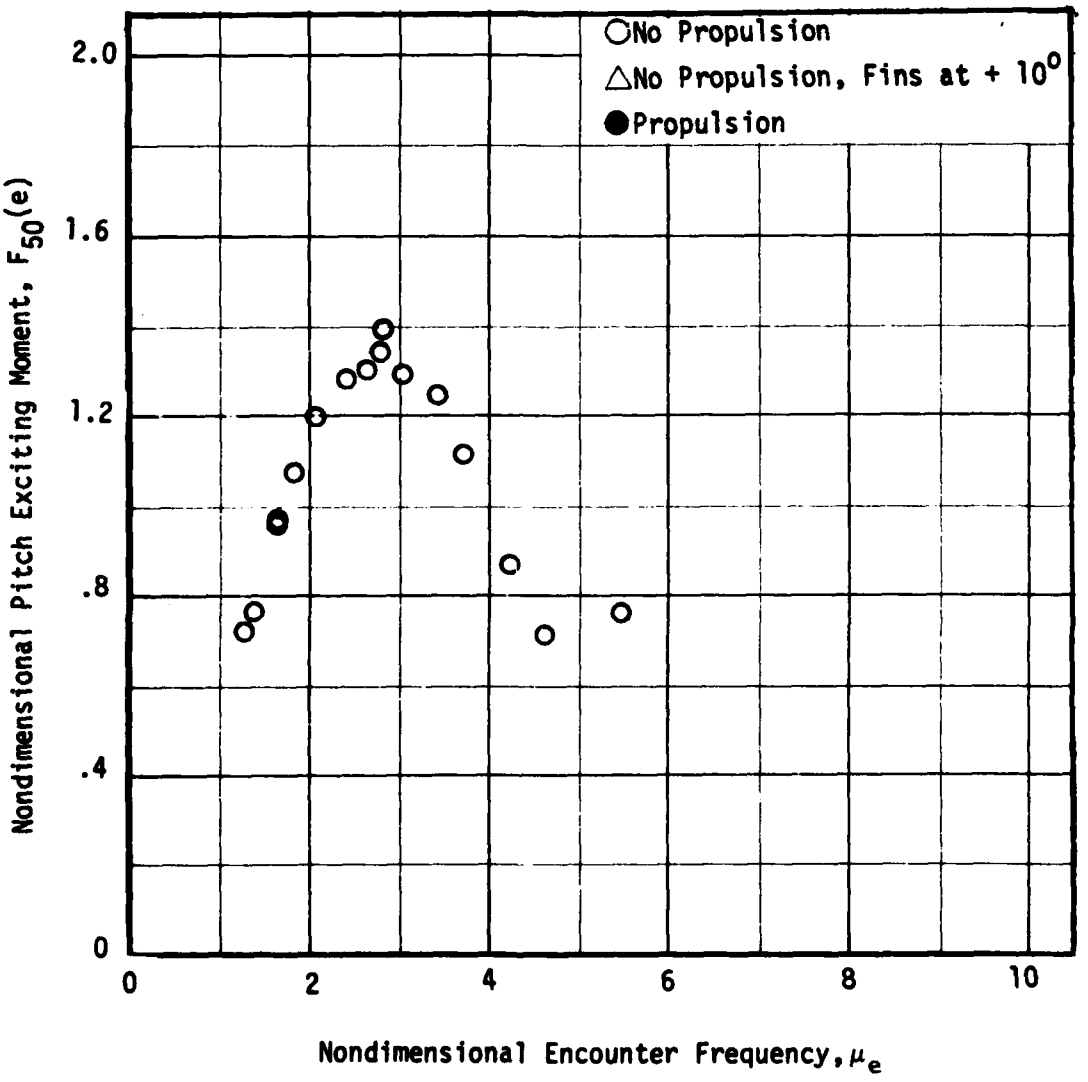

Figure 86 - Variation of Nondimensional Pitch Exciting Moment, $F_{50}(e)$, with Nondimensional Encounter Frequency, μ_e, at a Full Scale Speed of 10 Knots for the SSP in Head Waves

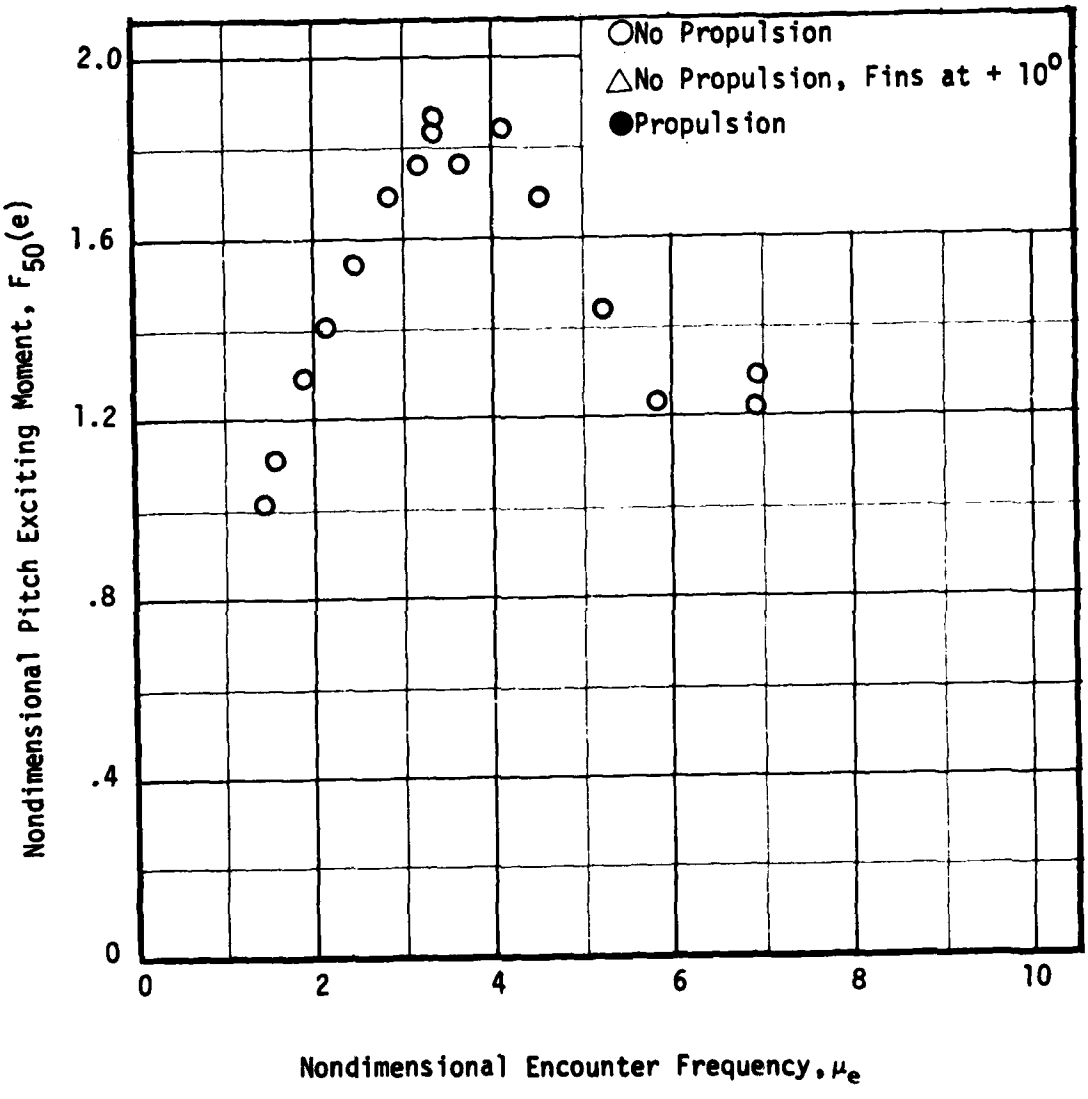

Figure 87 - Variation of Nondimensional Pitch Exciting Moment, $F_{50}(e)$, with Nondimensional Encounter Frequency, μ_e, at a Full Scale of 15.5 Knots for the SSP in Head Waves

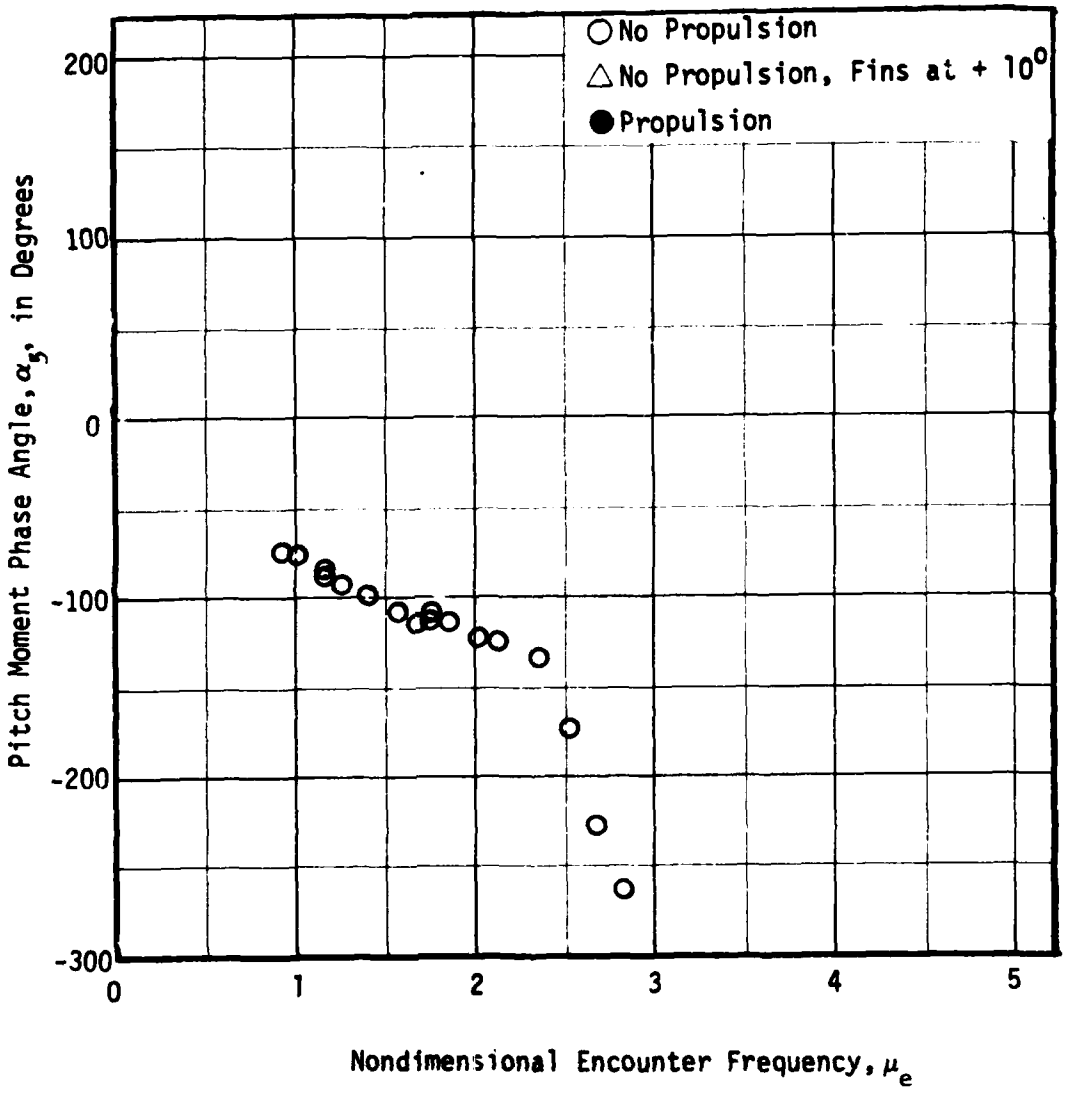

Figure 88 - Variation of Pitch Moment Phase Angle, α_5, with Nondimensional Encounter Frequency, μ_e, at Zero Speed for the SSP in Head Waves

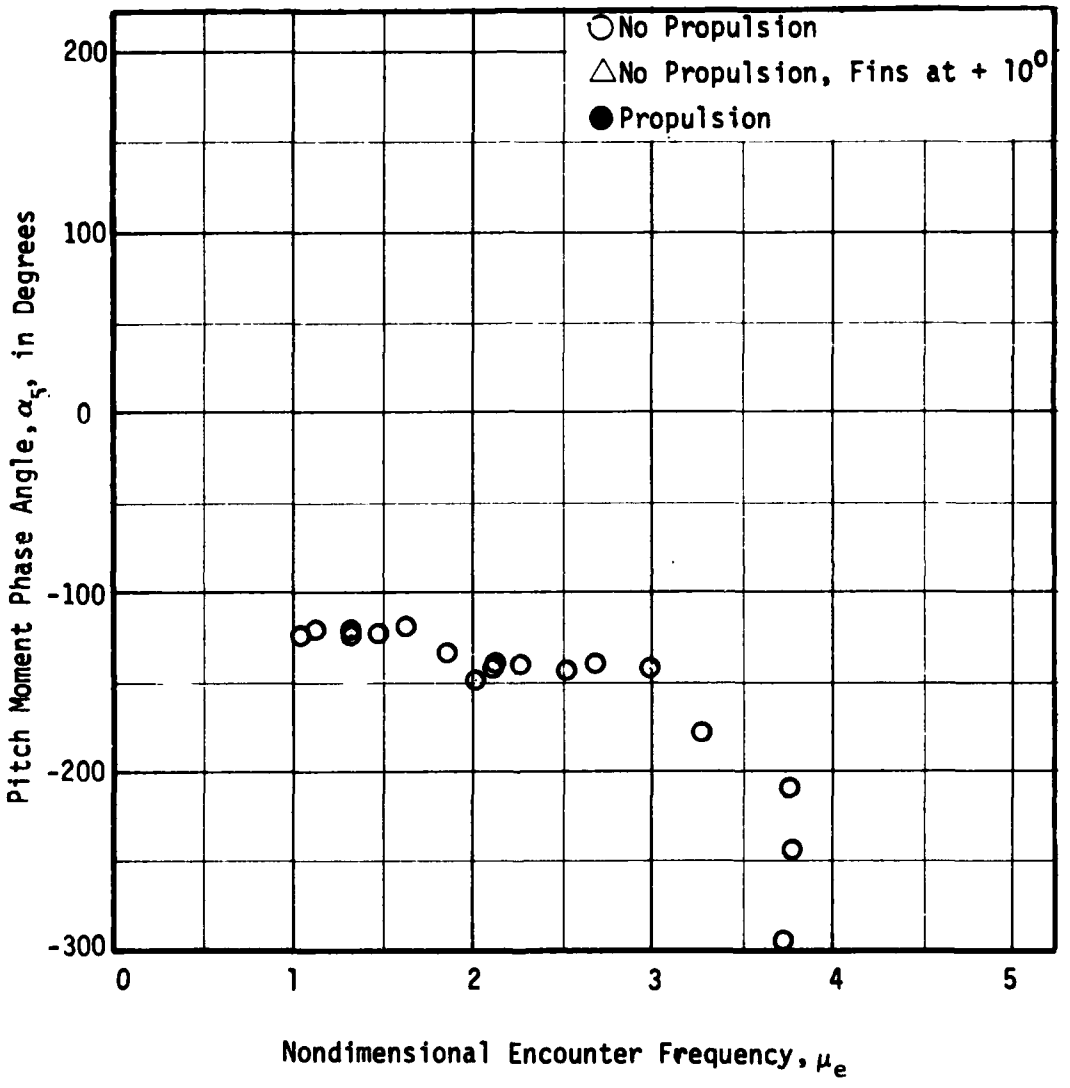

Figure 89 - Variation of Pitch Moment Phase Angle, α_5, with Nondimensional Encounter Frequency, μ_e, at a Full Scale Speed of 3 Knots for the SSP in Head Waves

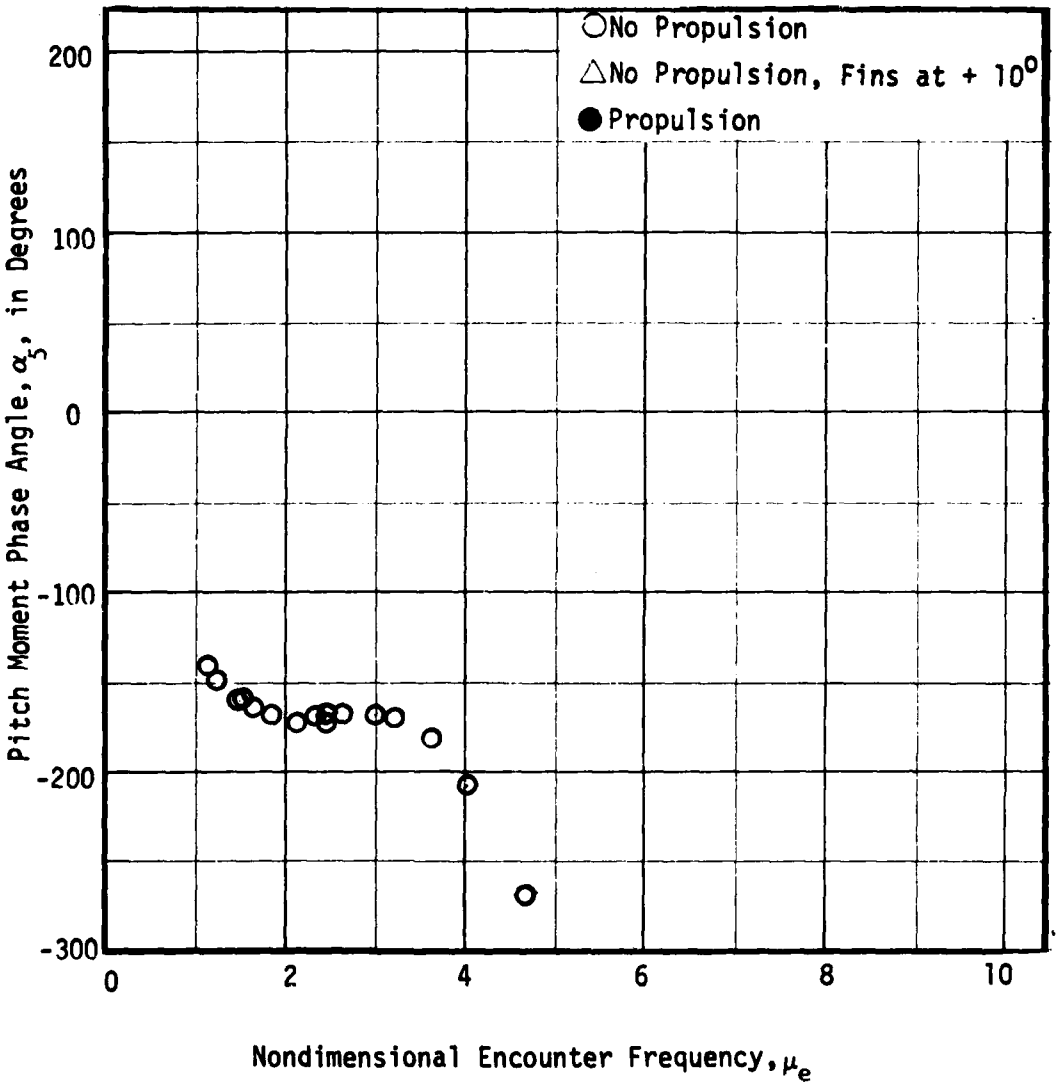

Figure 90 - Variation of Pitch Moment Phase Angle, α_5, with Nondimensional Encounter Frequency, μ_e, at a Full Scale Speed of 7 Knots for the SSP in Head Waves

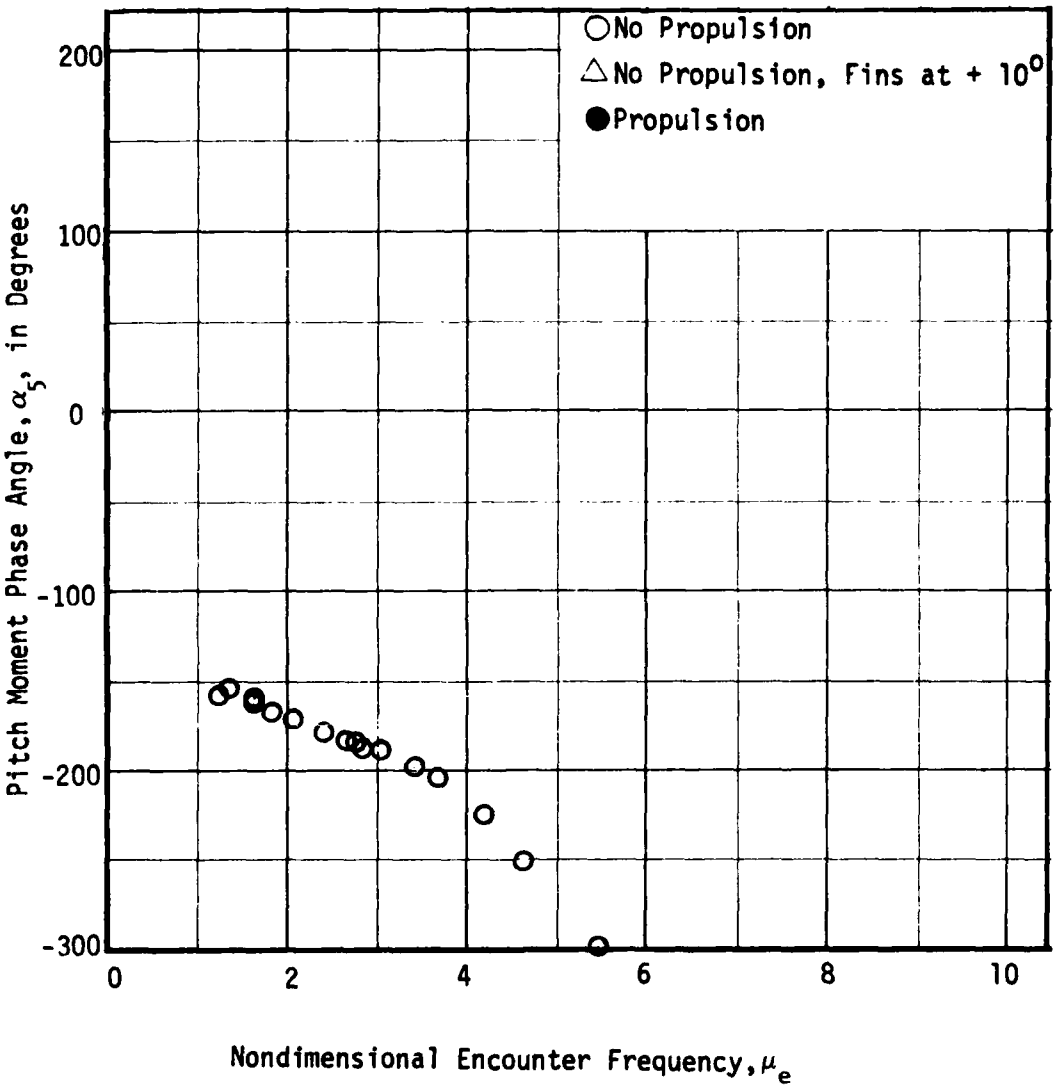

Figure 91 - Variation of Pitch Moment Phase Angle, α_5, with Nondimensional Encounter Frequency, μ_e, at a Full Scale Speed of 10 Knots for the SSP in Head Waves

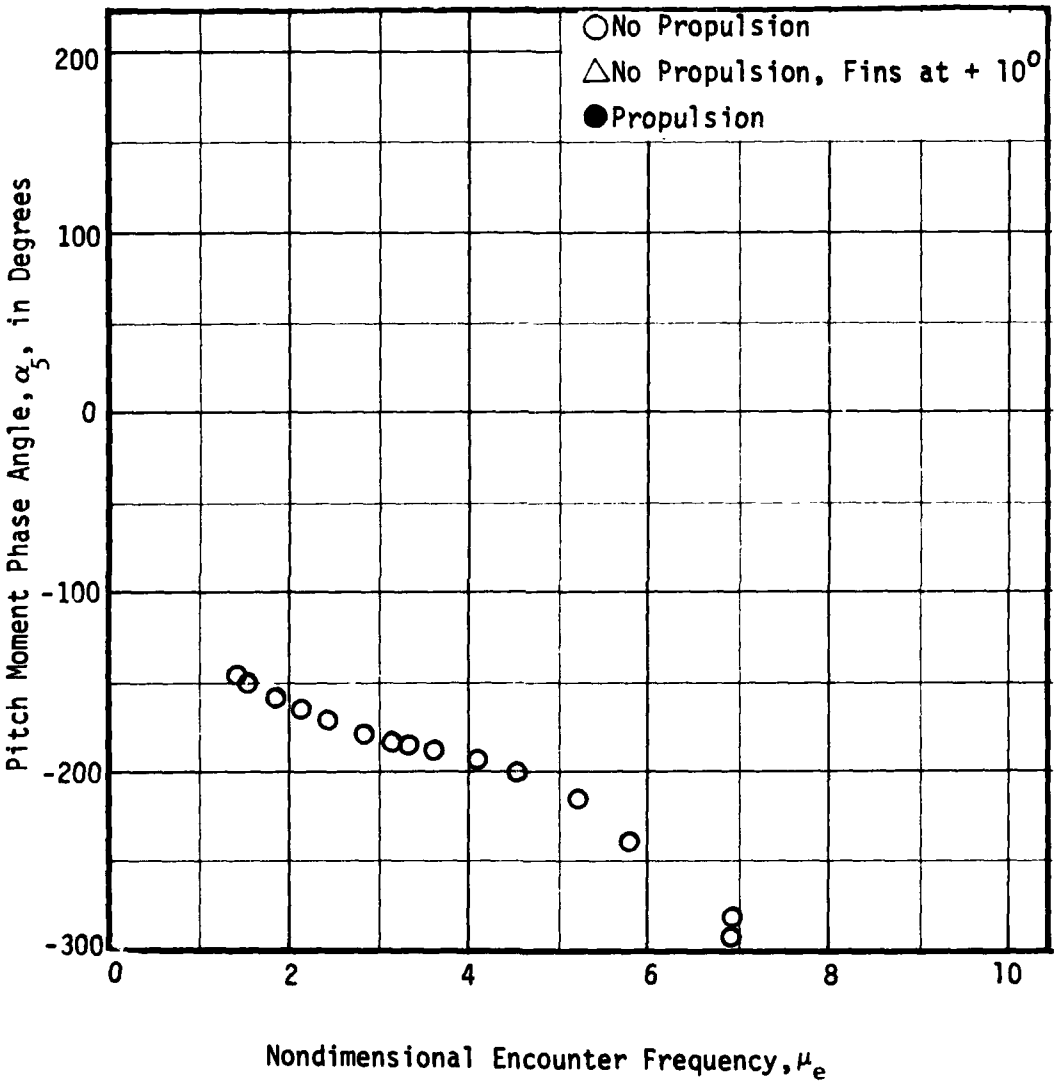

Figure 92 - Variation of Pitch Moment Phase Angle, α_5, with Nondimensional Encounter Frequency, μ_e, at a Full Scale Speed of 15.5 Knots for the SSP in Head Waves

DTNSRDC ISSUES THREE TYPES OF REPORTS

1. DTNSRDC REPORTS, A FORMAL SERIES, CONTAIN INFORMATION OF PERMANENT TECHNICAL VALUE. THEY CARRY A CONSECUTIVE NUMERICAL IDENTIFICATION REGARDLESS OF THEIR CLASSIFICATION OR THE ORIGINATING DEPARTMENT.

2. DEPARTMENTAL REPORTS, A SEMIFORMAL SERIES, CONTAIN INFORMATION OF A PRELIMINARY, TEMPORARY, OR PROPRIETARY NATURE OR OF LIMITED INTEREST OR SIGNIFICANCE. THEY CARRY A DEPARTMENTAL ALPHANUMERICAL IDENTIFICATION.

3. TECHNICAL MEMORANDA, AN INFORMAL SERIES, CONTAIN TECHNICAL DOCUMENTATION OF LIMITED USE AND INTEREST. THEY ARE PRIMARILY WORKING PAPERS INTENDED FOR INTERNAL USE. THEY CARRY AN IDENTIFYING NUMBER WHICH INDICATES THEIR TYPE AND THE NUMERICAL CODE OF THE ORIGINATING DEPARTMENT. ANY DISTRIBUTION OUTSIDE DTNSRDC MUST BE APPROVED BY THE HEAD OF THE ORIGINATING DEPARTMENT ON A CASE-BY-CASE BASIS.